AD-A175 205 CHEMICAL LASER PHASE CONJUGATION TECHNOLOGY (CLPCT)(U) 1/2
TRW DEFENSE AND SPACE SYSTEMS GROUP REDONDO BEACH CA
APPLIED TECHNOLOGY DIV A D SCHNURR ET AL. 30 NOV 86
UNCLASSIFIED TRW-AP-0923 F/G 20/5 NL

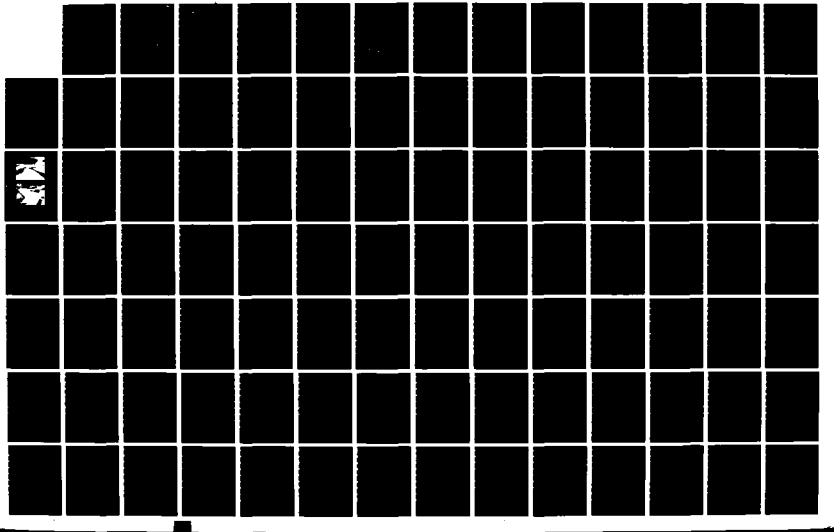

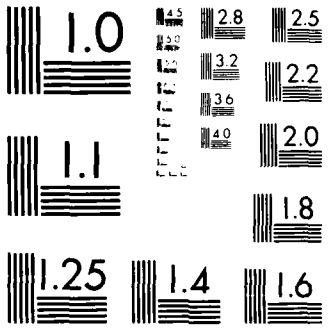

TRW

12

CHEMICAL LASER PHASE CONJUGATION TECHNOLOGY (CLPCT)

Alvin D. Schnurr, et al.
TRW Inc.
One Space Park, 01/1270
Redondo Beach, CA 90278

30 November 1986

Final Report 10 July 1985 to 9 November 1986

Prepared for
STRATEGIC DEFENSE INITIATIVE OFFICE
1717 H Street
Washington D.C.

NAVAL RESEARCH LABORATORY
4555 Overlook Avenue
Washington, D.C. 20375

SECURITY CLASSIFICATION OF THIS PAGE

AD-A175205

REPORT DOCUMENTATION PAGE

1a. REPORT SECURITY CLASSIFICATION Unclassified	1b. RESTRICTIVE MARKINGS Per clause H-9
2a. SECURITY CLASSIFICATION AUTHORITY [redacted]	3. DISTRIBUTION/AVAILABILITY OF REPORT Unlimited
2b. DECLASSIFICATION/DOWNGRADING SCHEDULE [redacted]	
4. PERFORMING ORGANIZATION REPORT NUMBER(S) AP-0923	5. MONITORING ORGANIZATION REPORT NUMBER(S) Naval Research Laboratory Contract N00014-85-C-2337
6a. NAME OF PERFORMING ORGANIZATION Applied Technology Division Space & Technology Group, TRW 6b. OFFICE SYMBOL (If applicable)	7a. NAME OF MONITORING ORGANIZATION Naval Research Laboratory
6c. ADDRESS (City, State, and ZIP code) One Space Park Redondo Beach, CA 90278	7b. ADDRESS (City, State, and ZIP code) Washington, D.C. 20375-5000
8a. NAME OF FUNDING/SPONSORING ORGANIZATION Naval Research Laboratory 8b. OFFICE SYMBOL (If applicable)	9. PROCUREMENT INSTRUMENT IDENTIFICATION NUMBER
8c. ADDRESS (City, State, and ZIP code) Washington, D.C. 20375-5000	10. SOURCE OF FUNDING NOS PROGRAM ELEMENT NO. / PROJECT NO / TASK NO / WORK UNIT NO
11. TITLE (Include Security Classification) Chemical Laser Phase Conjugation Technology (CLPCT)	
12. PERSONAL AUTHOR(S) A. Schnurr, S. Meisenholder, S. Quon, J. Betts, J. Doyle, G. Koop, J. Reeve, and M. Valley	
13a. TYPE OF REPORT Final	13b. TIME COVERED FROM 10 Jul 1985 TO ~~Sept.~~ 9 Nov. 1986
14. DATE OF REPORT (Yr., Mo., Day) 1986, November, 30	15. PAGE COUNT 125
16. SUPPLEMENTARY NOTATION	

17. COSATI CODES		
FIELD	GROUP	SUB. GR.

18. SUBJECT TERMS (Continue on reverse if necessary and identify by block number)
HF pulsed chemical laser experimental facility, high energy laser, nonlinear optics, stimulated Brillioun scattering, phase conjugation.

19. ABSTRACT (Continue on reverse if necessary and identify by block number)

The final report for the Chemical Laser Phase Conjugation Technology (CLPCT) project presents the detailed design for an experimental facility for use in future phase conjugation experiments which will be conducted under a separate project. The objective of the CLPCT program was to design a facility that (1) is compatible with the use of an existing 50-liter repetitively HF pulsed chemical laser (RPCL) device and (2) would allow design flexibility/growth potential for other more complex experiments.

The detailed design of the facility for the HF Conjugation experiment is described. Phase conjugation is developed by the nonlinear optical process wherein the high energy HF chemical laser beam is focused within a stimulated Brillioun scattering (SBS) cell which is filled with xenon at 40 atmospheres. The experimental facility consists of the oscillator subsystem, RPCL subsystem, diagnostics subsystem and phase conjugation subsystem. The detailed design o. each subsystem is described. In addition, the conceptual design of additional hardware for a future Conjugation Subsystem (COS) experiment is described. A flowing SBS cell was developed for this experiment.

20. DISTRIBUTION/AVAILABILITY OF ABSTRACT UNCLASSIFIED/UNLIMITED [X] SAME AS RPT [ ] DTIC USERS [ ]	21. ABSTRACT SECURITY CLASSIFICATION Unclassified
22a. NAME OF RESPONSIBLE INDIVIDUAL A. D. Schnurr	22b. TELEPHONE NUMBER (Include Area Code) (213) 536-1078
	22c. OFFICE SYMBOL

DD FORM 1473, 83 APR — EDITION OF 1 JAN 73 IS OBSOLETE

Unclassified
SECURITY CLASSIFICATION OF THIS PAGE

CONTENTS

CONTENTS (Continued)

CONTENTS (Continued)

ILLUSTRATIONS

ILLUSTRATIONS (Continued)

ILLUSTRATIONS (Continued)

ILLUSTRATIONS (Continued)

TABLES

TABLES (Continued)

1. INTRODUCTION AND SUMMARY

1.1 GENERAL PROJECT SUMMARY

This report presents the results of the Chemical Laser Phase Conjugation Technology (CLPCT) project. The overall objective of this project was to design a major phase conjugation experimental capability that uses the stimulated Brillouin scattering (SBS) process and hydrogen fluoride (HF) chemical lasers. SBS phase conjugation is a nonlinear process which requires a high power laser. Therefore, the experiments developed under the CLPCT project are based on the use of an existing high energy device, the repetitively pulsed chemical laser (RPCL), which would be used in a single-pulse mode to provide high peak power over a wide parametric range of experiment conditions. This project has resulted in the detailed design of an HF phase conjugation experiment [HF conjugation demonstration (HFC) experiment] and conceptual design of key hardware elements of an advanced experiment that would use an extension of the same hardware [conjugation subsystem (COS) experiment]. Figure 1-1 is a perspective showing the principal elements of the detailed design for the HFC experiment. Long lead hardware was also procured as part of this activity, thus allowing an accelerated schedule for the HFC test activity as part of a follow-on program.

Before discussing the details, it is appropriate to review the motivation for exploration of this new technology. It is anticipated that the HF phase conjugation technology development, made possible by this project, may become the basis for a Strategic Defense Initiative (SDI) space based laser (SBL) system design. Such a system has substantial advantages of design and performance margin over more conventional, non-phase-conjugate systems. In a phase conjugate system, device beam quality is limited primarily by the beam quality of a small oscillator which, given the low oscillator power requirement, can be near diffraction-limited. Furthermore, the key requirement of multiple device coupling requires minimal alignment control in comparison to conventional electro-optical coupling approaches. The APACHE MOPA subsystem would require ~5 waves of angular alignment and ~10 cm of piston control whereas the beam direction segmented primary may have

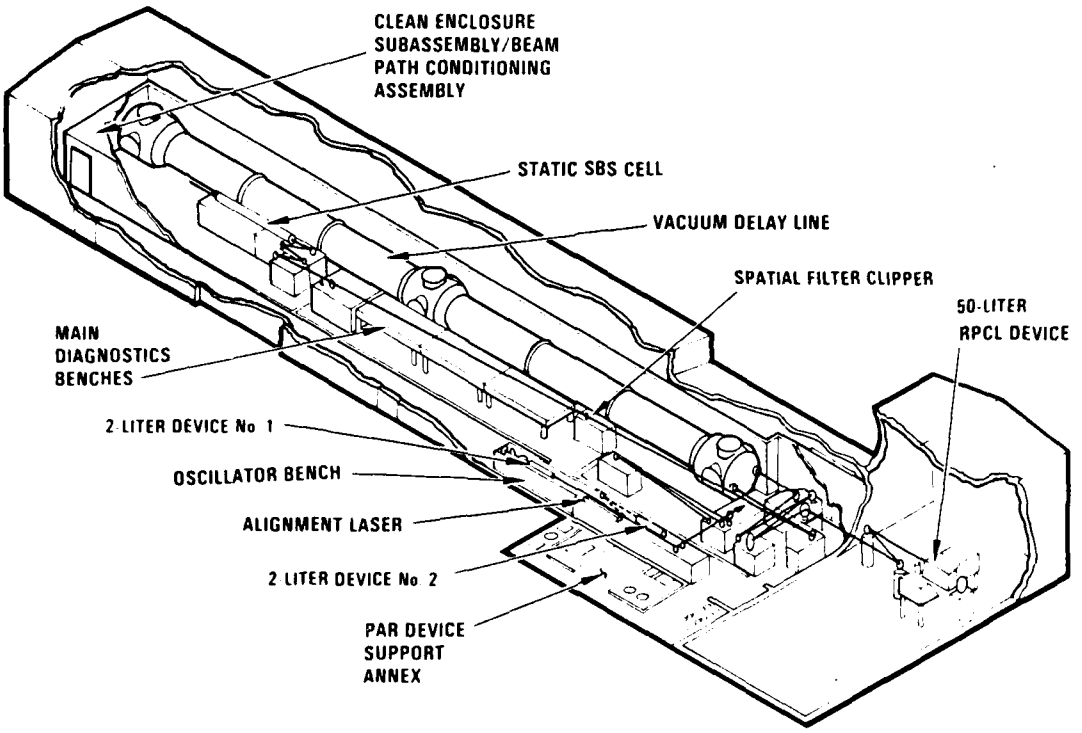

Figure 1-1. Perspective of HFC facility, (shown for the RPCL oscillator, configuration B).

piston errors of $\simeq 10\lambda$. Similarly, output device jitter depends only on the jitter of the small oscillator, with high energy laser (HEL) device jitter corrected to a bandwidth of greater than 1 MHz. These performance and design advantages provide a powerful motivation for the CLPCT project, which has designed experiments that would develop the required technology base.

The output of the designed experiments would include three key dependent parameters, namely:

- Reflectivity
- SBS threshold
- Conjugation fidelity.

These would be investigated as a function of a number of independent parameters, including:

- Aberrator beam quality (OPD power spectral density)
- SBS cell pressure
- f/number
- Absorption effects
- Power deposition
- Transverse medium velocity
- Polarization.

The design process was also guided by the desire to design a flexible hardware configuration that would allow use on possible future experiments that would look at oscillator isolation, beam combination, and other configuration changes with minimal hardware changes.

1.2 SUMMARY OF HFC EXPERIMENT DETAILED DESIGN

1.2.1 Optical Design

The HFC experiment apparatus was designed, to a critical design review (CDR) level, to allow demonstration of good conjugation fidelity at HF wavelengths using the 50-liter RPCL (single-pulse mode) at TRW's Capistrano Test Site (CTS). The key HFC optical design tasks were as follows:

- Develop a detailed optical design with adequate flexibility to accommodate a number of alternative configurations and future experiments, including:

  1) Configuration C - Low power SBS tests, using the 2-liter oscillator-preamp pulsed chemical lasers (PCL). This would provide a low power capability, useful over a restricted parametric range, or when the larger system is unavailable.

  2) Configuration B - RPCL configured as an oscillator. This configuration provides a basic data set for beam quality, bandwidth, phonon rise time, power deposition, mode control and pulse length effects. It has the advantage of less complexity and less hardware than the MOPA configuration.

  3) Configuration A&D - RPCL configured as MOPA (Config. A has slit spatial filter and Config. B has low Fresnel No. Spatial filter). This is the most robust configuration and allows use of oscillator controls such as bandwidth without any impact on power,

providing power margin if needed for jitter or BQ control, or for extending parametric range.

4) Future anticipated configurations. As mentioned above.

- Long lead hardware procurement.

1.2.1.1 Oscillator Subsystem

The oscillator subsystem provides a single HF line, polarized mode to the RPCL subsystem to allow amplifier saturation. The oscillator design was based on analysis to assure good RPCL extraction efficiency, amplified stimulated emission (ASE) suppression and pulse length matching. This analysis involved the use of the SOSHF kinetics code, the PSTAR one-dimensional MOPA $g_0 I_{sat}$ model, and the large Fresnel number conjugated MOPA (LFCM) two-dimensional wave optics MOPA model.

The final design, illustrated in Figure 1-2, is the result of design trades made to select the highest performance option, while minimizing parasitics. The design was constructed to accommodate both a single-head oscillator or an oscillator/preamplifier configuration for enhanced power performance.

1.2.1.2 RPCL and Phase Conjugation Subsystems

The RPCL and phase conjugation subsystems were designed to provide a substantial margin above SBS threshold, including the effects of spatial filtering and aberration.

The optical train design provides a reference beam quality which is near the diffraction limit. This approach allows the parameterization of conjugation fidelity using known aberrators. The use of spatial filtering to assure reference beam quality also required an alignment control capability. A delay line prevents feedback into the oscillator Fresnel core during the pulse, which might degrade oscillator performance.

The method used to separate reference and conjugate beams is polarization rotation, in combination with polarizers which divert the returning conjugate beam onto a different optical path and provide further isolation of the oscillator. The optical layout and amplifier configuration are also set up to assure ASE control and line selection.

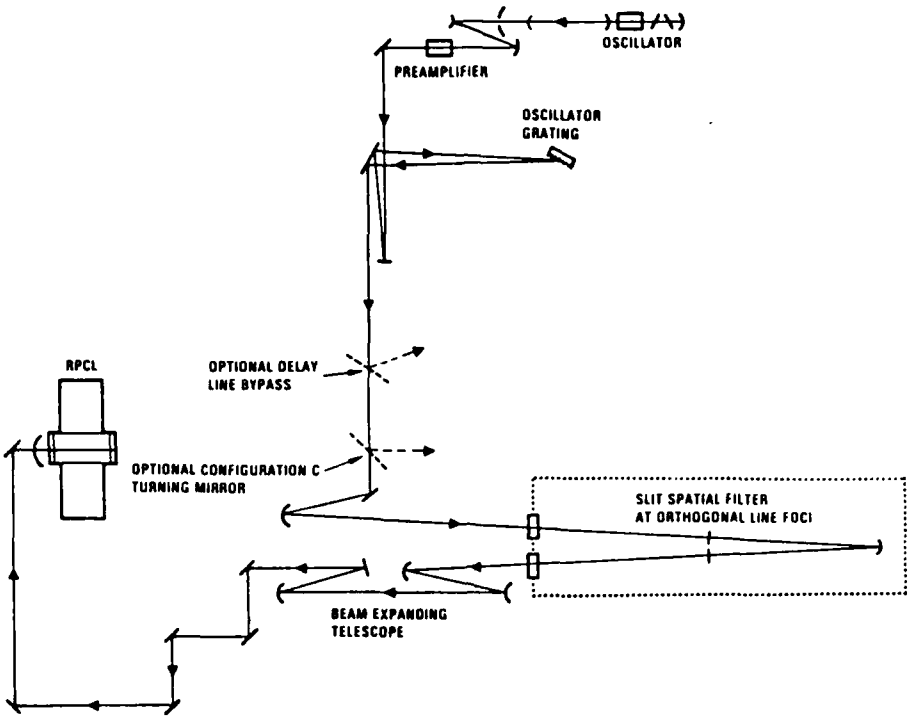

Figure 1-2. Oscillator subsystem beam train schematic (MOPA/configuration A).

The static SBS cell design uses 40 atmospheres of xenon as the baseline medium, and incorporates a number of features that allow use over a very wide f/number range and minimize uncertainties in the data that might arise due to variations in medium optical path difference (OPD).

A number of models were used in performance analysis of these subsystems. Beam propagation modeling included TPROP and CODE V, wave optics propagation codes, two-dimensional thermal models of the beam path and SBS cell, and closed form analysis of spatial filter beam cleanup. Material window analysis was used to examine stress-handling and birefringence performance.

In arriving at the final design for these subsystems, design trades were made on the basis of performance budgets and hardware cost/availability (Figure 1-3).

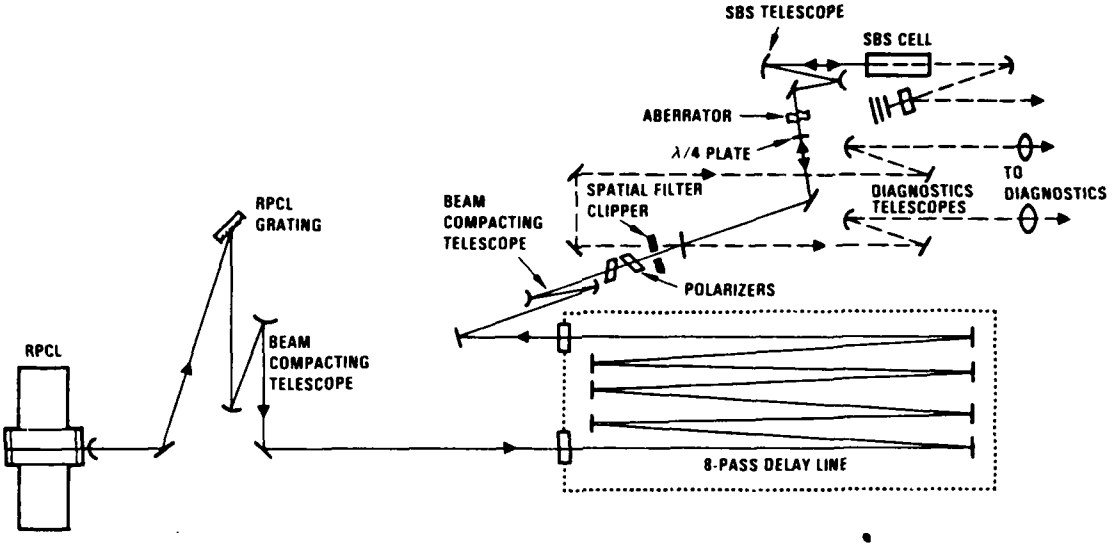

Figure 1-3. RPCL subsystem beam train schematic for RPCL and phase conjugation subsystems (baseline configuration).

1.2.1.3 Diagnostic Subsystem

The diagnostic subsystem (Figure 1-4) provides the capability to take beam quality, phase measurement and other critical data on both reference and conjugate beams. A basic requirement for this subsystem was the capability for near diffraction-limited performance assessment. Instruments included are:

- Beam quality
- Energy [total power, P(t) and spectrum]
- Polarization
- Near-field irradiance and phase
- Bandwidth
- ASE

Design analyses were used to guide the design process in the areas of electromagnetic interference (EMI) environment, instrument resolution/error budgeting, power budgeting and beam quality budgeting.

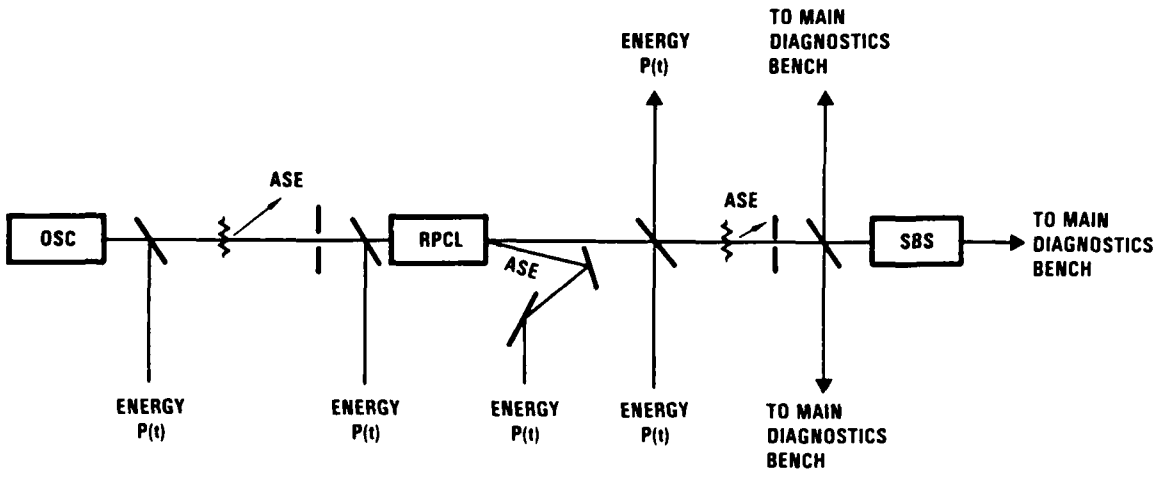

Figure 1-4. Beam diagnostics subsystem.

1.2.2 Mechanical Design

The HF conjugation experiment mechanical design provides the mounting, ducting, structural support and environmental conditioning hardware needed by the optical system design. The overall layout was guided by the basic requirement to allow flexibility to accommodate alternative configurations, as in the optical design effort, as well as by constraints imposed by the existing facility.

1.2.2.1 Mounting Hardware

The mounting hardware design was driven by the requirement to allow repeatable, nondrifting optical beam pointing/alignment to the spatial filter clippers and SBS cell. In making the trade between ease of adjustment and stability, this requirement drove the selection to very high stability approaches, although this would pose a more difficult, time-consuming initial alignment task.

Also for this reason, all highly alignment-sensitive piers will use mass stabilization, while piers used in the vacuum delay line will use a nontorquing vacuum interface technique (see Figure 1-5).

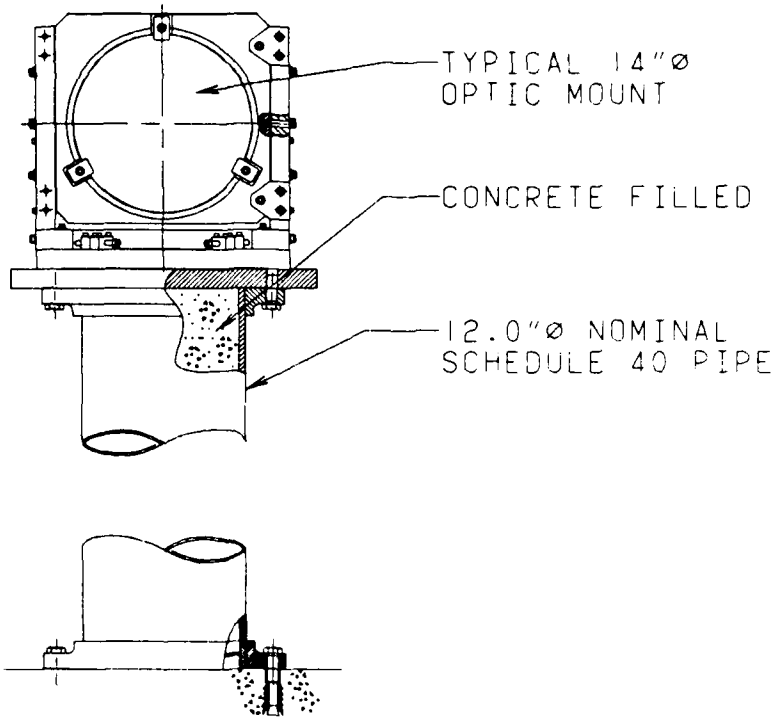

Figure 1-5. Optical pier.

1.2.2.2 SBS Cell

The SBS cell design reflects the need for maximum flexibility to allow taking a complete parametric range of relevant data. The purpose of this static cell is to function as a technology test bed, and as such it is important that the cell be well-characterized and that it provide a well-defined environment for the SBS process, over the full range of conditions at which data will be taken. This has driven the design to prevent non-deterministic uncertainties which might cloud the data, such as transient medium inhomogeneities. For this reason, the cell design includes a recirculation loop to ensure thermal homogeneity before testing.

A number of important requirements have gone into the design of the cell, primarily in the following areas:

- Medium pressure, purity, thermal uniformity
- Size required to accommodate full f/number range
- Safety

Extensive design analysis was required to demonstrate acceptable performance to the complete set of requirements, including window stress and birefringence analysis, recirculation thermal modeling and medium thermal analysis (Figure 1-6).

1.2.2.3 Beam Path Conditioning

The most important requirements on environment conditioning were the control of beam quality degradation and absorption. The optical beam path was provided with a benign, low absorptivity gaseous environment. The final design avoids the use of complex beam ducting by using the much more flexible approach of conditioned rooms for major segments of the optical train. For convenience in working in these enclosures, manufactured temperature controlled air will be used, which is free of absorptive gases such as H_2O and CO_2 (see Figure 1-7).

The longest segment of the optical path is the delay line, which allows completion of the RPCL pulse before possible contamination by returning conjugate energy. This long optical path led to the use of a vacuum duct for this piece of the optical system.

For all of the beam path conditioning enclosures, alignment and beam quality sensitivity analyses were performed, using algorithms anchored to data from similar propagation situations.

1.3 SUMMARY OF COS EXPERIMENT CONCEPTUAL DESIGN

The COS experiment will require that the HFC experiment apparatus, as described in the previous section, be used and/or modified to conduct extensively parameterized HF SBS nonlinear phase conjugation tests and to explore related phase conjugate system design approaches. The CLPCT project brought the design of this experiment to a conceptual design review (CoDR) level on key hardware, including a flowing gas SBS cell, which was brought to a concept design level to lead to meaningful optical simulation and top level aerodynamic demonstration in a COS experiment. This concept design task was particularly important in showing the compatibility of an SBL cell design with ground-based testing. Developing an experiment design compatible with accurate optical simulation of such a cell would allow simulation of continuous wave (CW) beam deposition into an SBS cell, as

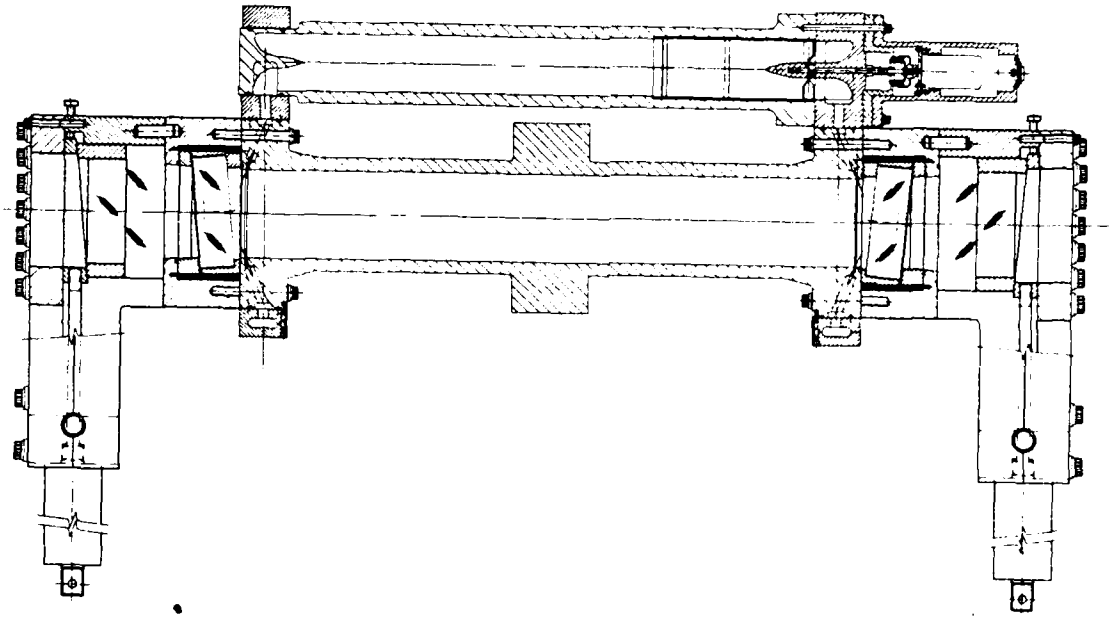

Figure 1-6. SBS static cell assembly.

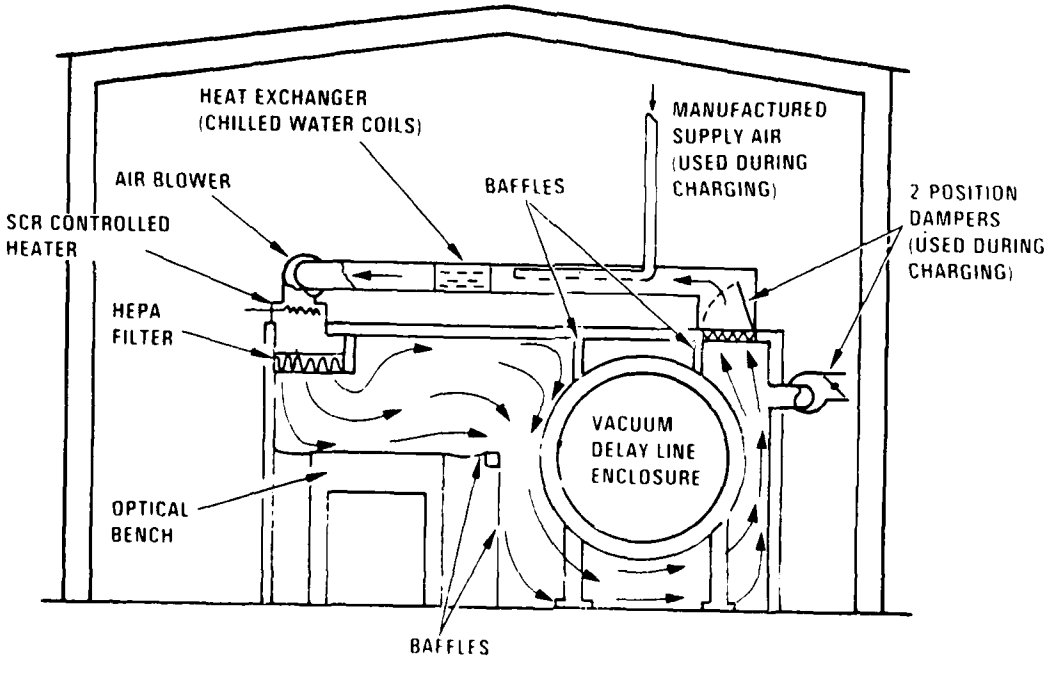

Figure 1-7. Beam path conditioning assembly design concept.

long as the pulse length is adequate to exceed the medium dwell-time in the beam. If utilized in some future experiment, the cell concept that has been developed would be within scale for a full-size, space-based weapon system.

Major requirements of this experiment include:

- Beam quality versus f/number, power, aberration parameterization
- Reflectivity versus cell pressure, phonon lifetime, f/number, aberrator
- Absorption effects
- Low SBS medium disturbance to simplify data reduction
- Two-line conjugation.

1.3.1 Phase Conjugation Subsystem

The SBS flowing cell concept design would allow use in the current estimated CW design range, in a 10-80 m/sec, 40-atm flowing cell. Since a basic requirement of cell design was compatibility with use, conceptually, in an SBL system, the design is usable at the conceptual level for a full-power SBL phase conjugation subsystem. The cell would allow operation over an f/number range of 15 to 30. The baseline cell design selected is for transverse flow, a much simpler approach than the near-sonic axial flow design previously considered as an approach to correct the SBS Doppler shift. MOPA extraction efficiency studies showed adequate extraction is possible without resorting to the much more complex axial flow design.

Extensive fluid mechanic analysis was performed to anchor the design to a CoDR level. Test cell requirements may in fact be more stringent than space-based cell requirements because medium OPD limits are driven by the need for data clarity and not by beam quality fidelity (an easier requirement level). As part of this process, thermal blooming and self-focusing requirements were reviewed to begin setting requirements on transverse flow speed and deposited power (Figure 1-8).

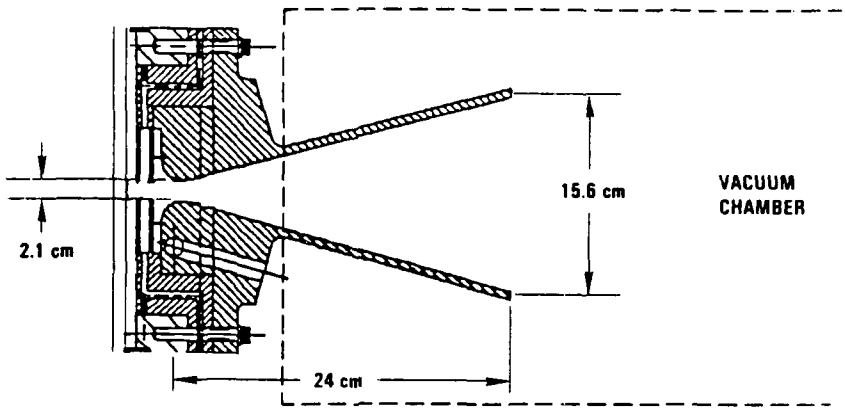

Helium supplied aerodynamic window to interface SBS cell to outside environment to prevent xenon condensation

Low index of refraction helium provides a smooth transition to a vacuum environment to reduce optical distortion

Helium exhausted by nozzle into a vacuum chamber

Helium flow rate 3 lbm/s

Figure 1-8. Aerodynamic window (conceptual design).

1.3.2 Initiation Assembly

During the CLPCT project, initiation system improvement was considered as an option to enhance the power delivery capability of the experiment. An improvement factor of more than three in ultraviolet (UV) energy over conventional design approaches was demonstrated in breadboard tests, and further UV coupling enhancement possibilities were suggested by preliminary testing of a new reflector configuration.

Although the final experiment power budget showed adequate power without this improvement, the success of this concept suggests possible future use on a stand-alone device (see Figure 1-9).

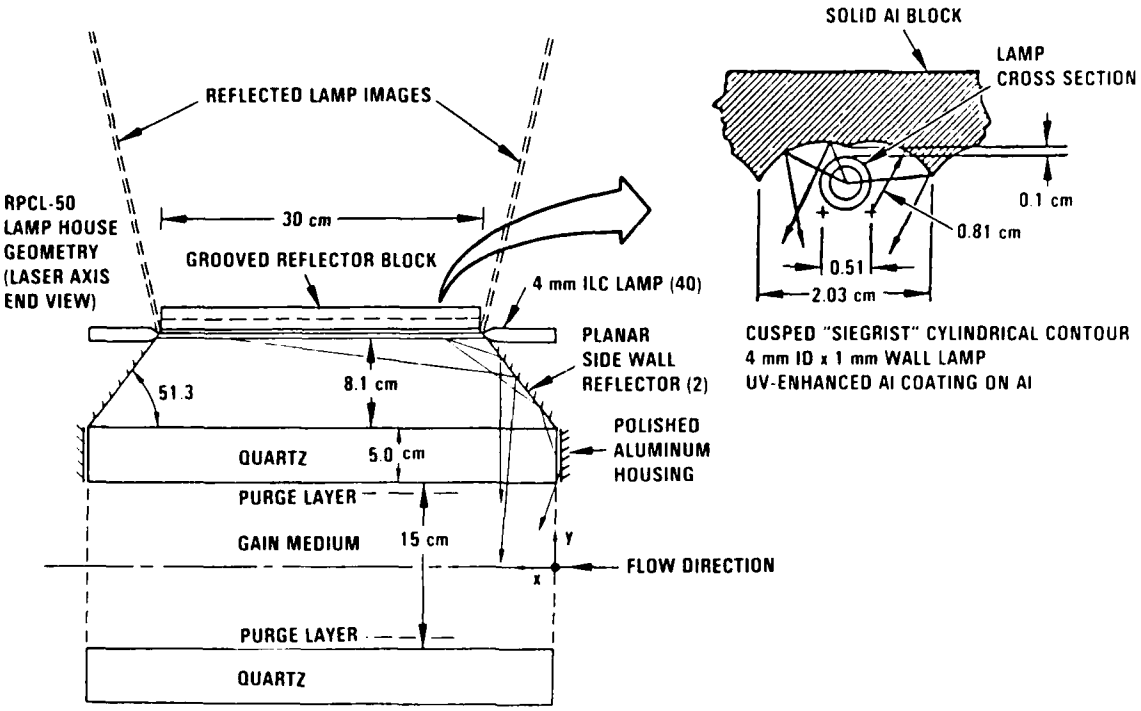

Figure 1-9. Review of existing RPCL-50 initiation assembly design.

2. OVERVIEW OF HFC FACILITY/EXPERIMENT DESIGN

2.1 OVERVIEW OF THE HFC FACILITY

2.1.1 Related TRW Capital Procurement Activities

There are three TRW capital funded activities that are related to the CLPCT and the future APACHE programs. These are summarized in Table 2-1.

TABLE 2-1. Capital Funded Activities to Prepare for APACHE Experiments.

Activity	Status	Description
Construction of APACHE facility	**100% completed**	**New building adjacent to RPCL building**
Procurement of 2 pulsed chemical lasers for use as a master oscillator	**100% completed**	**2-liter photoinitiated device from Pacific Applied Research**
Procurement of beam quality sensor	**30% completed**	**RCA IR CCD**

2.1.2 APACHE Facility

The APACHE facility, shown in Figure 2-1, consists of a prefabricated building which is approximately 130 feet long by 25 feet wide. This building was constructed on a concrete slab to the east of the existing Building 43G which houses the RPCL-50 device.

The final APACHE facility consists of a completed structural steel building which is erected on the concrete slab. Also included are a 22-ton government-furnished air conditioner, thermal insulation and provisions for electrical power.

Figure 2-2 shows the early stages of facility construction. These photographs show the excavated area, new access road, existing Building 43G, existing "cross-country" feed lines, existing steam ejector, etc.

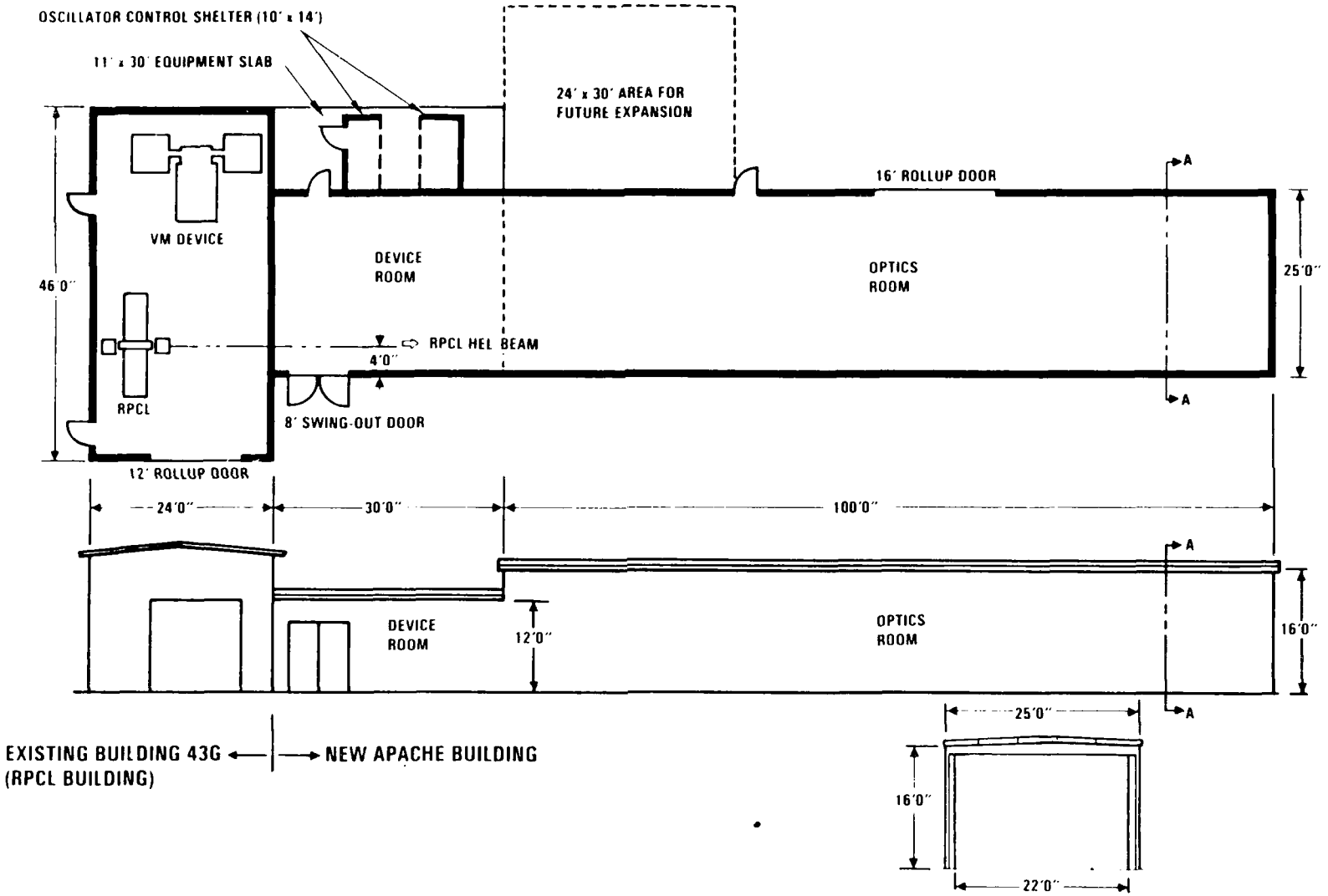

Figure 2-1. APACHE capital procurement facility.

APACHE building looking southwest

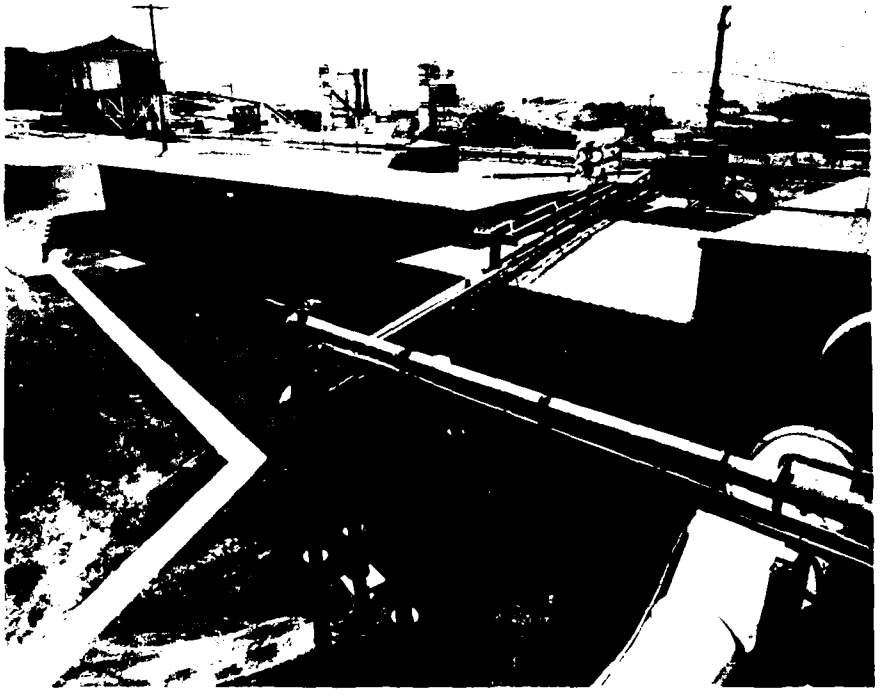

APACHE building looking southeast

Figure 2-2. APACHE facility building.

2.1.3 Pacific Applied Research (PAR) Pulsed Chemical Lasers

Two model 105 pulsed chemical laser (PCL) devices were procured with TRW capital resources from Pacific Applied Research (PAR). Each PAR device is a photoinitiated HF chemical laser consisting of the following assemblies:

- Laser head (2-liter cavity)
- Pulse power network
- Variable delay trigger circuit
- Flow control console.

These devices will be available for use as a OSC-preamp beam source (for Configuration C) or a master oscillator in the MOPA configuration, or to perform subsystem checkout tests and off-line SBS experiments.

2.1.4 Beam Quality Sensor

A 2-dimensional IR CCD camera is currently under procurement with TRW capital resources. This camera will be used to determine the far-field intensity/fluence distribution in order to measure the beam quality.

2.2 OVERVIEW OF THE HPC EXPERIMENT DESIGN

2.2.1 Objective of the CLPCT Activities for the HPC Experiment

As discussed in Section 1.1, the HF conjugation (HFC) demonstration experiment involves the use of a pulsed HF high energy laser to demonstrate phase conjugation with a static gas SBS cell. This experiment will be one of several experiments conducted under the future Advanced Phased-Array Chemical High Energy (APACHE) Laser System Program. The principal objective of the HFC experiment is to provide an early demonstration of the SBS phase conjugation process for a single line within the HF spectrum. The intent is to demonstrate single-line phase conjugation of an aberrated beam with good fidelity and high reflectivity, as well as to make the following measurements:

- Reflectivity of SBS cell
- Beam quality (both input and output)

- Line width
- Temporally resolved power, P(t)

The HFC activities within the CLPCT Program involved the design of the HFC experiment facility [to critical design review (CDR) level] and the procurement of long-lead hardware. The primary constraints which guided the design of the experimental facility were that it should use the existing 50-liter repetitively pulsed chemical laser (RPCL-50) and be compatible with the APACHE facility building shown in Figure 2-1. Design criteria emphasized design flexibility, growth potential, and applicability to the following more complex APACHE experiments (which would follow the HF experiment):

- Conjugation subsystem (COS) experiment
- Oscillator isolation (OI) experiment
- Beam combination (BC) experiment
- MOPA experiment.

2.2.2 System Description for the HFC Experiment Facility

The HFC test facility is designed to be used in several different configurations using a common set of optics. This multiplicity in design allows for maximum flexibility and cost effectiveness in the experimental set ranging from use of small commercial pulsed chemical lasers for oscillator isolation and beam combination studies, to use of RPCL as an oscillator for power scaling studies, to the possibility of configuring the small PCLs with RPCL as an amplifier for MOPA testing.

Figure 2-3 is a block diagram of the HFC facility system which shows the principal subsystems and assemblies. In its most general configuration, the laser subsystem is configured as a MOPA wherein the oscillator subsystem transmits a pulsed HF chemical laser beam to the RPCL subsystem which functions as a pulsed power amplifier. All tests, for the HFC experiment and future experiments, would use the RPCL single-pulse operating mode (i.e., nonrepetitive). The oscillator subsystem provides a single-line, linearly polarized, single transverse mode beam with sufficient power to meet SBS experiment requirements or, in the MOPA mode, assure saturation

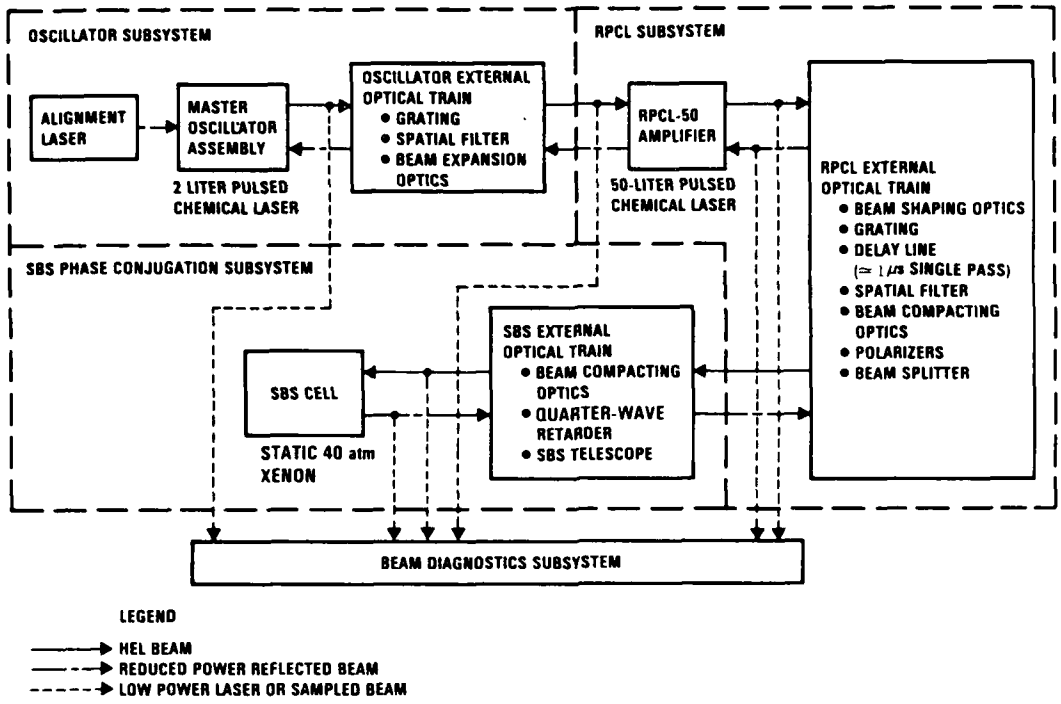

Figure 2-3. Simplified schematic of HFC experiment, showing major assemblies.

in the RPCL amplifier. In the MOPA mode, the oscillator pulse duration must exceed that of the RPCL amplifier and must be synchronized. The oscillator subsystem consists of the following assemblies:

- Alignment laser assembly. Contains a helium neon laser for oscillator cavity and external beam train alignment.
- Master oscillator assembly. Contains the PAR 2-liter PCL gain cell, cavity optics and Brewster windows for polarization control. This assembly also contains the second 2-liter PCL which can be used as a preamplifier or amplifier.
- Oscillator external optical train assembly. Contains the necessary beam shaping optics, diffraction grating (for line selection), spatial filter (for beam quality improvement) and beam expansion optics.

The RPCL subsystem provides a high energy, single-line HF beam with sufficient power to substantially exceed the SBS threshold power. The high energy laser beam from the RPCL assembly is transmitted through the RPCL

external optical train assembly to the SBS phase conjugation subsystem. The RPCL external optical train provides the necessary beam shaping optics, diffraction grating (for line selection), polarizers (for power variation) and beam splitters (to provide the diagnostics beams).

The SBS phase conjugation subsystem provides the necessary components to direct and focus the high energy beam to a high pressure static gaseous medium within the SBS cell. Thus, this subsystem contains the following two assemblies:

- SBS external optical train
- SBS cell.

Both assemblies provide for a variable f/number capability so that the effect of this parameter can be determined. The SBS medium is nominally xenon at 40 atmospheres although this pressure can be parametrically varied from 10 to 40 atmospheres.

The environmental conditioning subsystem (ECS) provides a benign environment along the beam path to minimize problems involving absorption of HF radiation, beam quality degradation/steering (caused by thermal blooming and turbulence) and gas dielectric breakdown. The ECS is comprised of the following subassemblies:

- Beam path conditioning assembly (BPCA). A large clean room type enclosure region containing atmospheric pressure, purified air (free of CO_2 and H_2O) which is recirculated to provide a transverse flow of a weakly absorbing gas. Beam ducts and small enclosures are provided at locations where the bulky clean room approach would be impractical.
- Vacuum duct assembly. A large vacuum enclosure containing dry air at low pressure (i.e., $\leq$5 torr).

The controls and instrumentation (C&I) subsystem provides controls and data acquisition for the HFC and future experiments.

The beam train for the HFC facility system design is shown schematically in Figure 2-4 and accurately in Figure 2-5. Figure 2-4 illustrates the various optical elements and identifies the subsystem. Figure 2-5 shows the actual optical layout within the APACHE building.

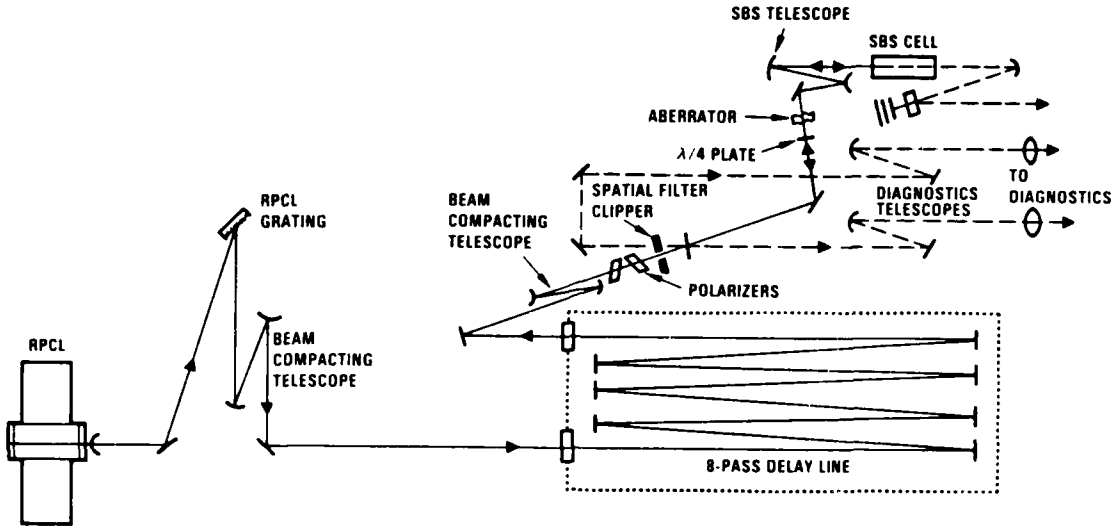

Figure 2-4. Overview of HFC system (configuration B) design with system identification.

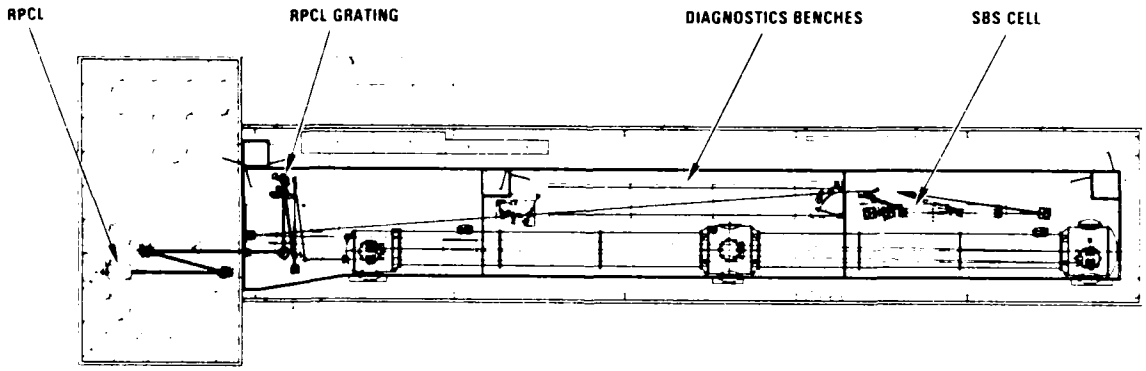

Figure 2-5. Baseline optical train (configuration B) layout for HFC experiment.

3. OPTICAL DESIGN

3.1 OPTICAL SYSTEMS ENGINEERING

3.1.1 Introduction

The major objectives of the HF conjugation optical design effort was to design an end-to-end optical train which experimentally demonstrates good phase-conjugation fidelity at HF wavelengths using the 50-liter RPCL at the Capistrano Test Site, ensure that the HFC facility will adapt to alternate configurations, and identify, specify, and order long-lead components for the optical train. Long-lead is defined to be items requiring greater than 3 months to receive.

The approach used in this task was to perform the optical design in subsystem units so that overall optical system requirements and performance budgets were met. The performance budgets included beam power, polarization, beam quality, and beam alignment. In the course of this work analytical support studies from the Phased Array Laser Systems (PALS) project were utilized to model oscillator and amplifier performance to establish derived subsystem-to-subsystem requirements.

The requirements for the HFC optical system tier down from overall end-to-end requirements to optical system interface requirements. The origins of these requirements lie in the basic requirement for good SBS conjugation fidelity, ALPHA bandwidth requirements, and the aforementioned subsystem-to-subsystem derived requirements.

3.1.2 Optical System and Subsystem Requirements Versus Capabilities

Table 3-1 summarizes the top-level optical system requirements versus capabilities. The SBS power threshold for 40 atm xenon is estimated to be 150 kW. It is expected that about three times the SBS threshold should saturate the SBS, and this is increased to a factor of 10 to ensure that the saturation curve will have, indeed, plateaued. The factor n is a classified number and represents the expected RPCL energy output in kilojoules when run as a resonator for HF operation. The good beam quality number at the diagnostics ensures that the phase conjugation process can, in fact, be maintained for a nearly unaberrated beam. Experiments under the

TABLE 3-1. HFC Optical System Requirements Versus Capabilities.

	REQUIREMENT	CAPABILITIES
o POWER TO SBS CELL	o AT LEAST 10 x SBS THRESHOLD	o 3.4n (WORST CASE) TO 35n (BEST CASE) X SBS THRESHOLD
o BEAM QUALITY AT DIAGNOSTICS	o 1.1	1.08 TO 1.12
o POLARIZATION @ SBS CELL	o GREATER THAN 95%	o 98%
o BANDWIDTH OF LASER TO SBS CELL	o LESS THAN 250 MHZ	o 50 MHZ PREDICTED
o SPECTRAL CONTENT TO SBS CELL	o SINGLE LINE P2(8)	o P(28)
o F-NUMBER	o VARIABLE F/10 TO F/50	o VARIABLE F/10 TO F/50

conjugation subsystem (COS) effort will address the problem of purposely aberrating the beam in a deterministic way. The spread in beam quality capability is due to uncertainties in the beam quality analysis and optical train. The bandwidth requirements of 250 MHz comes from ALPHA, and the predicted 50 MHz bandwidth is an estimate of what the homogeneously broadened oscillator will produce. The single line $P_2(8)$ requirement comes from a combination of being one of the stronger of the 20 or so RPCL lines, having good dispersion off the spectral separation grating, low water and CO_2 absorption, and being the strongest of the ALPHA output lines.

Table 3-2 summarizes the oscillator subsystem requirements versus capabilities for a MOPA configuration. These are derived requirements and find their origin in the Requirements and Technical Criteria Document. The output power of the oscillator must be sufficient to give total RPCL power extraction and provide a high level of ASE suppression. The details of this calculation are provided in the section on MOPA modeling. The pulse length requirement ensures that the oscillator pulse will totally enclose the amplifier gain pulse with margin for timing jitter. Oscillator spatial filters have been designed to assure that the oscillator input beam quality to RPCL is less than the expected output beam quality of RPCL run as a resonator. The intracavity Brewster windows set the linear output polarization from the oscillator which is then fixed again by the high polarization efficiency of the oscillator grating. The oscillator length

TABLE 3-2. Oscillator Subsystem Requirements Versus Capabilities.

	DESIGN ISSUE	REQUIREMENT	CAPABILITY
o OUTPUT POWER	o ASE SUPPRESSION; TOTAL RPCL POWER EXTRACTION	o GREATER THAN 50uJ/CM2	o 420 uJ/CM2
o PULSE LENGTH	o NESTING OF OSCILLATOR/ AMPLIFIER PULSE	o 1.7 uS FWHM	o 1.7 uS FWHM
o TIMING ACCURACY	o TIMING JITTER OF MO PULSE	o LESS THAN 0.1 uSEC	o COMPLIES
o BEAM QUALITY	o OSCILLATOR SPATIAL FILTERS	o LESS THAN 1.5	o 1.42
o POLARIZATION	o BREWSTER WINDOWS/GRATING	o GREATER THAN 90% HORIZONTAL	o 94 % HORIZONTAL
o BANDWIDTH	o OSCILLATOR BANDWIDTH	o LESS THAN 250 MHZ	o 50 MHZ PREDICTION
o OUTPUT SPECTRAL CONTENT	o WAVELENGTH SELECTION BY GRATING	o SINGLE LINE P2(8)	o P2(8)
o SINGLE TRANSVERSE MODE	o EQUIVALENT FRESNEL NUMBER	o HALF-INTEGER	o 8.5
o ALIGNMENT WITH RPCL	o ISOLATION OF OSCILLATOR FROM ASE PROPAGATING BACKWARD FROM AMPLIFIER	o ANGULAR SEPARATION	o COMPLIES
o ALIGNMENT AT SLITS	o POWER THROUGHPUT	o 0.5 LAMBDA/D	o 0.3 LAMBDA.D

and magnification have been chosen to give high single-transverse-mode discrimination (half-integer equivalent Fresnel number) and good oscillator power extraction (Rigrod curve). Both forward and backward propagating ASE from the RPCL cavity is angularly separated from the line-of-sight beam train by injecting the oscillator beam at a small angle with respect to the optic axis formed by the RPCL mirrors. Finally, the oscillator beam is aligned at the oscillator slits to within one-half a spot size to maintain adequate power throughput.

Table 3-3 shows the RPCL/SBS phase conjugation optical subsystem requirements versus capabilities. The first six requirements have previously been discussed. The RPCL cavity windows and mirrors have been designed to give maximum HF transmission, maximize usable gain volume, and maintain an output beam quality less than the predicted beam quality for the RPCL as a resonator. The delay line length was chosen to temporally

TABLE 3-3. RPCL/SBS Phase Conjugation Optical Subsystem Requirements Versus Capabilities.

	DESIGN ISSUE	REQUIREMENT	CAPABILITY
o POWER TO SBS CELL	o POWER EXTRACTION EFFICIENCY; EXTERNAL OPTICAL TRAIN POWER TRANSFER	o AT LEAST 10 X SBS THRESHOLD	o 3.4n (WORST CASE) TO 35n (BEST CASE) X SBS THRESHOLD
o PULSE LENGTH	o FLASHLAMP/GAS MIXTURE SETTINGS	o TO MEET POWER REQUIREMENT FOR AT LEAST 1uS	o COMPLIES
o BEAM QUALITY AT DIAGNOSTICS	o SPATIAL FILTERS	o 1.1	o 1.08 TO 1.12
o POLARIZATION AT SBS CELL	o RPCL POWER POLARIZERS	o GREATER THAN 95%	o 98%
o OUTPUT SPECTRAL CONTENT	o RPCL GRATING	o SINGLE LINE P2(8)	o P2(8)
o CAVITY WINDOWS	o MAXIMUM HF TRANSMISSION; NO SIGNIFICANT DEGRADATION OF RPCL BEAM QUALITY; MINIMIZE STRUT OBSCURATIONS	o TO MEET POWER REQUIREMENTS	o COMPLIES
o CAVITY MIRRORS	o MAXIMIZE USEABLE GAIN VOLUME; NO UNCORRECTABLE CONTRIBUTION TO BEAM QUALITY; ALLOW OFF-AXIS OSCILLATOR BEAM INJECTION	o TO MEET POWER/ BEAM QUALITY REQUIREMENTS	o COMPLIES
o DELAY LINE	o TEMPORAL SEPARATION OF OUTGOING FROM RETURN PULSE	o AT LEAST 2uS	o COMPLIES
o LESS THAN 25 JOULES/CM2	o 0.5n J/CM2	o RETURN POWER FLUENCE AT OSCILLATOR FRESNEL CORE	o MINIMIZE COMPONENT BIREFRINGENCE
o 10% MODE WIDTH + 1.5 MM FOR TRANSVERSE DISPLACEMENT (NEAR-FIELD), 0.5 CM (FAR-FIELD) @ SBS CELL	o COMPLIES	o EXTERNAL TRAIN ALIGNMENT	o ALIGNMENT
o LESS THAN 1.1 : 1	o 1.1:1	o BEAM ASPECT RATIO	o ASPECT RATIO TO SBS EXTERNAL OPTICAL TRAIN
o SPATIAL SEPARATION OF ASE	o COMPLIES	o ASE SEPARATION	o OFF-AXIS INJECTION OF OSCILLATOR BEAM TO RPCL
o VARIABLE F/10 TO F/50	o F/10 TO F/50 FOCAL LENGTH	o SBS TELESCOPE FOCAL LENGTH	o SBS TELESCOPE
o 90 DEGREES/PASS	o 90 DEGREES/PASS	o RETURN BEAM	o QUARTER-WAVE ISOLATION

isolate any return pulse from reentering the RPCL cavity before the forward propagating pulse had sufficient time to escape the cavity. Since perfect power isolation of the oscillator is difficult because of residual component birefringence, it was then necessary to maintain a maximum fluence level allowable back to the Fresnel core of the oscillator. The beam aspect ratio was kept low to avoid design of an anamorphic SBS telescope to account for axially different focal planes in the horizontal and vertical planes. Finally, return beam isolation was accomplished by the familiar technique of rotating the linear polarization of the return propagating beam by 90 degrees relative to the forward propagating beam via a quarter-wave retarder and using a polarizer to discriminate the polarization.

3.1.3 HFC Configurations

The optical facilities have been arranged to accommodate four basic configurations:

- Configurations A, D = master oscillator power amplifier to SBS cell
- Configuration B = RPCL resonator to SBS cell
- Configuration C = PAR oscillator to SBS cell.

The only difference between configuration A and D is that A has slit spatial filters at line foci whereas configuration D has a low Fresnel number spatial filter. These configurations will allow maximum flexibility during the integration and test period. First, configuration C will be integrated and tested to give initial SBS data. This will be followed by integration and testing of configuration B for full parametric SBS testing. Finally, the option of configuration A will be available for future tests.

Configuration D: MOPA to SBS Cell

Configuration D is shown in Figure 3-1. As discussed in the Requirements and Technical Criteria Document, each subsystem is further subdivided into assemblies. The oscillator subsystem is comprised of the following assemblies:

- Alignment laser assembly
- Master oscillator assembly
- Oscillator external optical train assembly.

The oscillator subsystem provides as its output, a linearly polarized single pulse, moderate power beam at a single HF spectral line. All assemblies are designed to satisfy the input beam requirements dictated by the RPCL subsystem which acts as a pulsed power amplifier. The principal oscillator subsystem requirements are that the input beam to the RPCL have adequate power to extract fully saturated output power from the RPCL and have very good beam quality.

As shown in Figure 3-1, the baseline oscillator uses a single 2-liter photoinitiated pulsed chemical laser (purchased from Pacific Applied Research) which provides the gain medium for the oscillator assembly resonator unit. Two intracavity Brewster windows reside upbeam of the gain generator and provide 95 percent polarization to the oscillator output beam. The resonator is configured to be an on-axis annular unstable resonator. The beam then enters into the oscillator external optical train assembly by reflecting off a high-efficiency grating which line selects the $P_2(8)$ line. The spectrally spread beam is then routed to a focusing cylinder which directs the beam into a vacuum duct where the beam passes through a high energy spatial filter. Clippers are placed at the line foci of the cylindrical telescopes which both spatially and spectrally filter the beam, thus providing enhanced beam quality and line selection, respectively. The beam then moves on to a beam shaping telescope that provides a beam that overfills the rectangular RPCL input aperture dimensions.

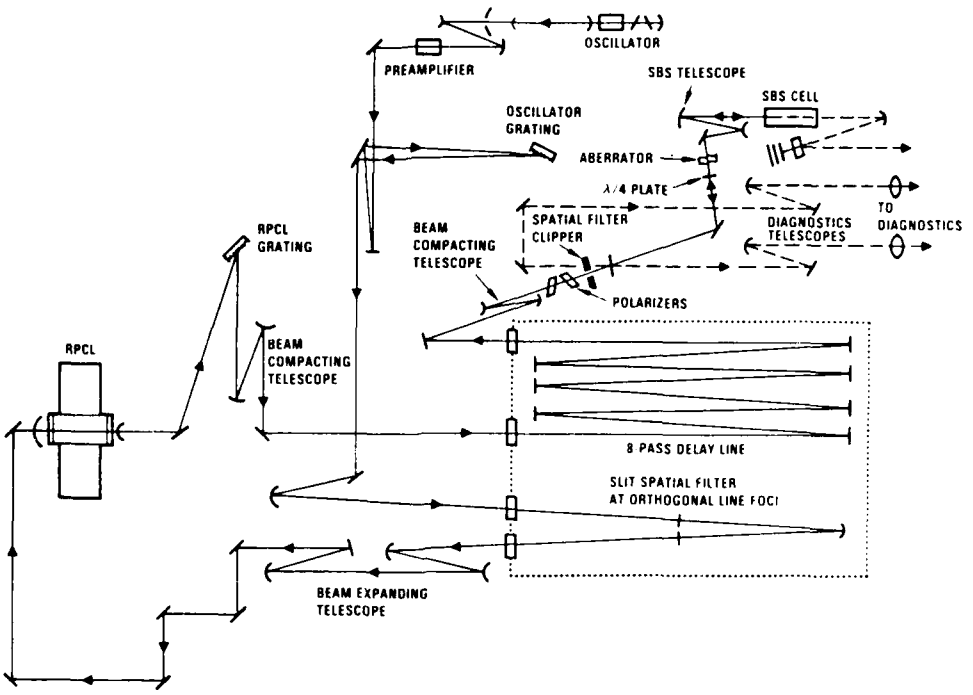

Figure 3-1. Configuration D: MOPA to SBS cell.

In order to protect the oscillator windows from any damage due to residual return beam from the SBS process which would demagnify on returning to the Fresnel core, the oscillator mirrors are spaced far enough apart such that the Fresnel core diameter is sufficiently large so that the fluence is well-below the oscillator window damage threshold.

The RPCL subsystem contains the MOPA power amplifier (i.e., the 50-liter repetitively pulsed chemical laser [RPCL-50] device) and the downbeam external optical train. The RPCL-50 is an existing photoinitiated, repetitively pulsed HF chemical laser which will be used in a single-pulse mode for the HFC experiment. The RPCL subsystem is composed of the following assemblies:

- RPCL amplifier assembly
- RPCL external optical train assembly.

The RPCL subsystem receives, as its input, the beam from the oscillator subsystem which is then amplified and injected into the SBS phase conjugation subsystem. It provides a means to extract the beam for some of the diagnostics purposes, and provides isolation for the RPCL device from potentially damaging return pulses. It also separates and dumps unwanted amplified stimulated emission (ASE) coming out of the RPCL amplifier.

In order to separate ASE from the amplified $P_2(8)$ pulse, the beam from the oscillator subsystem is injected at 1 degree with respect to the RPCL optic axis. The cavity is designed such that the $P_2(8)$ line traverses the cavity in five passes.

Referring to Figure 3-1, it is seen that the output beam from the RPCL amplifier enters the external optical train assembly, where an amplifier grating is used to spectrally spread any ASE that is collinear with the $P_2(8)$ line. The beam then moves into a long vacuum delay line which time-delays the return SBS pulse sufficiently such that the RPCL cavity has sufficient time to complete its pulse before any residual power due to birefringence reenters the RPCL cavity. In addition, the long propagation path yields a beam with a very low Fresnel number (~0.25) which is spatially filtered downstream resulting in a beam of excellent beam quality (~1.01). The delay line relay mirrors are high reflectivity coated and the CaF_2 delay line windows are anti-reflective coated in order to maximize energy throughput. The beam then moves on to a polarizer which consists of two CaF_2 windows set at the Brewster's angle to form a power controller. The forward and return propagating beam is extracted for diagnostics by means of a beam splitter.

The purpose of the SBS phase conjugation subsystem is to direct and focus the high energy beam to a high pressure gaseous medium within a static SBS cell. Xenon has been selected as the SBS medium. The SBS process requires high intensity light as input to the SBS cell in which light from the input laser is backscattered by acoustic waves resulting from optically induced electrostriction. SBS phase conjugation results when the phase information of the pump beam is transferred into an intensity grating either by focusing in the SBS medium or by placing the SBS medium in a multimode waveguide. In these cases, it has been shown

that the gain is largest for the Stokes component (generated from acoustical noise) that is the conjugate of the input beam. Thus, an SBS cell is a nonlinear optical element that will produce a reflected beam which is the phase conjugate of the input beam.

The SBS phase conjugation subsystem contains the following assemblies:

- SBS external optical train assembly
- SBS cell assembly.

The SBS phase conjugation subsystem takes the input beam from the RPCL subsystem, focuses it into the SBS cell, and directs the beam transmitted through the SBS cell into an appropriate set of diagnostics.

The focal length of the SBS telescope is adjustable between an f/number range of 10 to 50. This is to be done by five sets of different f/number telescopes. A quarter-wave retarder is used to rotate the polarization of the SBS reverse propagating beam by 90 degrees with respect to the forward propagating beam so as to achieve beam isolation at the power polarizer in the RPCL subsystem. An insertable aberrator plate allows future experiments to study effects of gross beam aberrations. Because the SBS cell entrance window is expected to introduce significant spherical aberrations in the beam, there is also provision for a phase corrector plate.

Static SBS Cell Assembly

The static SBS cell assembly consists of all hardware required to allow the phase conjugation process to proceed in a pulsed mode. The cell consists of a variable length metallic pressure vessel with windows at each end for the input/conjugated beam and transmitted beam, respectively. The windows are long-lead hardware items, while all other components are not long lead. The cell includes provisions for (1) media filling and venting, (2) maintaining thermal homogeneity, and (3) monitoring the temperature, pressure and potential dielectric breakdown of the media. The cell assembly also includes components to evacuate and backfill the cell with media while controlling levels of particulate and trace gas contamination.

Configuration B: RPCL Resonator to SBS Cell

Configuration B, is shown in Figure 3-2. This configuration will be the primary system used for all experiments involving power scaling issues (e.g., threshold, aberrator, f/number studies). The optical train resembles configuration D. A noteworthy difference is the addition of Brewster plates in the RPCL resonator which polarizes the output beam from RPCL.

Configuration C: Oscillator to SBS Cell

Configuration C, shown in Figure 3-3, takes the oscillator beam and routes the single spectral line beam either through the delay line, or directly to the SBS subassembly via an optional delay line bypass.

Within the framework of the three configurations are subsystem assembly variations. These variations are listed in Table 3-4. The use of these variations will be determined by subsystem performance, schedule, and possible cost reduction. The oscillator subsystem can be operated in either a single-head or dual-head mode, relative to the number of 2-liter PCL heads. In the event that the power throughput is found to be inadequate, the single-head oscillator will be replaced with an oscillator/preamplifier plus intermodule telescope. Figure 3-3 illustrates this dual-head configuration. The purpose of the telescope, as detailed in Section 3.3, is to propagate the beam from the first oscillator module an equivalent 40 meters before entering the second module for preamplification so as to partially diffractively fill the beam obscuration. In the RPCL subsystem, the baseline amplifier assembly is a five-pass RPCL assembly using six CaF_2 windows. The amplifier windows are considered long-lead items. Finally, the assembly for beam quality cleanup is to use focused spatial filtering within the delay line. An early task in the APACHE project will be to study configuration D which is a low Fresnel number alternative which propagates the beam through the delay line without focusing and spatially filters the beam external to the delay line.

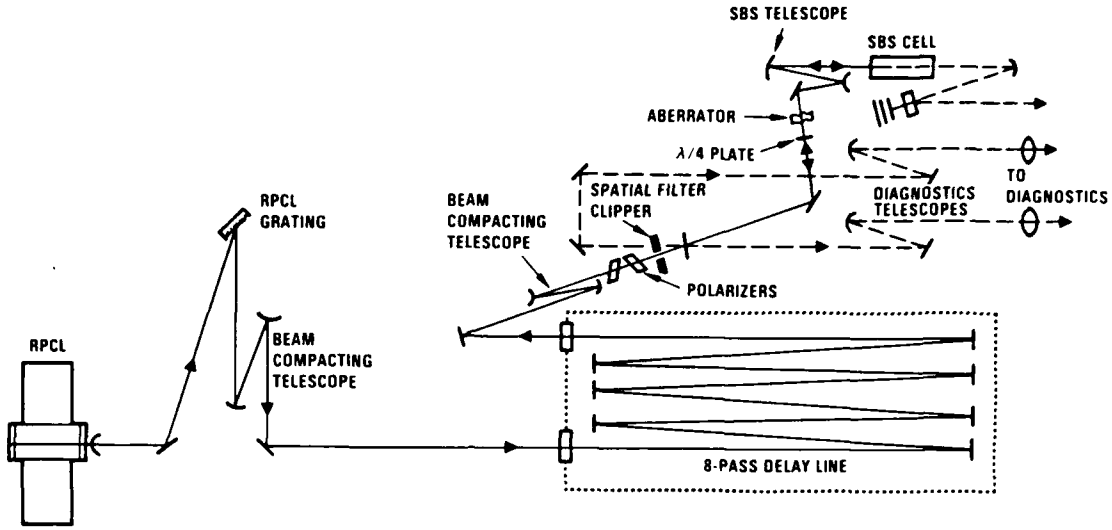

Figure 3-2. Configuration B: RPCL resonator to SBS cell

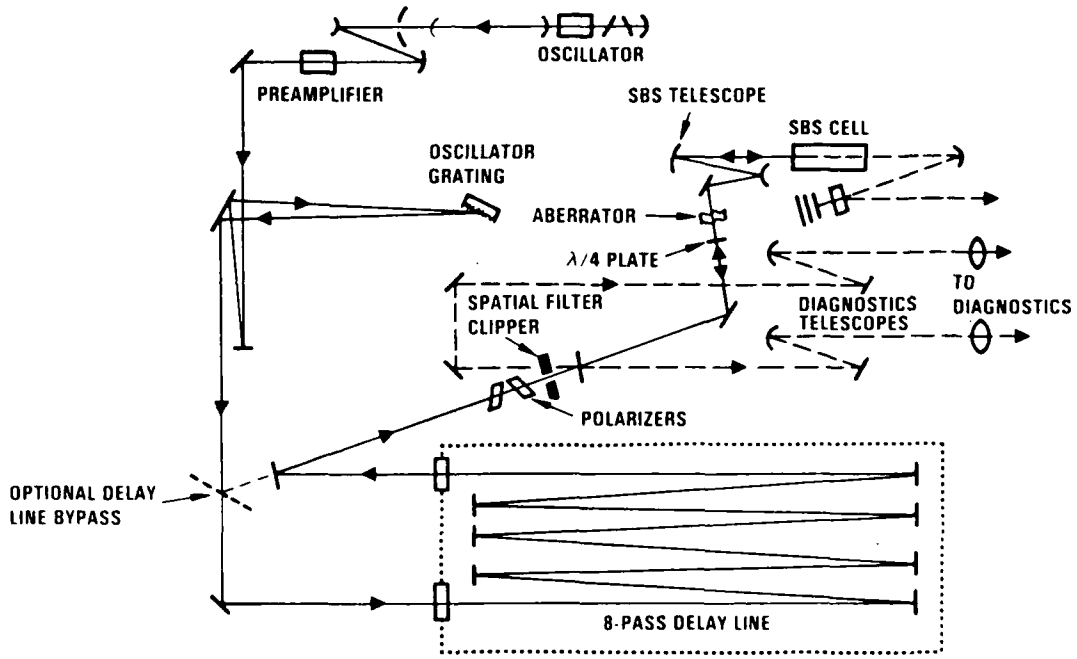

Figure 3-3. Configuration C: Oscillator to SBS cell.

TABLE 3-4. Subsystem Assembly Variations.

Subsystem	Baseline Assembly	Variation
Oscillator subsystem	**Single-head oscillator**	**Oscillator/preamplifier plus telescope**
RPCL Subsystem	**Three-pass RPCL plus four equal sized CaF_2 windows (MOPA only)**	**Five-pass RPCL plus six existing CaF_2 windows (MOPA only)**
	Low Fresnel number Spatial filtering	**Focused spatial filtering**

3.1.4 Long-lead Hardware

Long-lead hardware is defined as components requiring longer than 3 months to procure. Table 3-5 shows the list of long-lead items. The post-delay line optics are required to have excellent surface figure since they reside downstream to the clipper spatial filter. The quarter-wave retarder is a MgF_2 piece designed for $P_2(8)$. The RPCL delay line windows are CaF_2. The diagnostics Pockels cell is lithium niobate. The remaining components are CaF_2.

3.1.5 Summary

An optical system has been designed which complies with the Requirements and Technical Criteria Document for the CLPCT HFC and COS experiments. The optical system has been designed into three nested configurations for optimal flexibility in experiments. Variations of the optical assemblies have been designed in to allow for upgrading performance, adapting to component delivery schedules, and possible cost reduction. Finally, long-lead hardware has been identified with schedules for delivery currently being detailed.

TABLE 3-5. Long-Lead Hardware (≥3 Months).

Oscillator Subsystem	RPCL Subsystem	SBS Subsystem	ECS	Diagnostics Subsystem
Brewster windows	RPCL windows	SBS windows	Oscillator vacuum windows	Pockels cell
	RPCL polarizers	One-quarter-wave retarder	RPCL vacuum windows	
	Beam splitters			

3.2 MASTER OSCILLATOR POWER AMPLIFIER (MOPA) MODELING

3.2.1 Introduction

The objectives of the MOPA modeling were threefold:

1. To set the master oscillator injection level to ensure that all the RPCL power in the $P_2(8)$ line is extracted and that ASE in this line is suppressed

2. To ensure that the pulse length of the master oscillator overlaps the gain of the RPCL amplifier

3. To ensure that there is sufficient energy from the $P_2(8)$ line of the RPCL to achieve SBS threshold.

There were several analytical tools used in the MOPA modeling. These included the SOSHF kinetics code, the PSTAR amplifier code and the LFCM amplifier code. These codes are described below.

The SOSHF code was used as a tool to determine the properties of both the oscillator and amplifier medium. It is a time-dependent kinetics/laser model with a nonequilibrium rotational level model. It was modified to provide information about small signal gain, saturation flux and stimulated emission cross section versus time for input into the amplifier models. It was also run purely as an oscillator model to predict the performance of the PAR oscillators.

The PSTAR amplifier model was used for preliminary determination of injection requirements. It is a one-dimensional, steady-state amplifier model which includes both energy extraction and amplified spontaneous emission (ASE). The code had been developed exclusively for XeF. It was modified to be a general amplifier code with inputs of small signal gain, g_o, saturation flux, I_{sat}, stimulated emission cross section, σ, photon energy, $h\nu$, and Einstein A coefficient.

The LFCM amplifier code was used for some runs and also to anchor the PSTAR code. This code is a two-dimensional amplifier code with a more sophisticated geometry. The code is again a steady-state code. It has three possible gain models. The simplest is a g_o, I_{sat} gain model. It also has provision for two- and three-level gain models which require inputs of pumping and quenching rates of the upper and lower levels which must be derived from more detailed kinetics models. The g_o, I_{sat} gain model was used for the HF calculations because of difficulties in fitting the SOSHF kinetics code to the LFCM format. Because of the two-dimensional geometry, the ASE model in LFCM is more detailed than in the PSTAR code.

Some effort was spent in establishing the accuracy of the SOSHF code, especially as concerns its predictions of single-line performance. The major difficulty in establishing code accuracy was the lack of detailed line-by-line data in pulsed HF. Much of the data in the literature gives only total output energy. Most data on spectral distribution have been obtained from film burns which give very qualitative estimates. There is also uncertainty in the initiation fractions for specific experiments of interest. These fractions are often estimated, making model comparison more difficult.

The main data available for comparison come from AVCO (References 1 through 3), Aerospace Corporation (Reference 4), and Boeing (References 5 and 6).

3.2.2 Discussion

Figure 3-4 shows plots of experimental energies in J/liter versus $P_{F_2}\ F/F_2(\alpha_{th})^{1/3}$ where P_{F_2} is the pressure of fluorine in torr, F/F_2 is the fluorine dissociation fraction and and $\alpha_{th} = 1/L\ R_o R_L$ and L is the cavity length and R_o and R_L are mirror reflectivities. Inclusion of the

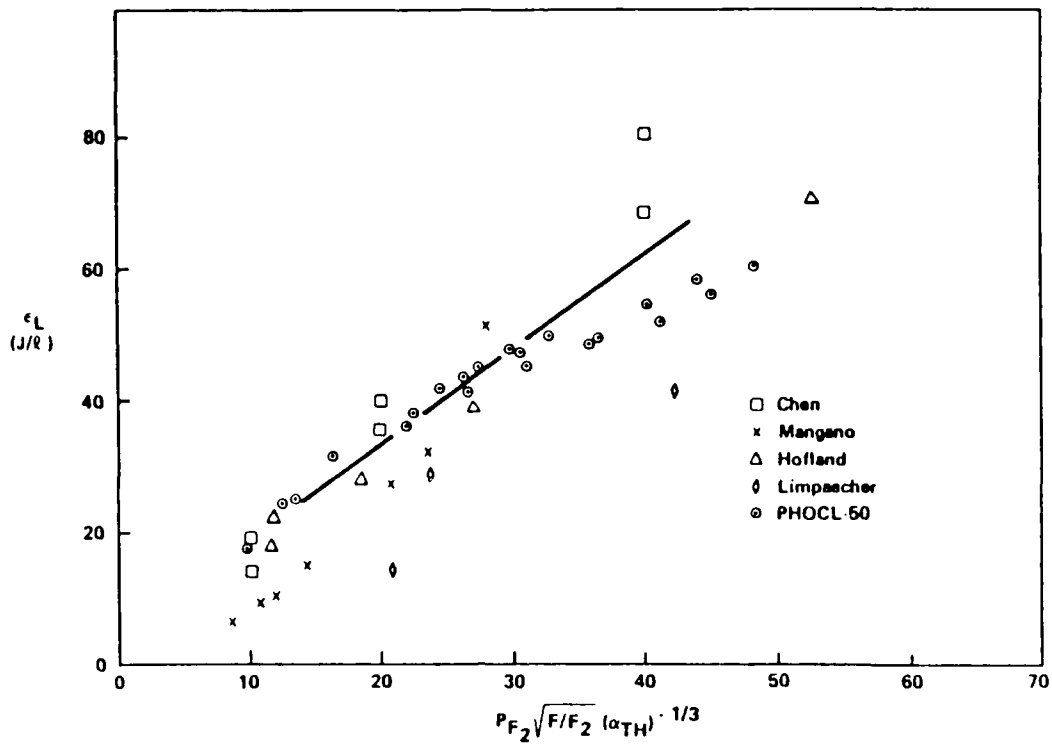

Figure 3-4. Summary of HF experimental data.

threshold energy factor allowed all experimental data to fall on a single curve. The SOSHF code was run for some of the data in the figure. It tended to overpredict the total pulse energy results by about 30 percent. However, it did substantiate the generally accepted scaling laws.

$$E_p \propto P_{F_2} F/F_2$$

and

$$\tau_p \propto 1/E_p$$

Measured pulse durations from the reference cited above are shown in Figure 3-5. One point of interest is that the pulse length can change as a function of laser outcoupling fraction which is related to the degree of gain saturation in the laser. Extrapolation of this result to an amplifier implies that the amplifier could have a longer pulse than the oscillator.

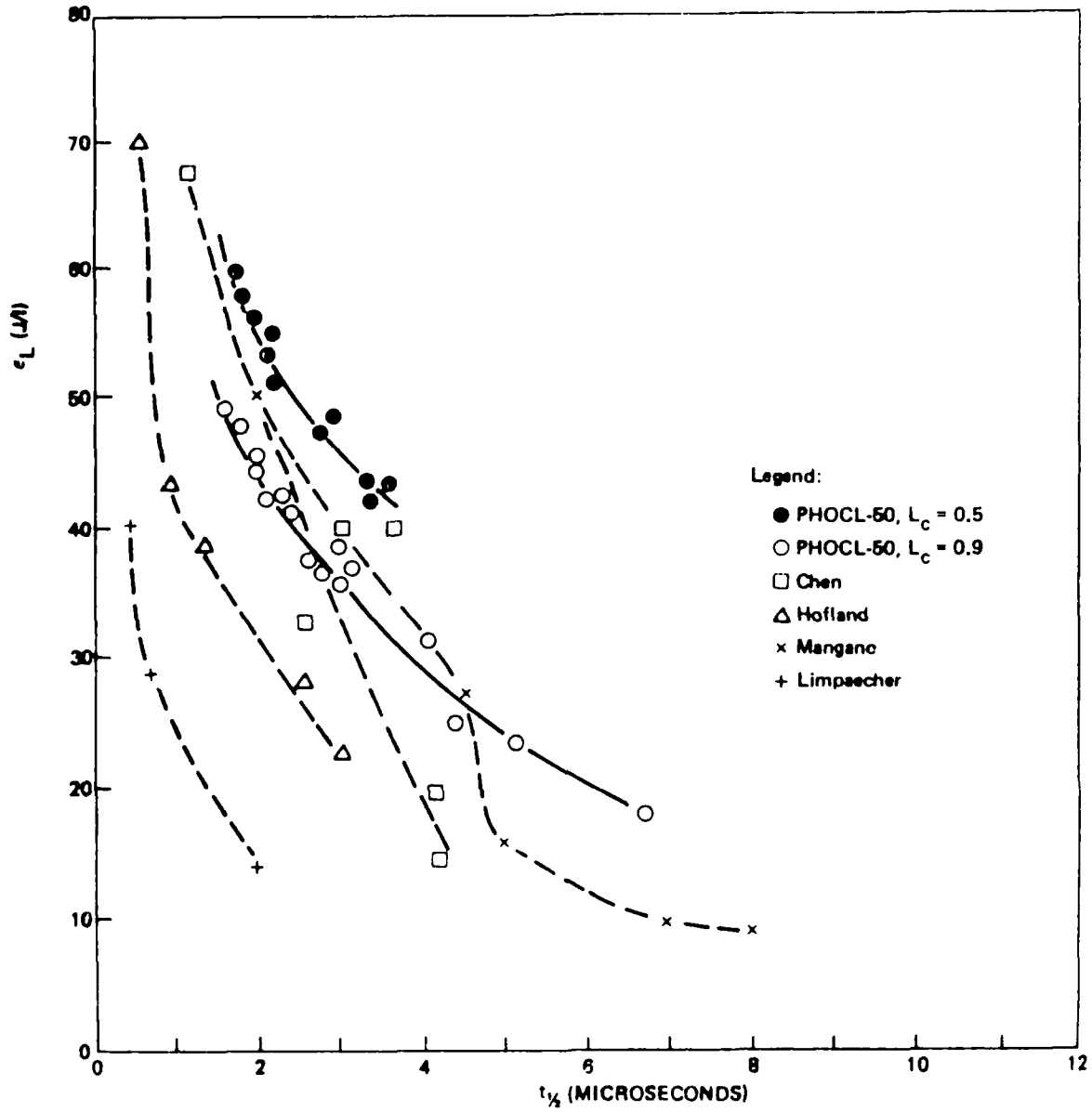

Figure 3-5. Measured pulse duration (FWHM) for pulsed HF lasers.

This is because gain at the beginning and end of a pulse, which is needed to reach lasing threshold in an oscillator, can be extracted by an amplifier.

The only available data where line-by-line temporal behavior was reported was in the previously cited AVCO report. In this report

oscillograph traces giving the intensity versus time behavior of approximately 40 lines in the HF spectrum were published.

An attempt was made to set up the SOSHF kinetics code to model the AVCO experimental condiitons to compare pulse lengths. These were:

F_2 = 4%

H_2 = 4%

He = 92%

Pressure = 1 atmosphere

Cavity length = 50 cm

Mirror reflectivities = 95%, 10%

The flashlamp pulse shape was digitized using an experimental trace appearing in the report. The major uncertainty in the experiments was the F/F_2. AVCO had used a diagnostic based on HCl absorption to measure the initiation. However, Boeing has attempted to correlate the total pulse energy from AVCO's experiments with other existing HF data and found that it was inconsistent. Boeing concluded that AVCO had an error in their F/F_2 diagnostic that resulted in a factor of 4 too low F/F_2. Thus, AVCO reports an F/F_2 of $(8 \pm 2) \times 10^{-3}$. Applying Boeing's correction factor makes F/F_2 = $(3.2 \pm 0.8) \times 10^{-2}$.

Code runs were performed with F/F_2 of 0.01, 0.03, 0.04 and 0.05. Two factors were compared, the pulse turn-on time and the full width at half maximum (FWHM) of the pulse. The best fit to the experiments was achieved with F/F_2 of 0.03. Some comparisons of the FWHM are shown below:

	Pulse Width (FWHM) (μsec)	
Line	Experimental	Code Prediction
$P_2(7)$	1.5	1.3
$P_2(8)$	1.2	1.05
$P_2(9)$	0.9	0.8

The above table shows that the code consistently underpredicts the pulse length for the set of experiments that were modeled but tends to predict the FWHM to within about 20 percent. There were some discrepancies in the detailed time histories of each line as predicted by the code and measured experimentally. Howver, the agreement was quite good considering the uncertainty in F/F_2 and the assumptions made in the code.

The above comparison shows that the code is a valid tool to use in guiding the experiemntal design and that it can be used to determine the feasibility of matching pulse lengths on a master oscillator with an amplifier. However, because of uncertainties in the experimental conditions, especially as regards F/F_2, it will be necessary to perform experiments on the PAR when it arrives to determine the exact pulse duration of the spectral line used.

A limitation of currently existing pulsed HF data is the lack of any single-line gain measurements. Consequently, even though the code calculates small signal gain and saturation flux, it cannot be anchored to any available experimental data.

The SOSHF kinetics code was run to determine the expected gain for the RPCL amplifier. A standard mixture of 20 percent F_2, 5 percent H_2 and 75 percent He was assumed. A plot of the calculated small signal gain of the $P_2(8)$ line versus time is shown in Figure 3-6. This plot shows that the average gain is about 0.2 cm^{-1} for this line. The saturation flux was also calculated and found to be fairly constant at about 25 kW/cm^2. Also shown in Figure 3-6 is a plot of a $P_2(8)$ oscillator pulse for a mixture of 10 percent F_2, 2 percent H_2 and 88 percent He. The plot shows that the oscillator pulse can be tailored to overlap the entire RPCL temporal gain. Fine adjustment of gas mixture and initiation level can be used for temporal adjustment of the oscillator pulse.

An additional oscillator issue addressed by the SOSHF kinetics code was the dependence of the $P_2(8)$ output on outcoupling fraction. A Rigrod curve plotting output power in the $P_2(8)$ line versus cavity outcoupling fraction is shown in Figure 3-7. The code indicates that the energy in the $P_2(8)$ line is relatatively constant with outcoupling, whereas the total power shows a substantial drop at both high and low outcoupling fractions.

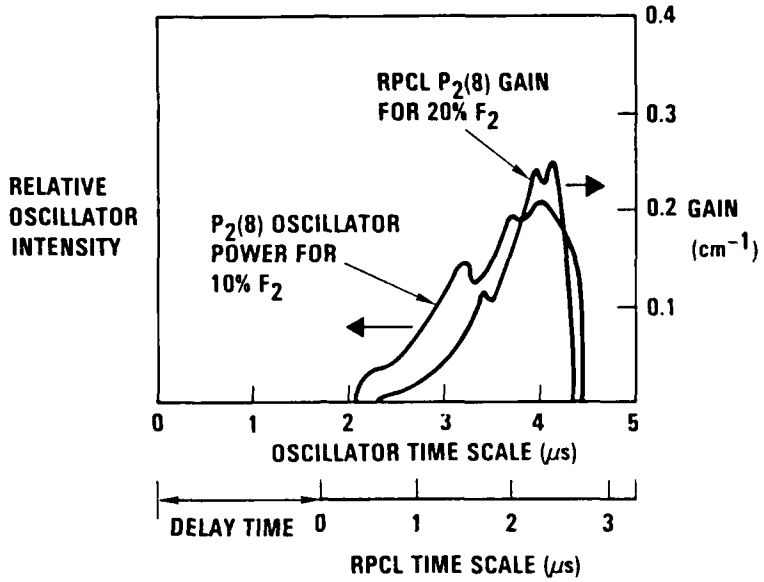

Figure 3-6. Temporal profiles of RPCL gain and oscillator output pulse.

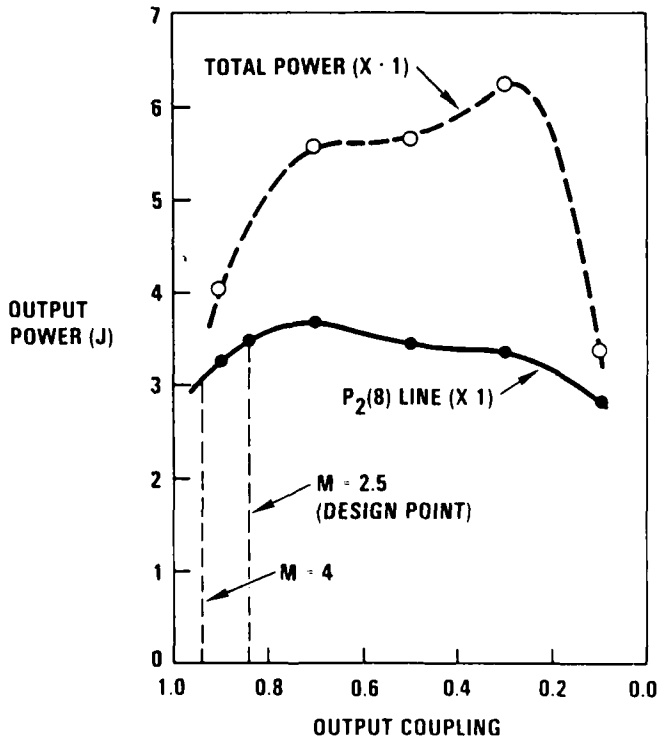

Figure 3-7. Rigrod curve for $P_2(8)$ line energy.

A design point with an outcoupling of 0.18 (magnification of 2) was chosen for the oscillator design. The plot in Figure 3-6 used this magnification.

Once the parameters for small signal gain and saturation flux were set by the kinetics code, an amplifier analysis was performed to determine the injection level needed to lock the RPCL amplifier and to suppress ASE. The amplifier parameters used were

$$g_o = 0.20 \text{ cm}^{-1}$$

$$I_{sat} = 25 \text{ kW/cm}^2$$

$$A = 194 \text{ sec}^{-1}$$

$$\sigma = 1.6 \times 10^{-16} \text{ cm}^2$$

The PSTAR amplifier code was used for the initial analysis. Later, the LFCM amplifier code was run to verify the PSTAR predictions. Both codes predicted the same MOPA output power shown in Figure 3-8. The ASE predictions of the two codes differed slightly, as shown in the two lower curves in Figure 3-8. However, the agreement between the codes was very good.

Because there is so little experimental data available to anchor any ASE code, a possible error of a factor of five in the ASE code results was assumed in making recommendations of the oscillator power required in the $P_2(8)$ line to lock the RPCL amplifier. When this assumption was made, it was recommended that from 30 to 50 W/cm^2 of oscillator input power would both allow efficient RPCL extraction and suppress ASE in that line.

3.2.3 Concluding Remarks

An unanswered question is how the time-dependence of the gain will affect the extration efficiency. The amplifier codes used were steady-state codes and could not predict the effects of the gain and saturation flux changing with time during the pulse. A range of small signal gains was analyzed indicating that the energy could be extracted over most of the pulse. However, a true time-dependent amplifier analysis was not performed.

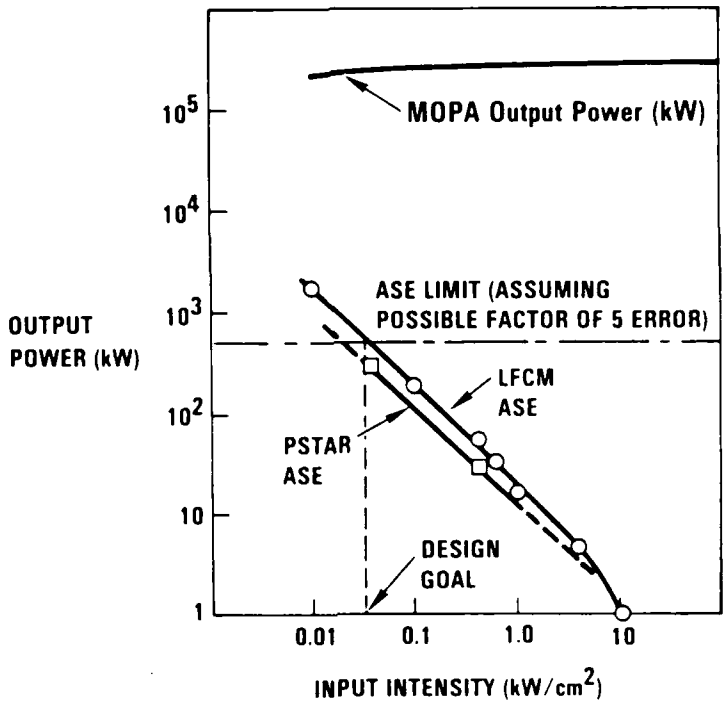

Figure 3-8. Results of amplifier analysis showing required input intensity.

An unanswered issue is how much energy will be extracted in the $P_2(8)$ line in the amplifier configuration compared to what would be extracted from an oscillator. The amount of ASE on the other lines may influence this. For example, if there is no ASE output on the lines feeding the upper level, $P_3(7)$, or depleting and lower level, $P_1(9)$, a bottlenecking in the lower level could occur and lead to less energy extraction. However, other kinetic processes could add to the upper laser level, compensating for this effect. In fact, oscillator experiments, done by Rolf Gross at Aerospace and Wayne Whitney at NRL, which have a grating in the cavity, allowing oscillation only on the $P_2(8)$ line, show more energy in this line than in a multiline oscillator. On the other hand, if the ASE on adjacent lines is almost equivalent to the energy in the multiline oscillator, the amplifier energy from the $P_2(8)$ line could be compared to the oscillator. Slightly more energy may be expected due to more efficient extraction at the beginning of the pulse. The ideal situation would be to have the

master oscillator lock the $P_3(7)$, $P_2(8)$, and $P_1(9)$ lines to ensure feeding of the upper level and depletion of the lower level. Joe Hough looked at this type of situation in an oscillator (Reference 7). For a multiline oscillator case he had 1.56 J/l energy for the case he was running. When he let only the $P_2(8)$ line oscillate, he has 0.19 J/l or 12.3 percent of the multiline energy in a single line. This could be compared to an amplifier case with no ASE on adjoining lines. When he had the lines cascading, i.e., $P_1(9)$, $P_2(8)$, $P_3(7)$, $P_4(6)$, he obtained 0.33 J/l in the $P_2(8)$ line or 21 percent of the multiline energy.

In the summary, the analyses described above were used to set requirements for the optical system. These requirements are summarized in Table 3-6. The input power at RPCL was derived from the amplifier analysis, the pulse length was derived from the temporal shape of the RPCL gain profile, the magnification was obtained from a Rigrod analysis performed with the SOSHF kinetics code and the F_2 mole fraction was obtained from pulse matching the predicted RPCL gain with the predicted oscillator pulse shape. Finally, the path length from RPCL to the SBS cell was determined by the time that the RPCL gain would be on, during which return from the SBS cell would interfere with the amplifier. The analysis was also used to predict the performance of both the oscillator and amplifier. These performance predictions are summarized in Table 3-7. The largest uncertainty is the percent of single line energy expected in the $P_2(8)$ line when RPCL is run as an amplifier. As discussed above, this is dependent on the amount of ASE coming from adjacent lines which could not be precisely predicted.

3.3 DETAILED DESIGN OF OSCILLATOR SUBSYSTEM

3.3.1 Introduction

The purpose of the oscillator subsystem is to provide either (a) single-line input beam to the RPCL used in the MOPA configuration; or (b) a beam directly to the phase conjugation subsystem when the RPCL device is not available. The subsystem design utilizes laser heads from PAR to supply the power, an external grating to select a single line, and a spatial filter and shaping optics to improve beam quality. The requirements on the beam parameters used to drive the design are listed in Table 3-8 along with the predicted subsystem capabilities and the design feature

TABLE 3-6. MOPA Requirements Derived from Analyis.

Parameter	Requirement
Oscillator Subsystem	
Input power at RPCL	> 30 W/cm^2 (50 μJ/cm^2)
Pulse length	> 2 μs start to end (1.7 μs FWHM)
Magnification	< 2.5
F_2 mole fraction	$< 10\%$
RPCL Subsystem	
Path length (RPCL to SBS cell)	300 m (2 μs round-trip delay)

TABLE 3-7. MOPA Performance Predictions.

Oscillator

• Total	35 J
• Percent on $P_2(8)$ line	6.5%
• Pulse length	2.5 μs start to end (1.7 FWHM)

Amplifier

• Total	1.00 * n x (V/V_0)
• Single-line fraction	5-15%
• Pulse length	2.0 μs (start to end of gain)

TABLE 3-8. Oscillator Subsystem Requirements.

	Requirement	Capability	Required Design Feature
Power	$> 50\ \mu J/cm^2$	$420\ \mu J/cm^2$	Spatially filtered single-head oscillator
Pulse length	1.7 μs FWHM	Complies	Set by using proper gain mixture
Beam quality	< 1.5	1.42	Spatial filters
Polarization	$> 90\%$ horizontal	94%	Brewster plates intracavity
Bandwidth	< 250 MHz	50 MHz	Homogeneous broadening
Spectrum	HF $P_2(8)$ line	Complies	Grating
Oscillator magnification	2.5	Complies	Oscillator design
Oscillator Fresnel number	1/2 integer	8.5	304 cm cavity length

imposed to satisfy each requirement. A sketch of the oscillator subsystem appears in Figure 3-9.

3.3.2 Detailed Discussion

The oscillator assembly consists of an on-axis unstable resonator and preamplifier. This configuration was chosen because it has the maximum transverse mode separation. Also, the resonator length of 304 cm was chosen so that the resonator equivalent Fresnel number would be a half-integer, where the transverse mode separation reaches a relative maxima. Intracavity Brewster windows are used to polarize the beam and a magnification of 2.5 is chosen to get the smallest possible beam obscuration while retaining good efficiency. Since the oscillator gain medium is homogeneously broadened, the output bandwidth is expected to be a fraction of the longitudinal mode spacing, on the order of 50 MHz.

In order to increase power in the oscillator assembly, if required, a backup preamplifier assembly has been designed. This employs a second PAR laser head used as a single-pass preamp and a pair of telescopes between

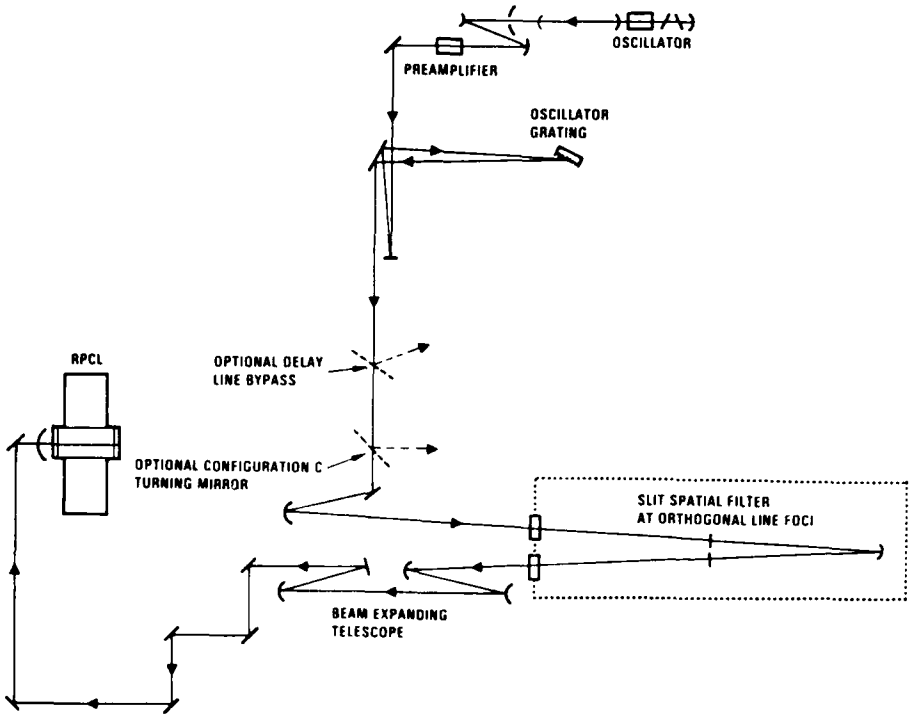

Figure 3-9. Oscillator subsystem beam train schematic.

the oscillator and preamp. The equivalent Fresnel number of the beam propagation through the telescope system is low enough so that the central obscuration in the oscillator beam is filled in by diffraction before reaching the preamp. Without these telescopes the shadow of the oscillator convex mirror would reach the preamp and a central core of unsaturated gain would exist that could degrade the output beam or perturb the resonant mode in the oscillator. In this backup configuration an etalon may be installed between the oscillator and preamplifier if the oscillator bandwidth does not meet the requirement. Additional detail and trade studies on the oscillator and preamplifier design can be found in Reference 8. The oscillator assembly is sketched in Figure 3-10.

From the oscillator, the beam is sent to the oscillator subsystem grating. The 632 lines/mm (mm^{-1}) gold coated blazed grating is supplied by Milton Roy. Fold mirrors are used so that there is a 10-meter optical path length from the oscillator to the grating so that lines that are diffracted near the Litrow angle are prevented from reaching the oscillator cavity.

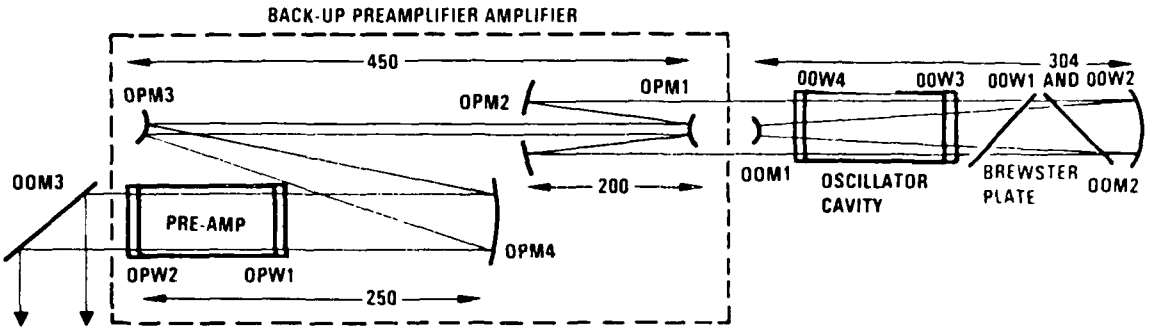

Figure 3-10. Oscillator assembly.

The beam next goes (if required) to the spatial filter assembly which is located inside the vacuum enclosure. Spatial filtering is accomplished with slits at two separate line foci: one in the vertical plane and one in the horizontal. The beam is brought to the first, horizontal line focus using a cylindrical mirror outside the enclosure, relayed via a spherical mirror to form a vertical line focus, and collimated again with a second cylinder outside the enclosure. Figure 3-11 shows the spatial filter assembly. If oscillator BQ is adequate, spatial filtering at this point is not used.

After the spatial filter, the beam is expanded so that it can fill the RPCL entrance aperture. A series of turning flats is used to steer the beam from the APACHE building to the entrance aperture of the RPCL amplifier.

The oscillator subsystem can also be configured as a stand-alone system (Figure 3-3). The oscillator/preamplifier assembly remains the same, and the delay line forms a low Fresnel number spatial filter for beam quality cleanup. Two joules per pulse are expected from the oscillator assembly (Table 3-9). Including the effects of component reflectivities, spatial filter losses, clipping at the RPCL entrance (from eliptical to rectangular), and beam path absorption, there are 108 mJ of energy per pulse at the RPCL entrance aperture. Assuming a 2:1 ratio between average and minimum power in the near field of the beam, the minimum fluence on the beam at RPCL is 404 $\mu J/cm^2$. This is eight times the required fluence derived in the previous section. The performance budgets (power, beam

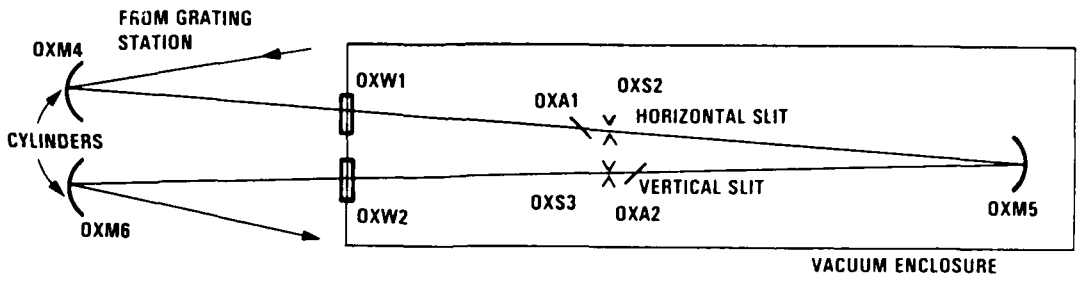

Figure 3-11. Oscillator spatial filter.

TABLE 3-9. Oscillator Subsystem Power Budget.

Oscillator assembly	
Energy per pulse (J)	80.0
Single line fraction:	6.5%
Net output energy (J)	2.08
External train	
Component transmission	0.408
Spatial filter:	0.250
Beam path absorption:	0.5%
Degree of polarization:	85%
Clipping:	0.60
Net train transmission:	0.052
Pulse energy at RPCL (mJ):	108
Beam size (cm^2)	134
Average fluence ($\mu J/cm^2$):	809
Minimum/average near-field intensity	0.50
Minimum fluence ($\mu J/cm^2$):	404
Required fluence ($\mu J/cm^2$):	50
Margin:	8.1

quality, and polarization), along with the subsystem ray trace and fluence loadings, are presented in greater detail in Reference 9.

3.3.3 Summary

All of the oscillator subsystem requirements have been met by specifying the technical criteria for subsystem assemblies or components. The power requirement is satisfied by using the PAR oscillator with the proper mixture to satisfy the pulse length requirement, and using the component efficiencies called out in the power budget. Homogeneous broadening of the oscillator gain medium will ensure compliance with the bandwidth requirement. The beam quality requirement is met by adding the spatial filter assembly, the spectrum requirement is met by adding the grating, and the polarization requirement is met by using the intracavity Brewster plates. The oscillator magnification and Fresnel number requirements are met by properly designing the oscillator geometry.

3.4 DETAILED DESIGN OF RPCL AND PHASE CONJUGATION SUBSYSTEMS

3.4.1 Introduction

The purpose of the RPCL and phase conjugation subsystem is to provide a beam for SBS phase conjugation and sample the beam appropriately for the diagnostics assembly so that the conjugation process can be assessed. The approach is to either use RPCL in its present resonator configuration, or to use RPCL in a MOPA configuration with the oscillator subsystem described in the preceeding section.

The requirements on the subsystems used to drive the design are listed in Table 3-10. Also shown are the predicted subsystem capabilities and the design feature imposed to satisfy each requirement. The RPCL and phase conjugation subsystems are sketched in Figure 3-12.

3.4.2 Detailed Discussion

A sketch of the RPCL assembly is shown in Figure 3-13. For a MOPA design (such as configuration D) the oscillator subsystem beam is injected into the RPCL amplifier assembly at an angle of 1.5 degrees from the amplifier optical axis. Since the ASE from all the HF transitions is nominally confined to some cone angle about the amplifier axis, the

TABLE 3-10. RPCL Subsystem Summary.

	Requirement	Capability	Required Design Feature
Power	≥ 10 x SBS threshold	3.4 n worst case 32 n maximum	RPCL MOPA configuration
Pulse length	Power requirement maintained by 1.0 μs	Complies	RPCL initiation system
BQ at diagnostics	< 1.10	1.08 to 1.12	Spatial filter
Polarization at SBS cell	> 95%	> 98%	Polarizers
Return power fluence in oscillator Fresnel core	< 25 J/cm^2	0.5 n J/cm^2	Polarizers and quarter-wave plate
Spectrum	HF $P_2(8)$	Complies	Grating
Path length (RPCL to SBS cell)	> 300 m	311 m	Delay line
SBS telescope f/number	f/10-f/50	Complies	SBS telescope
Aspect ratio	< 1.1:1	1.15:1	Beam shaping telescope (not required)

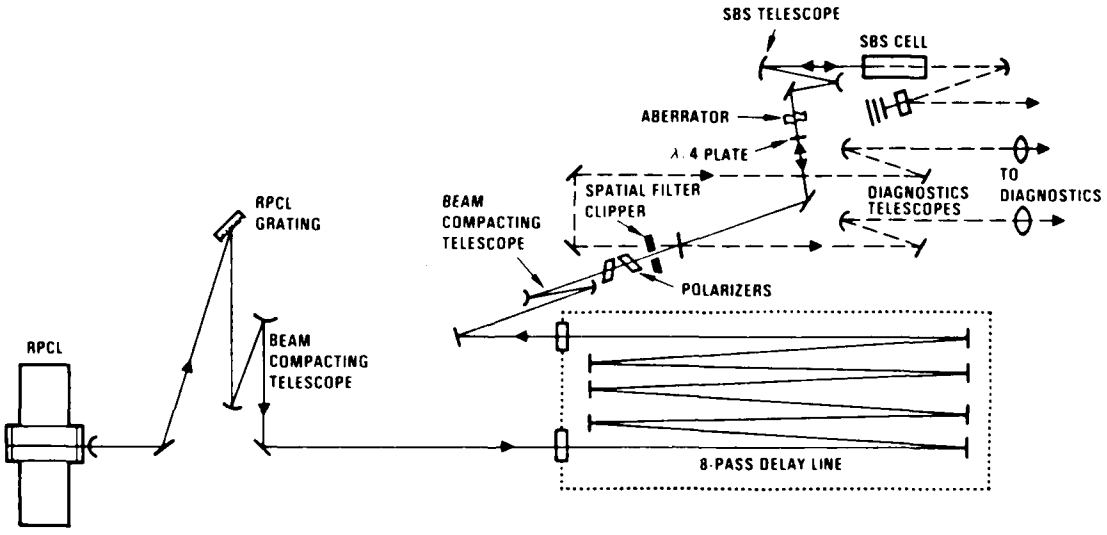

Figure 3-12. RPCL subsystem beam train schematic (baseline configuration).

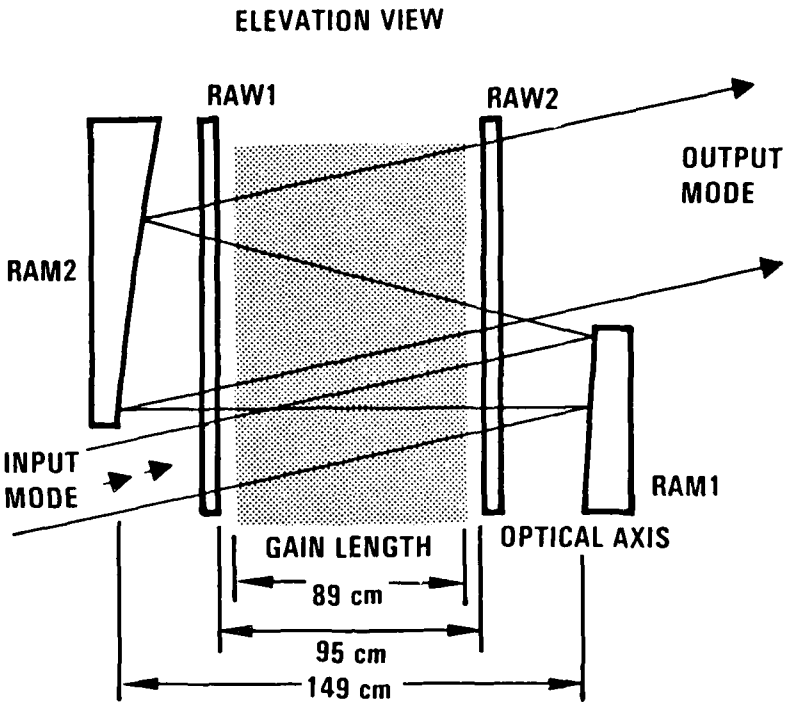

Figure 3-13. RPCL-50 amplifier.

amplified mode can be angularly separated from most of the ASE. Since the ASE cone angle cannot be accurately predicted, a grating downbeam from RPCL removes ASE that may propagate along the mode axis.

For a resonator design, the grating in the RPCL subsystem is identical to that used in the oscillator subsystem except for the size. Dumps are located around the RPCL entrance and exit apertures, and at various upbeam and downbeam locations, to collect the ASE at all angles relative to the nominal mode axis.

The RPCL subsystem optical train is designed so that RPCL may also be used in a resonator (i.e., configuration B) without any modifications to the downbeam external train.

From the amplifier and grating, the beam is compacted to 3 cm and sent through the eight-pass delay line. A sketch of the delay line and spatial filter assembly appears in Figure 3-14. The compacting telescope and delay line work in conjunction with a clipper 280 m downbeam from the telescope

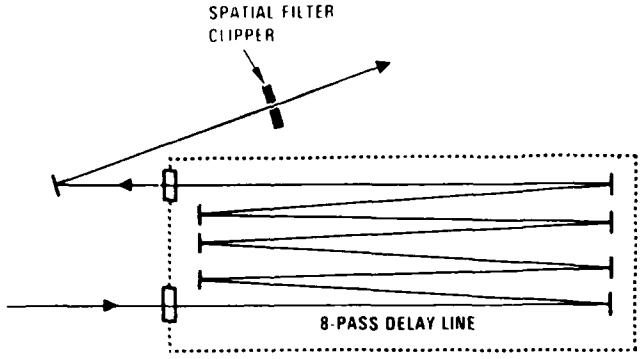

Figure 3-14. Delay line/low Fresnel number filter.

to spatially filter the beam. Propogation code runs predict that the beam quality through the clipper is less than 1.05. This is accomplished because the clipper is distant enough from the compacting telescope to be considered in the far-field (Fresnel number of 0.20). The delay line also serves to delay the return beam from the SBS cell for the required 2 μs before it returns to RPCL.

The beam is then passed through two polarizers and a sampling beamsplitter, all made from CaF_2 substrates. The polarizers are coated to pass only p-polarized light (100:1 extinction) when mounted at Brewster's angle. The first polarizer may be rotated so that the net transmission through both polarizers can be throttled while the polarization state remains fixed as determined by the second polarizer. The beamsplitter is AR coated on one side and uncoated on the other to reflect energy to the diagnostics. For very low power testing, coated beamsplitters will be used to meet the diagnostics area energy requirement.

A MgF_2 quarter-wave plate downbeam of the beamsplitter is used in conjuction with the polarizers to isolate the beam from the RPCL. Light incident on the plate is horizontally, linearly polarized, circularly polarized at the SBS cell, and vertically polarized after two passes through the quarter-wave plate. Most of the return power is eliminated at the polarizers; however, because of birefringence in windows, on mirrors, and error in the quarter-wave plate, some power does reach the amplifier and therefore the oscillator Fresnel core. The polarization budget accounts for these factors and predicts the return energy at the Fresnel

core to have a fluence of 0.5*n J/cm^2. (n is a confidential number used to normalize power and energy values so that they become unclassified. It is the full, multiline, HF output power of the RPCL in kilojoules.)

The SBS telescope is used to supply a converging beam to the SBS cell. The telescope design uses an interchangeable convex mirror to adjust the telescope f/number, followed by a large concave. Using five different convex mirrors, the f/number can be adjusted between the required f/10 and f/50 beams in increments of f/10. Detailed design of the SBS telescope (Reference 10) shows the wavefront degradation to less than 1/50 wave, RMS, for all five positions.

Reflected from the sampling beamsplitter, the sampled incident and SBS return beams are relayed to the diagnostics area. As shown in Figure 3-15, telescopes in each leg of the beam provide the required 1.5 cm beam to the diagnostics area. The telescopes also image the beamsplitter to the middle of the diagnostics area, thus preventing Fresnel diffraction from significantly degrading the sampled beam. The beam transmitted through the SBS cell is also sampled and relayed to the diagnostics area. The imaging characteristics of the transmitted beam train are not critical because this beam is sampled only for spectrum and power measurements.

A 59*n J per pulse is expected from the RPCL amplifier in the $P_2(8)$ line (see Table 3-11). Including the effects of component efficiencies, spatial filter losses, loss from Fresnel diffraction, and beam path absorption, there are 9.2*n J at the SBS cell. From examination of typical RPCL expected pulse shapes as determined by kinetics codes, the expected power over the required 1 μs pulse length is 4.85*n MW. This is 32*n times the predicted threshold for SBS phase conjugation of 150 kW. The performance budgets (power, beam quality, and polarization), along with the subsystem ray traces and component fluence loadings, are presented in greater detail in Reference 9.

3.4.3 Summary

There are three alternate approaches for providing power to the SBS cell for phase conjugation: RPCL MOPA, RPCL resonator, and PAR resonator direct to the SBS cell. While the MOPA configuration is the most robust,

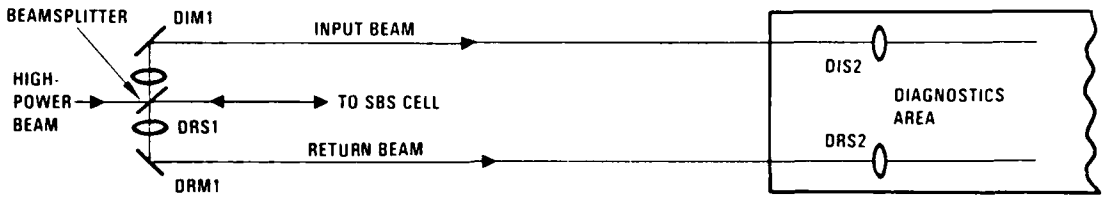

Figure 3-15. Diagnostics external train.

TABLE 3-11. RPCL/Phase-Conjugation Subsystems Power Budget.

RPCL subsystem	
Energy per pulse (kJ)	1.00 n
Single line fraction:	6.5%
Net single line energy (J)	59 n
External train	
Component transmission:	0.663
Spatial filter:	0.250
Beam path absorption:	0.5%
Degree of polarization:	94%
Net train transmission:	0.155
Pulse energy at SBS cell (J):	9.17 n
Pulse length (μs):	1.70
Average power (MW):	5.39 n
Average power in 1μs (MW)	4.85 n
SBS threshold (kW):	150
X Threshold:	32

(n = Normalization factor)

the other configurations offer a simplified alignment procedure and quicker setup times. The RPCL resonator has less power than the MOPA due to losses in the "fang" beam. The PAR lasers are small and have less output power.

All of the RPCL and phase conjugation subsystem requirements have been met by specifying the technical criteria for subsystem assemblies of components. The power and pulse length requirements are satisfied by using the RPCL in its MOPA or resonator configuration. The PAR resonator configuration can meet most test requirements while being the easiest to implement. The beam quality requirement is met by using the delay as a spatial filter. The polarizers and quarter-wave plates are used to satisfy the polarization and return power requirements. The tilted input design of the RPCL amplifier assembly, in conjunction with the external train grating, are needed to comply with the single-line requirement. The path length requirement is met by using the eight-pass delay line, and the SBS telescope satisfies the f/number requirements.

3.5 BEAM PROPAGATION ANALYSIS

3.5.1 Introduction

The purpose of the beam propagation analysis was to use diffractive analysis to propagate a given intensity profile and phase screen from the output plane of the oscillator to the plane of the oscillator spatial filters and determine what slit widths would be required to obtain good spatial filtering. Similarly, a diffractive optics code (TPROP) was used to propagate a given intensity profile and phase screen from the output plane of the RPCL to the plane of the RPCL spatial filters to determine its slit width settings. Both analyses were done for configuration C, which is a MOPA with slit spatial filters at orthogonal line foci.

3.5.2 Oscillator Beam Propagation

The propagation analysis was analytically performed in two steps. First, a top hat annular beam was launched from the oscillator output and propagated to the delay line focusing cylinder (f = 20.3 meters). Second, this near-field intensity/phase profile was propagated into the far-field. Figure 3-16 shows the far-field intensity profile of the beam at focus.

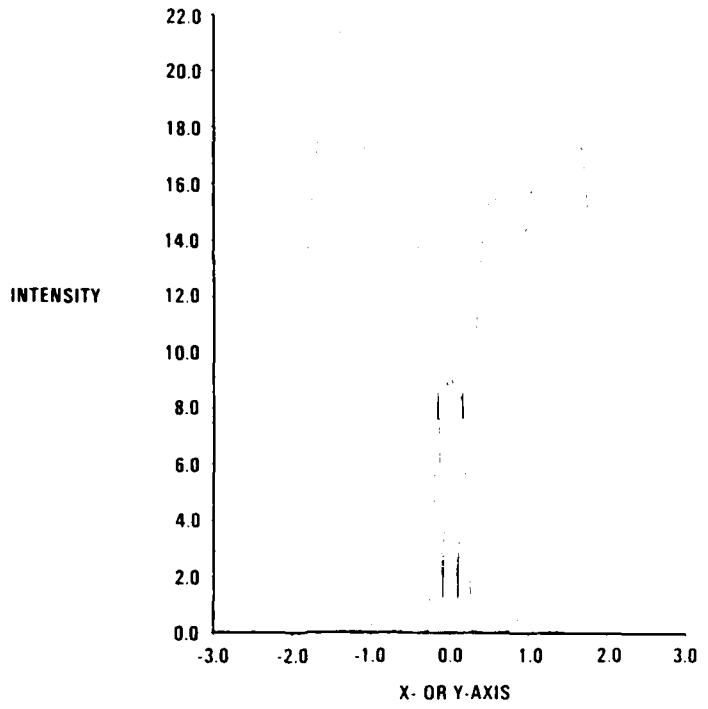

Figure 3-16. Field at X-focus (uniform field on annulus propagated to Z = 2100, X-focus at 4130).

The width between the first set of minima at focus is 1.9 mm, and will be the design setting of the horizontal oscillator spatial filter jaws. It is to be noted that the obscured portion in the nonfocused dimension (y-axis) fills in considerably, far more than near-field filling due to propagation to 41.3 meters (Reference 11). This is because a one-dimensional (x-axis) Fourier transform is performed on a nonseparable two-dimensional field, i.e., the spatial frequency distribution is radial.

After the cylindrical focus, the beam propagates 16.5 meters to a spherical mirror (f = 16.5 meters) where the orthogonal (y, vertical) direction is focused. The analytical expressions become cumbersome to handle after the first spatial filtering because of the large number of Bessel functions that need to be retained in the infinite series expansion representing the field. We can argue, however, that because the first (x, horizontal) spatial filtering has removed some high frequency content over the entire radial field, the orthogonal (y, vertical) focused beam should have intensity nulls farther apart than the horizontal focused beam.

Therefore, a conservative approach would be to set the jaw separation of the second spatial filter equal to the first.

3.5.3 RPCL Beam Propagation

Slit spatial filtering of the RPCL beam was studied in a separate effort (Reference 12). Essentially, if defocus can be spatially filtered, all higher order aberrations can be spatially filtered; therefore, the problem reduces to analyzing beam quality as a function of defocus. Figure 3-17, extracted from Reference 12, plots equivalent beam quality (any aberrations other than tilt) versus an equivalent amount of defocus (T), and Figure 3-18 plots cleaned up beam quality versus slit width, with T as a parameter.

Figure 3-19 shows the layout of the copper jaw design. The jaws are axially separated to avoid axial ringing of rays. Each jaw will be remotely actuated. The jaws will be radiused to avoid breakdown at sharp edges. Tungsten "V" structures or possibly Shott glass will serve as dumps.

TPROP was used to generate the far-field intensity profile at the plane of the horizontal spatial filter. The case of top hat intensity/flat phase screen and top hat intensity/autozoom phase screen at the RPCL output were considered. The autozoom phase screen for HF was derived from a screen for DF which can be used as a first approximation (Reference 13).

Figure 3-20 shows the intensity isocontours of the focused geometry for flat phase screen and indicates jaw separation and jaw position for Q = 0.3 both for the beam aligned and beam misaligned (misalignment = 0.8 Q). The misalignment is based on a figure of 0.3 λ/D for shot-to-shot misalignment and 0.5 λ/D for oscillator spatial filter to RPCL spatial filter misalignment. The peak-to-average intensity is about 2. The results for an autozoom phase screen were essentially the same.

From Reference 14, the damage fluence threshold for copper at a grazing incidence of 45 degrees is experimentally determined to be greater than 358 J/cm^2 for s-polarization (100 nsec pulse). This does not include surface plasma considerations. Reference 14 recommends that tests be performed to assure that 5 torr vacuum is sufficiently low to prevent surface

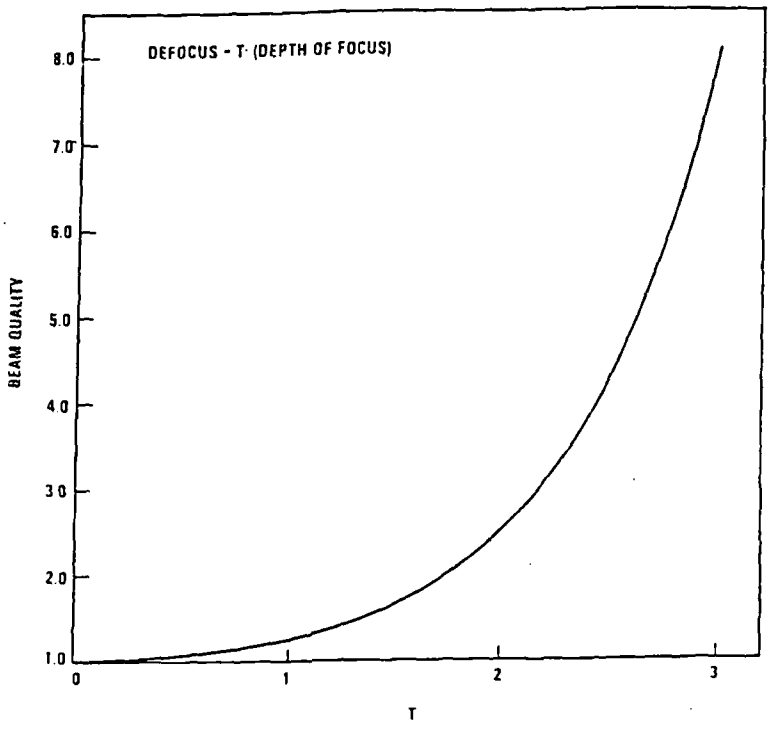

Figure 3-17. Beam quality of uniform field with defocus aberration.

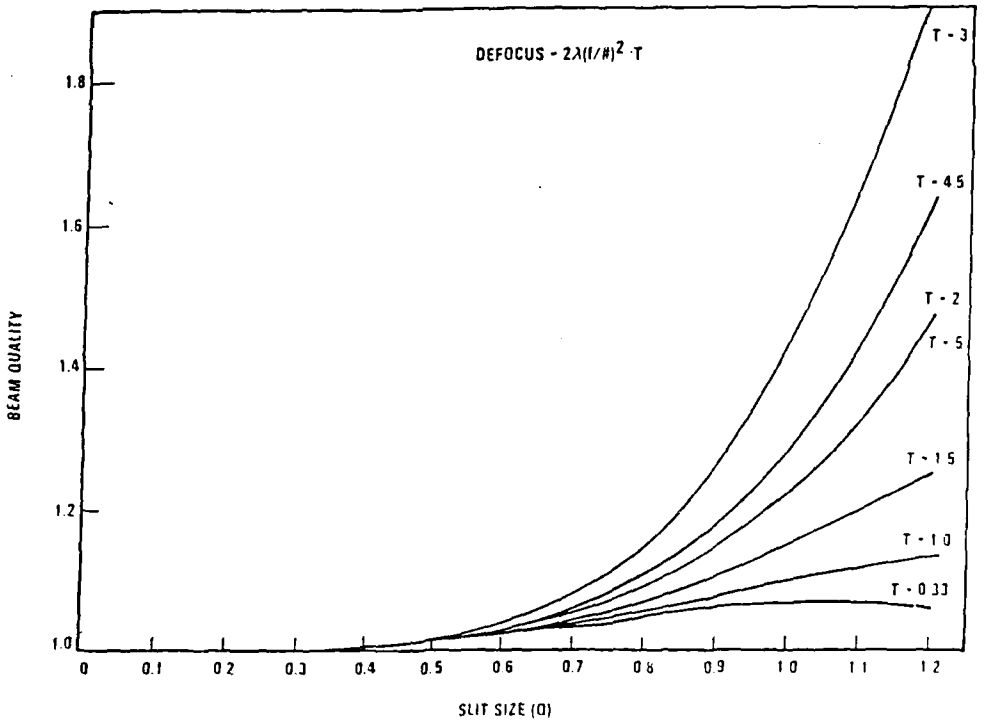

Figure 3-18. Single slit spatial filter output beam quality (peak intensity definition).

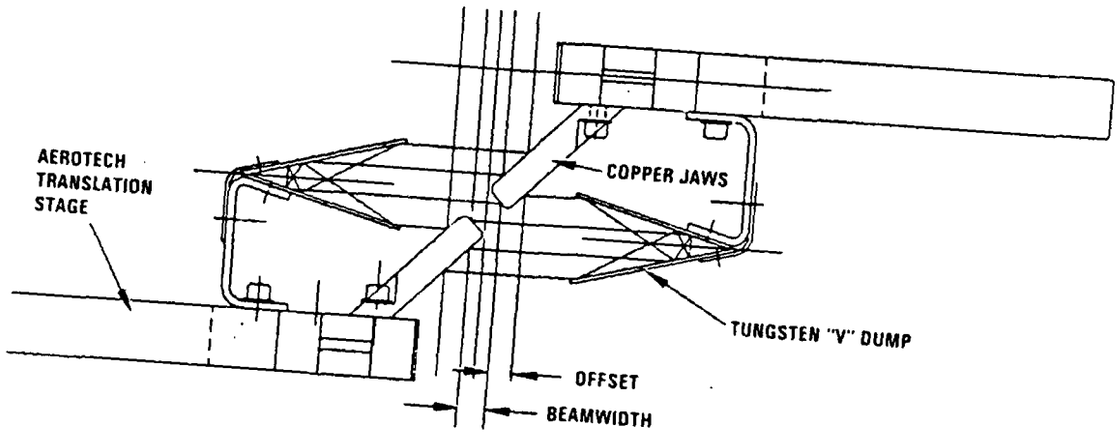

Figure 3-19. Copper spatial filters.

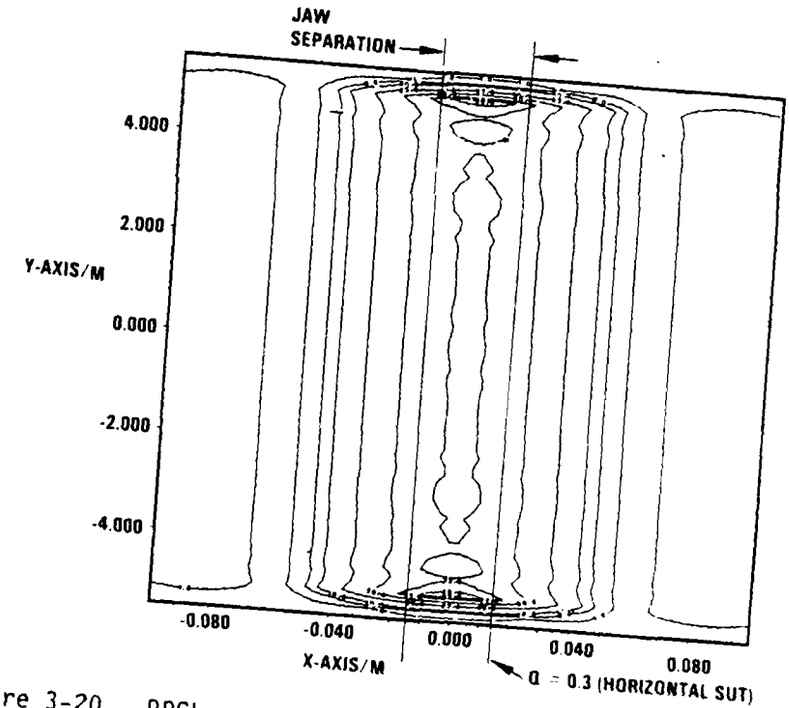

Figure 3-20. RPCL spatial filter at slit CLPCT 0.1 x 5.5.

plasma ignition. The current (12 February 1986) jaw design utilizes a grazing angle of 45 degrees, and the maximum average fluence normal to the spatial filter focal plane is 155*n J/cm^2. This translates to a peak fluence level of 310*n J/cm^2. Therefore, the peak fluence safety factor is greater than 23/n.

3.5.4 Summary

An intensity/phase profile propagation of the annular oscillator beam to the oscillator spatial filter shows that for an outer annular diameter of 5 cm and an obscuration diameter of 2 cm, the spatial filter jaw setting should be 1.9 mm. It is also concluded that, if the RPCL intensity output is nearly a "top hat" and the phase screen has low frequency content as in the case of autozoom, and if surface plasma is not a problem (i.e., 5 torr He is sufficient to prevent surface plasma initiation), the RPCL copper jaws should survive the case of maximum RPCL fluence both in the aligned and worst misaligned case.

4. DIAGNOSTICS SUBSYSTEM DESIGN

4.1 BEAM DIAGNOSTICS DESIGN

The diagnostics subsystem provides instrumentation for monitoring the performance of the oscillator and amplifier subsystems (power, energy, bandwidth, spectral characteristics) and characterizes the fidelity of the phase conjugation process using SBS. Table 4-1 tabulates the measurements required for the HFC experiment. The phase conjugation diagnostics have been divided into three categories to delineate between the beam incident upon the SBS cell, the Stokes return, and the beam transmitted through the cell. The phase conjugation diagnostics include measurements of energy and instantaneous power, time-integrated and time-resolved beam quality, near-field irradiance and phase, and polarization state. The remaining diagnostics, including bandwidth, power spectrum, PAR laser energy and power, and RPCL energy and power, as well as generally monitoring the laser performance.

TABLE 4-1. Measurement Requirements for the Beam Diagnostics Subsystem.

Measurements	SBS Incident Beam	SBS Reflected Beam	SBS Transmitted Beam	Other Selected Locations
Beam Quality				
$\langle BQ \rangle$	X	X		
BQ(t)	X	X		
Energy, $\langle E \rangle$	X	X	X	
Temporal power, P(t)	X	X	X	
Power spectrum, S(t)	X			
Near-field irradiance, $\langle I(X,Y) \rangle$	X	X		
Near-field phase, $\langle \phi(X,Y) \rangle$	X	X		
Polarization, PO(t)	X	X		
Bandwidth, $\langle BW \rangle$	X			
ASE measurement, ASE(t)				X
PAR osc/preamp power and energy, $P_o(t)$ and $\langle E_o \rangle$				X
RPCL power and energy, $P_a(t)$ & $\langle E_a \rangle$				X

$\langle\ \rangle$ denotes measurements which are temporally integrated over the duration of the pulse

(t) denoted temporally resolved measurements (with resolution of much less than the pulse duration)

4.2 DISCUSSION

Figure 4-1 shows the schematic layout of the diagnostics subsystem. Energy and power meters are positioned downstream of either the PAR lasers (for Configuration C) or RPCL (for Configuration A, B, or D). Following the amplifier grating and spatial filter, the beam incident upon the SBS cell is picked off by the main diagnostics beam splitter and directed to the diagnostics bench which is located as shown in Figure 4-2. The Stokes return from the SBS cell is likewise directed to the diagnostics bench using the same beam splitter. The beam transmitted through the cell is monitored on a small bench located in the vicinity of the SBS cell exit.

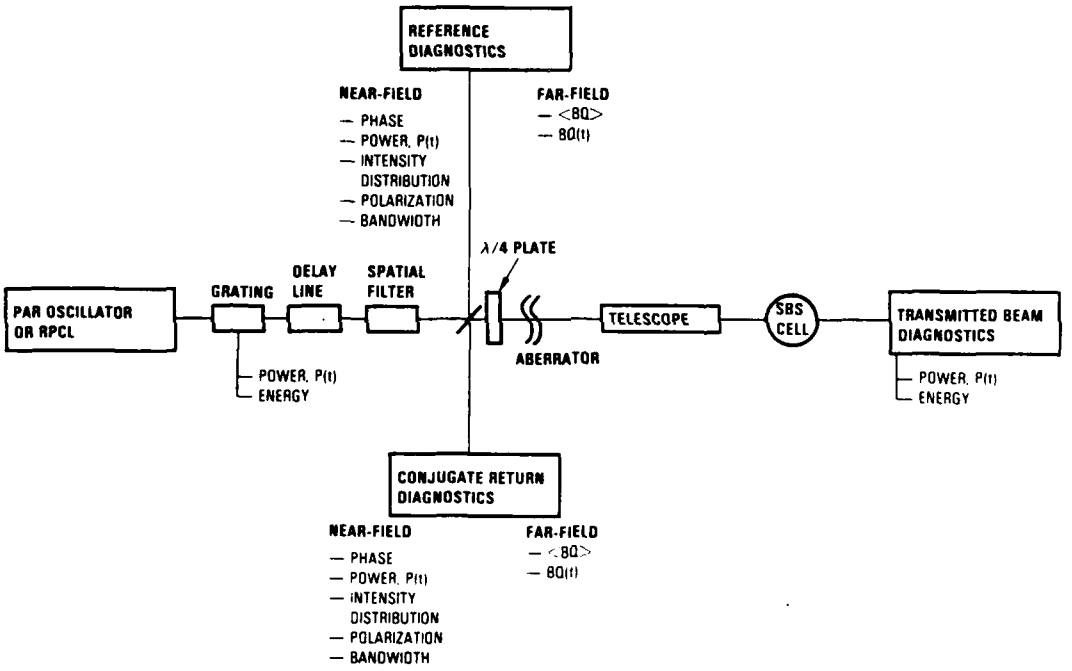

Figure 4-1. Measurement requirements for the beam diagnostics subsystem.

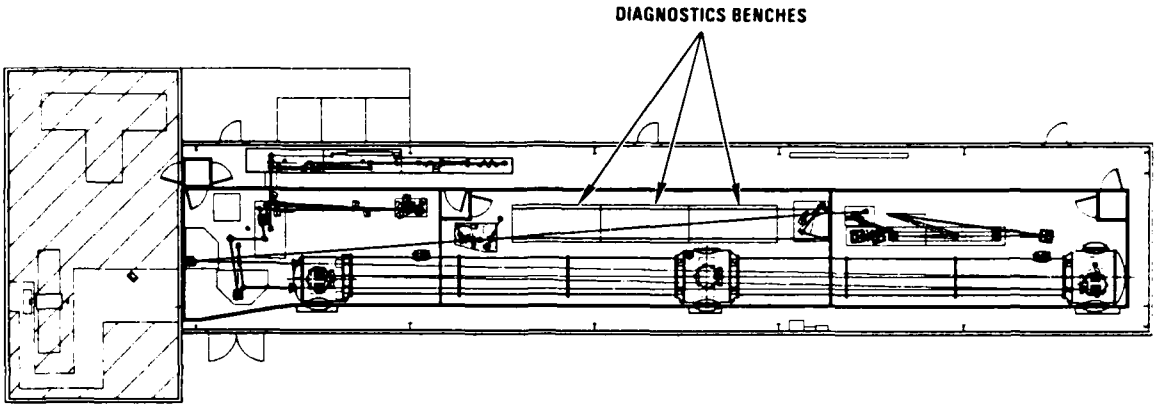

Figure 4-2. Location of measurement stations in diagnostics subsystem.

Figure 4-3 shows schematically the diagnostics beam train layout for the beam incident to the SBS cell on the main diagnostics bench. The diagnostics train for the reflected beam is identical to that of the incident beam. The first measurements made on the incoming beam are energy and power in order to ascertain how much energy and power are delivered to the SBS cell. Because polarization fidelity of the SBS process is critical for oscillator isolation, the second measurement in the beam train is polarization. Downstream of the polarization measurement, is a Pockels cell used for power control and to act as a shutter to isolate the diagnostics beam train before possible leakage of energy back into RCPL or the PAR oscillator arising from accumulated system birefringence can propagate to the diagnostics bench.

Following the Pockels cell, the beam is divided into two parts; one leg is directed to the near-field instruments and the second leg is propagated to the far-field using a 5-meter telescope. Two orthogonally oriented, time-integrated beam quality sensors are located in the far-field leg along with a single time-resolved beam quality diagnostic. The last measurement in the far-field beam is a DP-4 film burn which provides semiquantitative information on beam quality in the event of a failure of either time-integrated sensors. Within the near-field leg, a measurement of near-field intensity distribution is made using a two-dimensional array. Near-field phase is to be measured using a Mach-Zender interferometer with

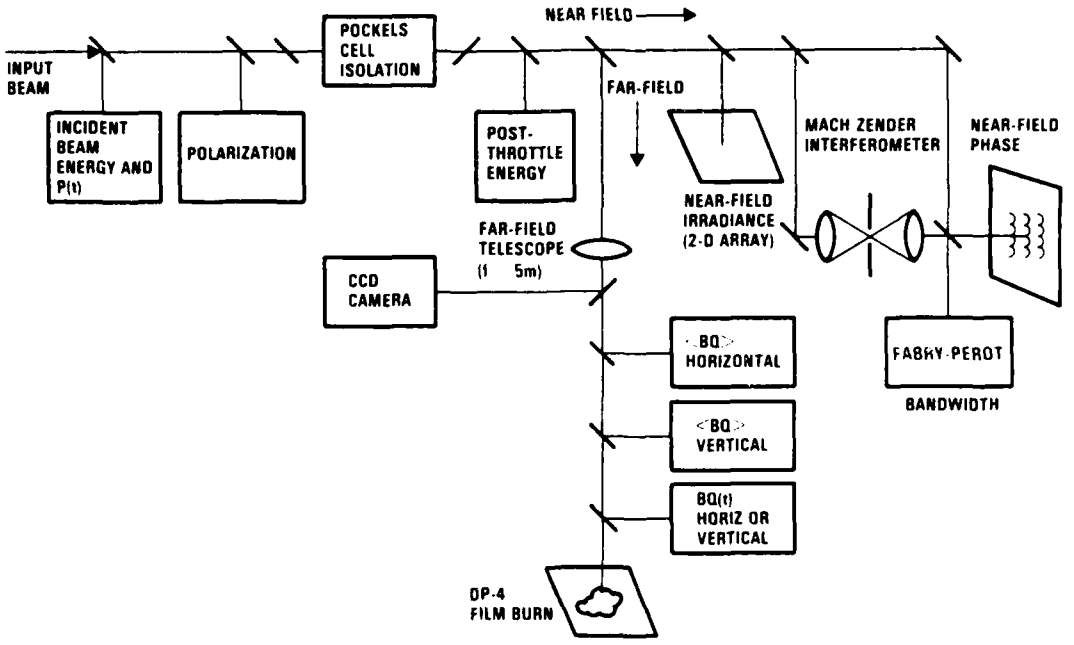

Figure 4-3. Schematic representation of diagnostic beam train for incident beam on main diagnostics bench. Beam train for reflected beam is identical to that of incident beam.

one leg spatially filtered to provide a uniform reference beam. Finally, a Fabry-Perot interferometer is to be used on the incident beam to measure the bandwidth of the laser pulse.

Figure 4-4 shows a layout of the time-integrated beam quality diagnostic. The basic concept utilizes two 256-element linear arrays positioned at the focus of a 5-m telescope coupled with a 16 x 16 element area array located in the far field of a 30-m telescope. Cylindrical lenses are positioned in front of the linear arrays to compress all of the energy orthogonal to the long axis of the array onto the detectors. The telescope for the linear arrays was designed such that the length of the 256-element array corresponds to approximately 13 diffraction-limited spot diameters. Coupled with the cylindrical lenses in front of the arrays, these detectors capture more than 99% of the incident energy. By using the arrays orthogonally oriented, the crossed arrays provide a measure of the

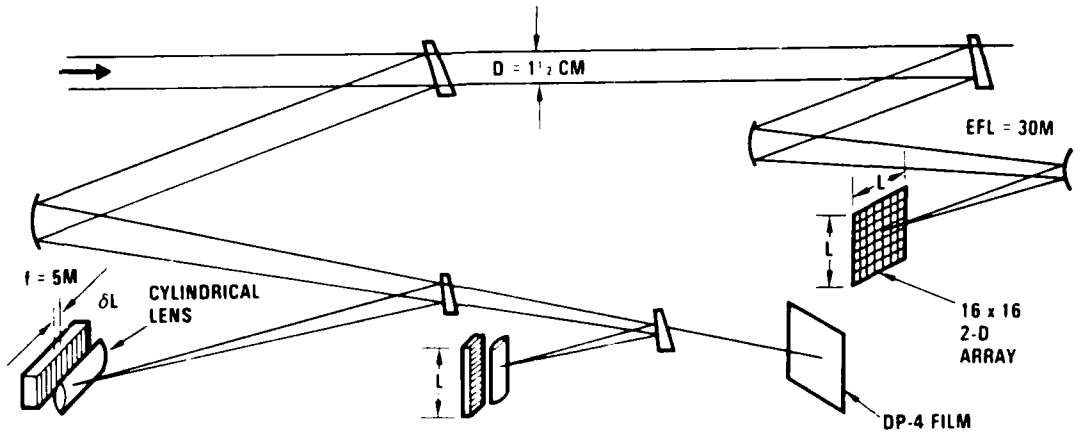

Orthogonally oriented linear arrays

- 256 elements
- $\frac{L}{2f\lambda/D} = 13.6$ $\frac{\delta L}{2f\lambda/D} = 0.05$
- Centroid and P_0 measurement

Area array

- 16 x 16 elements, $\frac{L}{2f\lambda/D} = 2.0$
- Maps 2-D intensity distribution in Q = 1 bucket
- Q = 1 bucket centered on centroid determined by linear arrays

Figure 4-4. Layout of design for time-integrated beam quality diagnostic.

total power P_0 in the beam and the location of the centroid of the far-field spot. The telescope for the 16 x 16 element area array is designed such that the physical dimensions of the detector correspond to 1.5 diffraction-limited spot diameters. Using the total power and centroid information obtained from the crossed linear arrays, the two-dimensional intensity distribution on the area array can be integrated within the Q=1 bucket around the centroid, and an unambiguous beam quality measurement results, defined as

$$BQ = \left[\frac{P_0}{\int_A I(x,y)dxdy} \right]^{1/2}$$

where A is that area on the 16 x 16 element area array centered about the centroid (as determined by the linear arrays) of size Q=1.

Table 4-2 presents the results of a beam quality error analysis on the light condenser diagnostic, including optical component aberrations in the

TABLE 4-2. Beam Quality Error Analysis for Time-Integrated Beam Quality Diagnostic.

Source of Degradation	BQ-1
Diagnostics optical component aberration ($\lambda/20$ optics)	0.02
Medium aberration along diagnostics beam train	0.01
<BQ> diagnostics errors	
• Decentration (0.3 $f\lambda/D$)	0.0036
• Misalignment (0.3 λ/D)	0
• Sensor electronic noise (S/N = 10^3)	0.001
• Error in P_0 measurement	0.005
• Finite detector resolution and length	0.01
EMI effects	0.001
Digital quantization error	0.01
<BQ> diagnostic measurement error	0.027

diagnostics beam train, medium-induced aberration, EMI effects, and digital quantization errors. These results show that the measurement error associated with the time-integrated beam quality diagnostic for a diffraction-limit beam quantified in terms of $\Delta BQ/BQ$ is approximately 0.03.

The time-resolved beam quality diagnostic utilizes the same linear array concept with a 64-element linear array that has parallel output with a time-resolving capability. Figure 4-5 shows the control logic and data acquisition system to be used for the time-resolved beam quality diagnostic. To reduce the number of channels required, bistatic FET switches are used to sample two channels at a rate of 50 MHz, and the resulting data are digitized using a flash A/D and temporarily stored in a memory buffer. Following the test and using the addressing logic, the data are read out using an IBM personal computer (PC) and linked with the HFC experiment data acquisition system for subsequent processing.

BQ(t) diagnostics

- **Same light condensor concept as <BQ> sensor**
- **Sixty-four-element parallel output time resolved linear array with 400 μm resolution**
- **100 ns sampling time**

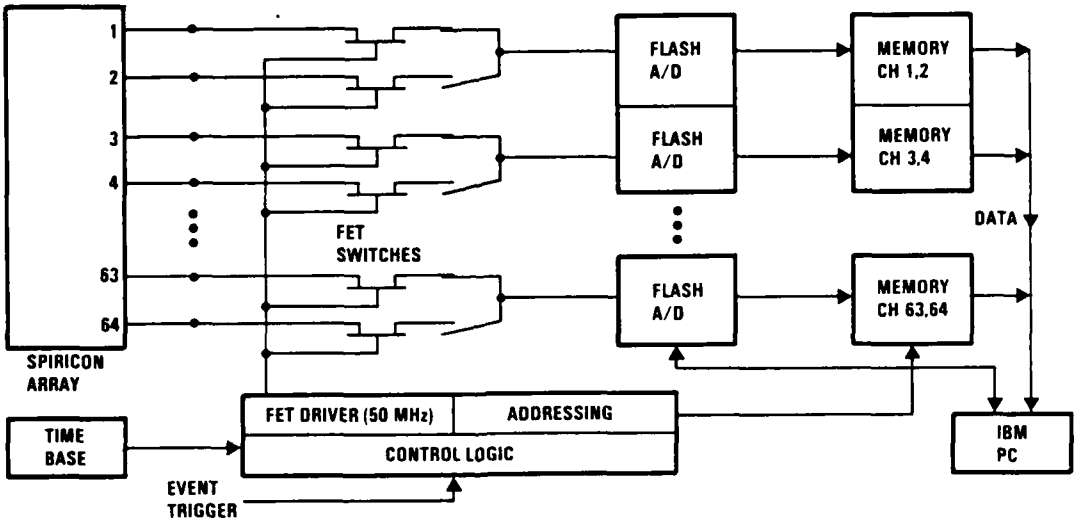

Figure 4-5. Block diagram layout of data acquisition system for time-resolved beam quality diagnostic.

The remaining near-field diagnostics are summarized in Table 4-3. Energy measurements on the bench are to be made using Scientek calorimeters. Power measurements are to be made with Judsen J-12 InAs detectors utilizing an integrating sphere. Polarization measurements will be performed using dual Judsen InAs detectors with orthogonally oriented polarizers within the input aperture of two integrating spheres giving time-resolved capability to the polarization measurement. Time-averaged near-field irradiance is to be measured using a 16 by 16 element, two-dimensional array manufactured by Spiracon using InAs detectors. Near-field phase measurements will be performed using a Mach-Zender interferometer. To provide a high quality reference beam to facilitate interpretation of the phase measurements, one leg of the interferometer is spatially filtered. The fringes are to be detected using an IR CCD camera being purchased with capital funds. Bandwidth data are to be measured using a Fabry-Perot with a finesse of 50 and a free spectral range of 2.5 GHz; fringes are to be detected using a Spiricon 256-element linear array.

TABLE 4-3. Summary of Near Field Diagnostics Design.

Measurement	Diagnostic Description
Energy	Scientek calorimeter with integrating sphere • 5 percent FS accuracy
Power	Judsen InAs detector with integrating sphere • 50 ns response time • 10^3 signal/noise
Polarization	Dual Judsen InAs detectors with crossed polarizers within input aperture of integrating spheres
Near-field irradiance	Spiricon 16 x 32 element two-dimensional array • Spatial resolution: 3-6% of beam diameter • 10^3 signal/noise
Near-field phase	Mach-Zender interferometer, one-leg spatially filtered • Fringes recorded using DP-4 film
Bandwidth	Fabry-Perot interferometer • Etalon: FSR = 2.5 GHz Finesse = 50 • Fringes recorded using 256 element linear array (Spiricon)
Time-resolved spectra	Time resolved spectrum analyzer (polychrometer) developed for use on RPCL technology program • Dispersive grating with 16 (position adjustable) pyroelectric P(t) sensors

Finally, time resolved spectra measurements are to be made using the polychometer which has been developed and used successfully on previous RPCL technology programs.

4.3 SUMMARY OF REQUIREMENTS VERSUS CAPABILITIES

Table 4-4 summarizes the diagnostics subsystem requirements and presents the projected performance capabilities of the present diagnostics design.

TABLE 4-4. Summary of Diagnostics Requirements and Projected Capabilities.

Measurement	Requirement	Capability
$\langle BQ \rangle$	Adequate resolution to measure BQ $\leq$ 1.15	1.03
BQ(t)	Adequate resolution to measure BQ $\leq$ 1.2	TBD
	Temporal resolution of BQ $\leq$ 100 ns	100 ns
Energy	Absolute accuracy to $\pm$ 5% of measurement	3%
Power	Power resolution of 1% of peak power	0.5%
	Temporal resolution $\leq$ *100 ns*	100 ns
Polarization	Accuracy of polarization measurement to $\leq$ 5%	1%
	Polarization measurement to $\leq$ 100 ns	100 ns
Near-field irradiance	Irradiance resolution to 1% of peak irradiance	0.1%
	Spatial resolution 10% of beam diameter	3-6%
Near-field phase	OPD resoltuion $\pm (\lambda/20)_{RMS}$	TBD
Bandwidth	Dynamic range from 50 MHz to 2.5 GHz	0.05 to 2.5 GHz
	Bandwidth measurement accurate to 50 MHz	50 MHz
Time-resolved spectra	Line power resolution to $\pm$ 1% peak line power	$\pm$ 0.25%
	Temporal resolution to $\pm$ 100 ns	100 ns
	Number of lines of simultaneous measurement $\geq$ 8	8

5. MECHANICAL DESIGN/HARDWARE ACQUISITION PLAN

The mechanical design of the HFC experiment includes the overall arrangement of the experiment components within the APACHE facility and the design of nonoptical hardware required to perform the experiment. Additionally, the analysis and design of the mechanical aspects of optical components, (e.g., pressure window mounting) are also performed under this subproject. Major nonoptical components and assemblies include optical mounts and supporting structures, the static SBS cell assembly, the beam path conditioning assembly, the vacuum duct assembly, and the controls and instrumentation subsystem.

5.1 OVERALL EXPERIMENT ARRANGEMENT

Any physical layout of HFC components within the APACHE and RPCL buildings must satisfy a variety of requirements. The building dimensions are fixed and moving a wall would produce significant cost escalation. The RPCL building presently exists, is shared by the ALPHA VM device, and is required by other programs. The sharing arrangement introduces "keep out" zones within the RPCL building and precludes major modifications to this building. The RPCL device location fixes the point and direction of entry of its output beam into the APACHE building. Similarly, concrete pads outside both buildings have been provided for PAR laser support equipment, for the APACHE building heat pump, and for the vacuum delay line pump. The direction of supply lines from this outside equipment is thus fixed.

The sizes of two major experiment components; the vacuum delay line enclosure assembly and, to a lesser extent, the main diagnostic assembly; dictate their placement along the long axis of the new building. The large number of long, small off-axis angle beam shaping telescope legs also package most compactly when oriented along the long axis of the room. A requirement to sweep the beam paths between mirrors with a flow of low absorption beam path conditioning gas dictates that this flow should be directed parallel to the short dimension of the room and the beam paths compacted as much as feasible to minimize the amount of gas and size of gas enclosures.

At both oscillator and amplifier line selection stations, the selected order beam is at a fixed angle from the surface normal of the grating, and the distance of the next component downbeam must be sufficient to spatially separate the orders and allow room for power dumps to absorb the unwanted energy.

Finally, safety considerations dictate a rapid evacuation route from the building for personnel anywhere in the building. This requires provision for unblocked aisles and building exits (in order to maintain thermal equilibration of the room, some exits will be covered with breakout panels for use in emergencies only).

The resulting physical arrangement of HFC equipment in the facility is shown in Figure 5-1. This figure describes the all-up monodirectional MOPA denoted configuration A. Larger scale breakdowns of the several optic trains are shown in Figures 5-2 and 5-3 (oscillator train), Figure 5-4 (RPCL train), Figure 5-5 (SBS injection train and diagnostics train).

5.2 Optical Mounts and Supporting Structure

Figure 5-6 shows a typical mirror mount designed for the HFC experiment. This design is based on similar designs used successfully on the 2454 Program. The mount is constructed of Meonite, a form of dimensionally stable cast iron. The concept is based on minimizing long-term alignment drift by providing a stiff, massive mount structure locked in position by preloading large areas in shear. While coarse adjustment screws are provided, they are backed off in the final aligned and locked position. This makes the mount laborious to align but minimizes repeated alignments. Near final alignment the locking bolts will be partially tightened, alignment varied with the adjustment screws, locking bolts fully tightened, and adjustment screws backed off. The HFC experiment requires 4-, 6-, 10- and 14-inch versions of this mount plus several custom mounts for the RPCL cavity mirrors, the amplifier grating and several remotely actuated mounts.

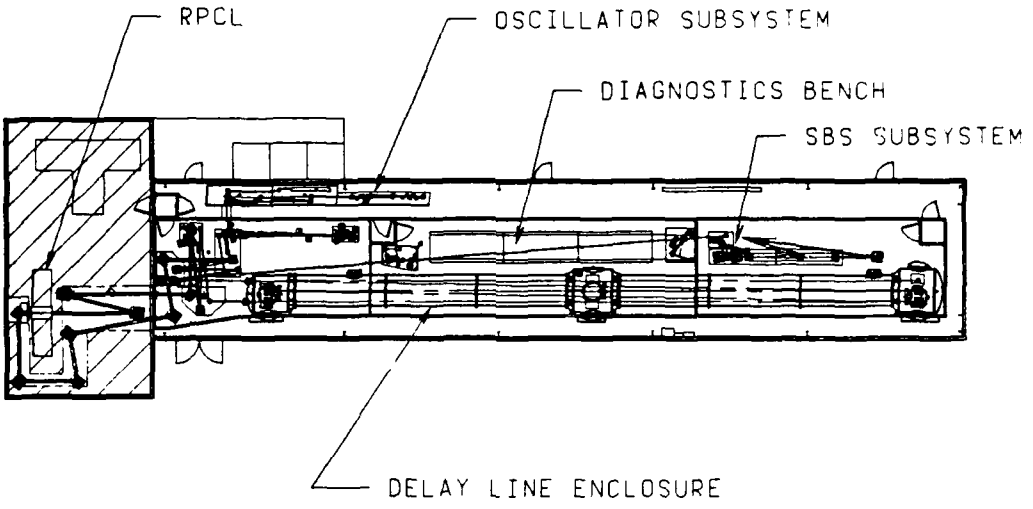

Figure 5-1. Layout of HFC optical train (configuration D).

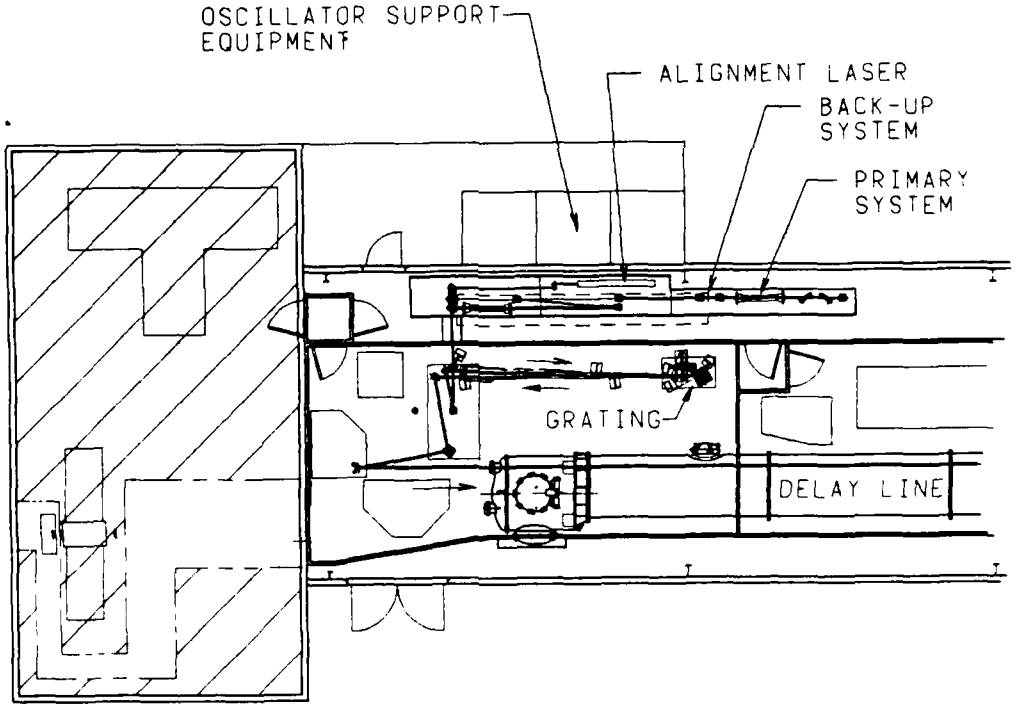

Figure 5-2. Level C of oscillator subsystem (configuration D).

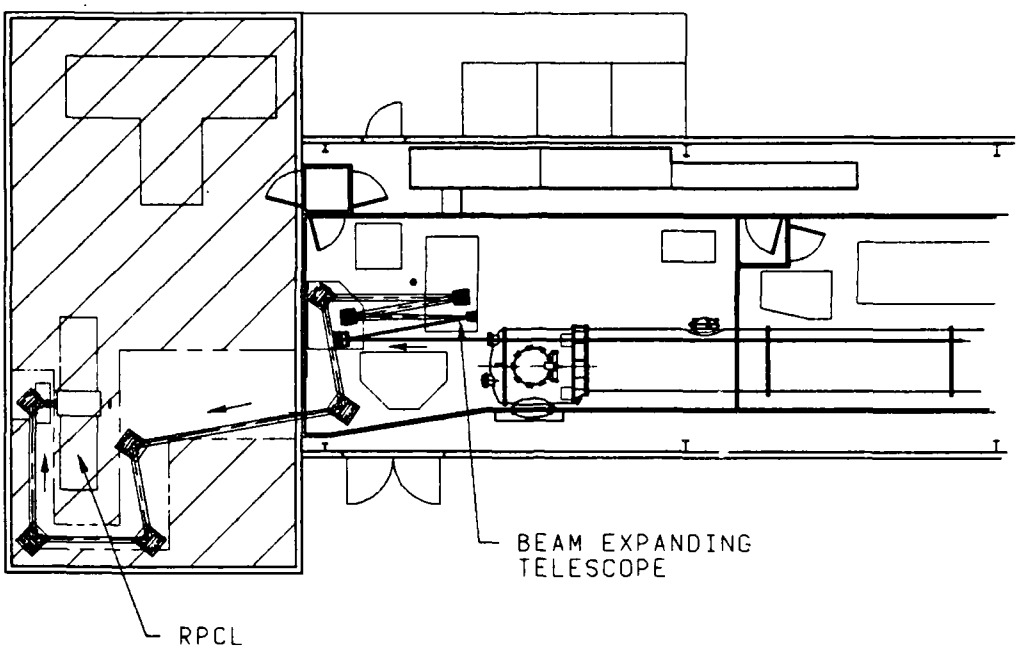

Figure 5-3. Level B of oscillator subsystem (configuration D).

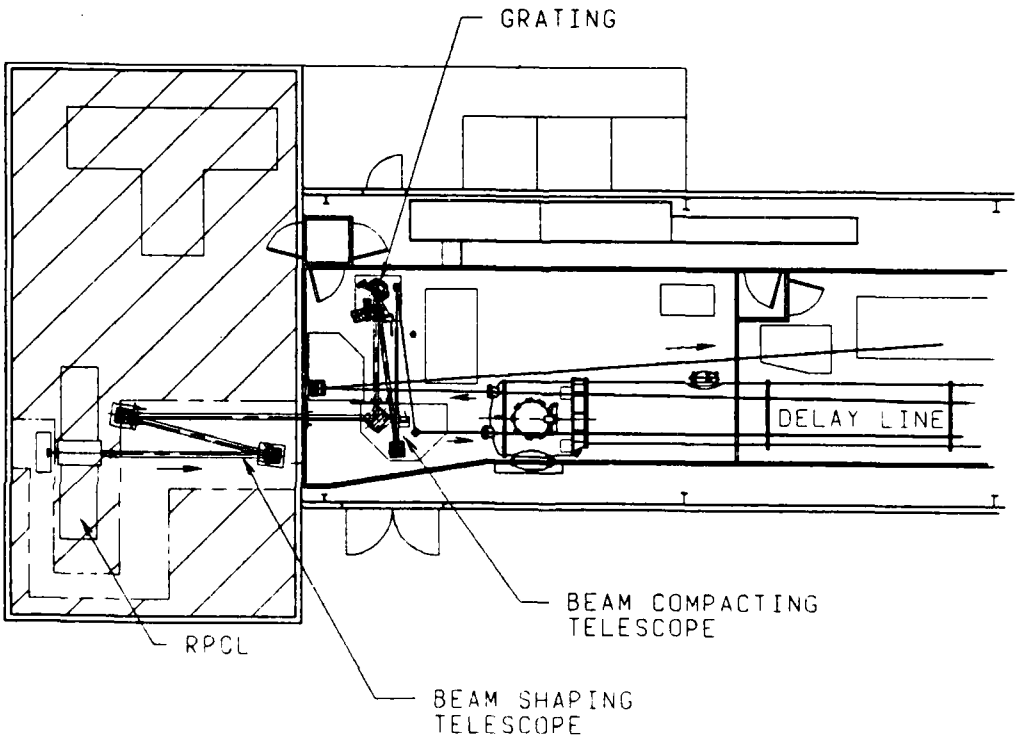

Figure 5-4. Level A of RPCL subsystem (configuration D).

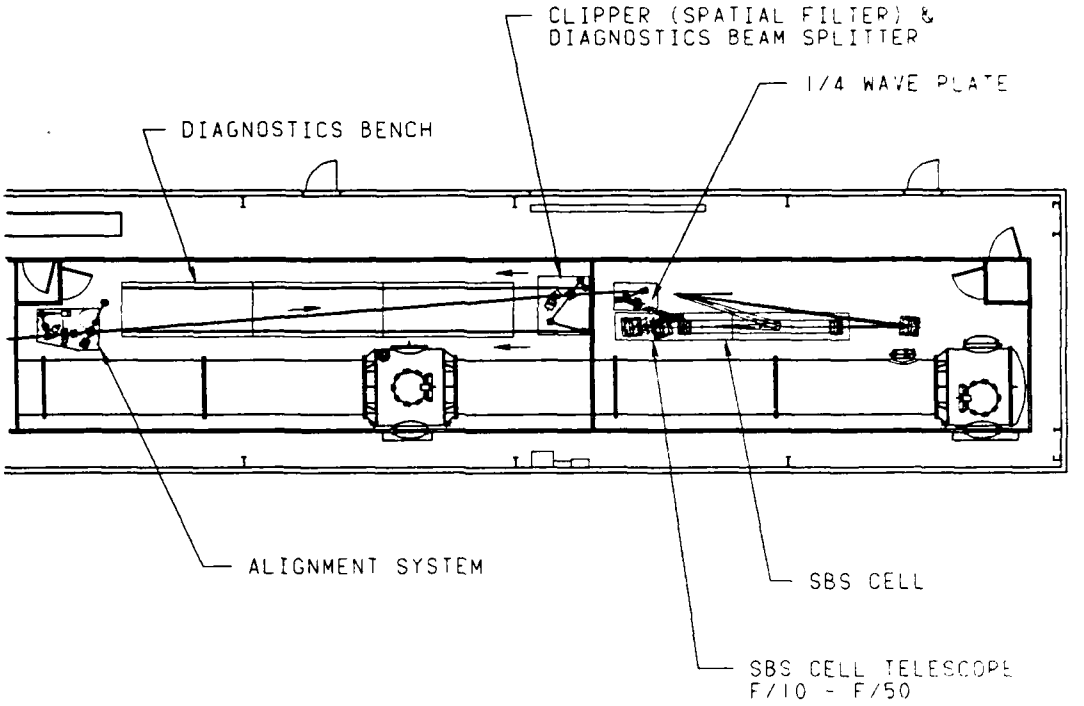

Figure 5-5. Level D of subsystem and levels A/D of the diagnostics subsystem.

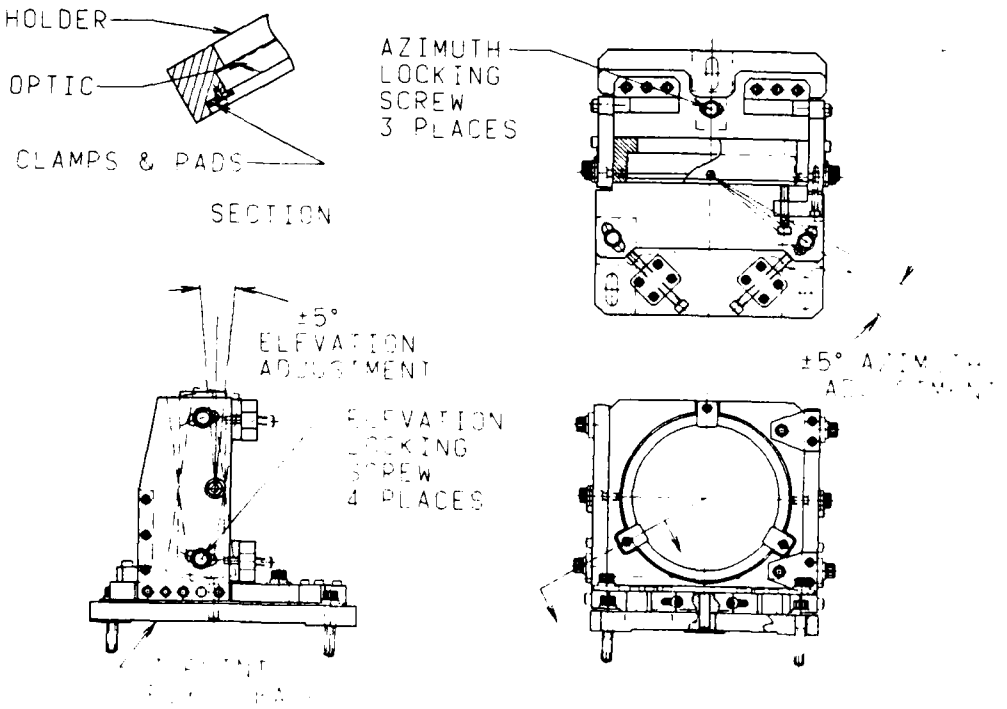

Figure 5-6. Typical optical mount.

5.3 SBS CELL ASSEMBLY

Figure 5-7 shows the essential requirements of and trade-offs performed for the static SBS cell assembly. More detailed requirements are summarized in Table 5-1. The cell is a long cylindrical pressure vessel containing xenon gas at 40 atmospheres pressure or alternate SBS media at higher pressures. Figure 5-8 shows an overall view of the cell.

Windows of CaF_2 are provided at both ends of the cell to transmit the input and SBS reflected beam and the transmitted beam, respectively. Brittle fracture of these windows is a safety concern and remotely operated polycarbonate safety windows are provided to shield personnel working near the cell. As f/number is varied through the test range of 10 to 50, the cell length must vary to keep the size of the beam footprint constant on the window. This variation maintains a constant safety factor on damage fluence. Cell length variation is accomplished by bolting together varying lengths of aluminum vessel as shown in Figure 5-9. A media recirculation loop has been added to control laminar free convection and equilibrate the cell.

Figure 5-10 shows a detail of the CaF_2 baseline window holder. A similar mount is provided for a set of ALON ($Al_{23}O_{27}N_5$) backup windows that could be used if the cell must be operated at pressures exceeding 40 atm (in evaluating alternate SBS media). The CaF_2 windows are mounted in fluorocarbon rubber flat gaskets in a carrier ring subassembly which is mechanically isolated from tilt and deflection of the main pressure vessel flanges to prevent secondary loading of the window. Final thickness selection for the baseline window is shown in Figure 5-11. A Weibull reliability analysis of CaF_2 window fracture was used to calculate the probability of a window withstanding exposure to a proof pressure 10 percent greater than the maximum to be used during testing. The 705 psi curve reflects this proof-pressure factor plus an allowance for shock wave overpressure against the windows after a breakdown at focus. As shown, a window thickness of 1.85 inches provides a reliability of 95 percent per window and is our design point. Similar analyses were performed for the other CaF_2 windows in the optic train.

- Maintain Xe purity to < 0.1 PPM of H_2O, CO_2, N_2O and < 1.0 μm particulates at up to 40 atm
- Insure personnel safety
- Provide high optical quality windows with clear aperture sufficient for two half beams
- Instrument for media temperature, pressure and breakdown
- Limit OPD from media density gradients to $\lambda/10$ between input window and focus
- Provide f number variation from 10 to 50

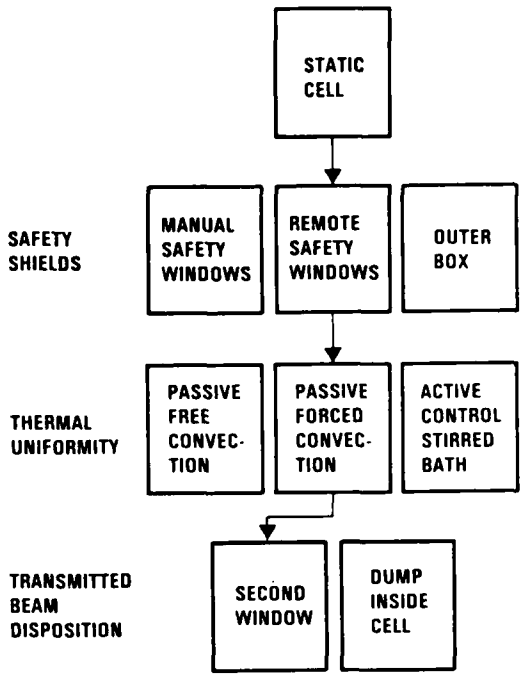

Figure 5-7. Static SBS cell (major requirements and trades).

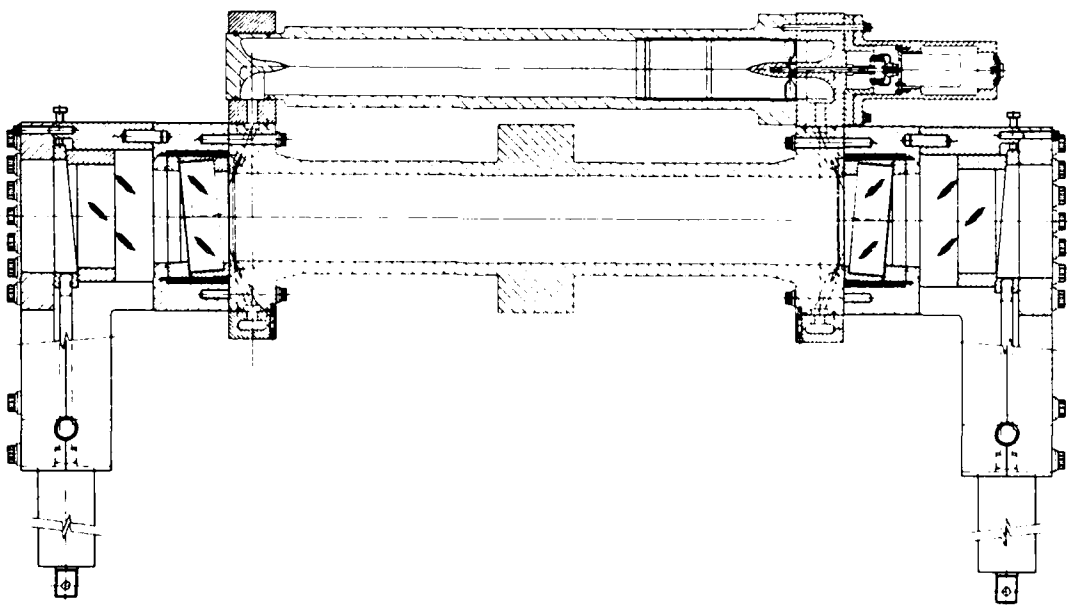

Figure 5-8. SBS static cell assembly.

TABLE 5-1. Static SBS Cell (Requirements Versus Capabilities).

Requirement	Relevant Features		Capability
Media • 40 atm xenon	2024-T4 aluminum cell walls to ASME code		Any noncorrosive media up to 130 atm
Media purity • H_2O, CO_2, N_2O $<$ 0.1 PPM each • Particulates $<$ 1.0 μm	Evacuation to 10^{-4} torr vacuum before fill LN_2 cold trap $<$ 1.0 μm filtration Getter pump in feed system		0.3 μm filtration 0.1 PPM trace gases
Storage duration • 1 week under pressure	Window aperture covers permit GN_2 pressurization to relieve stress in window between runs		Design may be operated in this manner
Pressure containment • Safety factor $\geq$ 4.0	40 atm baseline windows 130 atm vessel Provide backup window with 130 atm capability		Complies
Safety features • Pressure relief value • Prevention of window removal under pressure • External safety shields	Relief valve set to 43 atm Flange bolts require removal with wrench (also placarded) Polycarbonate outer window in place except when testing		Complies
Thermal uniformity • Sufficient so as to limit increase in far-field spot size	Equilibration period after fill Insulation blanket to attenuate spatial and temporal variations Wall and media RTDs Turbulent mixing loop added		Complies
Medium diagnostics • Temperature to $\pm$ 0.1 K res. • Pressure to $\pm$ 0.1 atm res. • Dielectric breakdown monitor	Platinum RTD probes each section Pressure gage and transducer Quartz window for monitor		Complies
Aperture • Space for two half beams separated by one half beam size in near field; 50 diffraction-limited spot diameters in far field	Window support radius	Complies	
Window orientation • Tilted from beam centerline	Tilted surface machined into mount	5° tilt	
Material compatability	Aluminum alloy walls, CRES flanges Fluorocarbon window elastomer has low off gassing and permeability	Complies	
Insulation	Mineral wool insulation enclosed in aluminum sheet	Complies	

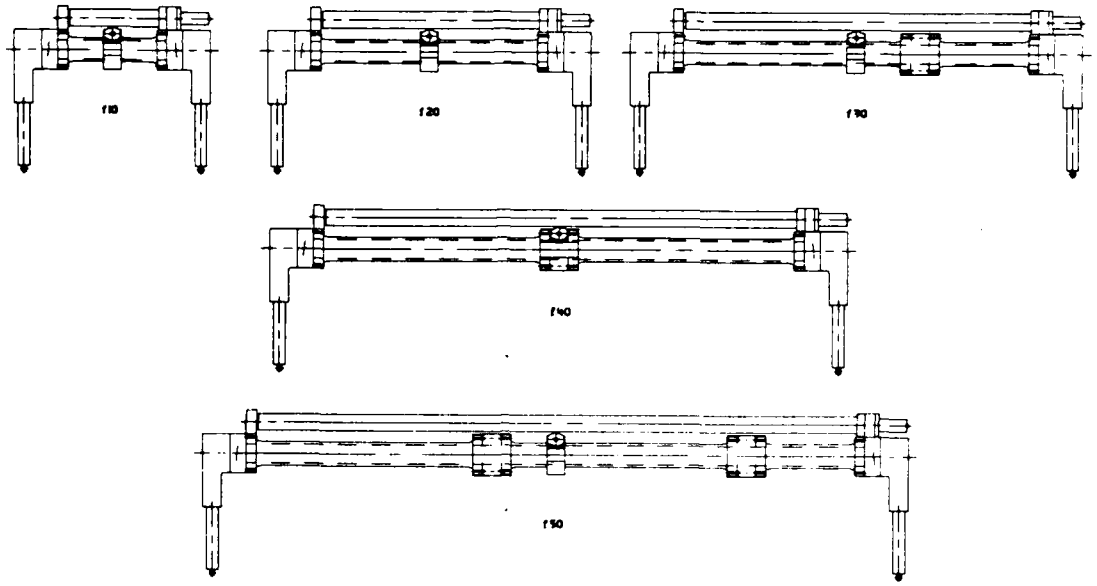

Figure 5-9. Cell and spacer assemblies.

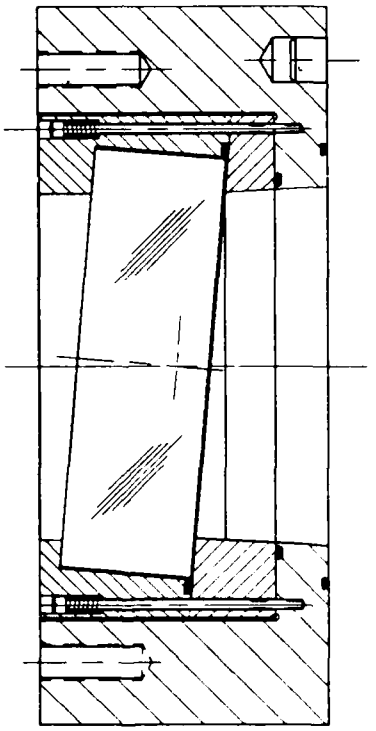

Figure 5-10. Window holder.

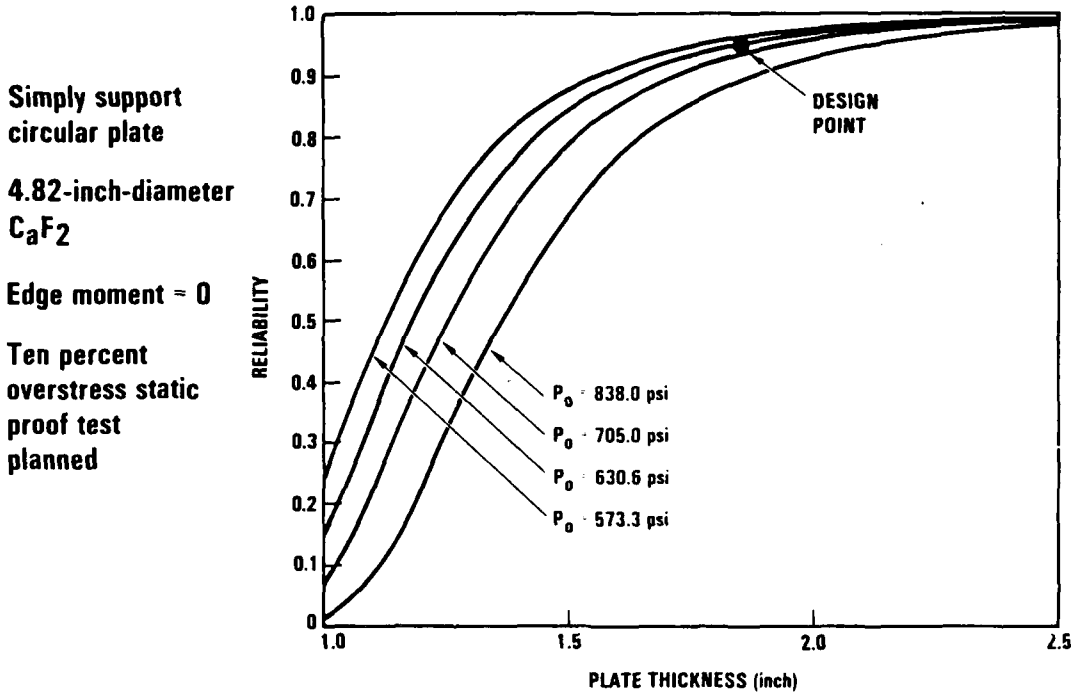

Figure 5-11. Window thickness selection by Weibull reliability analysis.

The media recirculation loop is shown in Figure 5-12. The loop consists of a set of passages and manifolds to inject and extract xenon from each end of the cell, a fan to circulate media around the loop, particulate filters to maintain media purity, a variable speed dc motor to drive the fan and a magnetic coupling to isolate the media from any trace contaminants generated by the motor. The loop maintains turbulent flow within the cell, suppressing free convection cells. Calculations indicate that, for a $\lambda/10$ OPD due to temperature-dependent index changes within the cell, a maximum thermal inhomogeneity of 0.002K is tolerable with free convection within the cell. Corresponding calculations for turbulent convection indicate that more than 0.1K thermal inhomogeneities are tolerable. While the cell exterior will be thermally insulated and surrounded with a temperature controlled environment it is unrealistic to expect cell uniformity greater than 0.1K. Figures 5-13 and 5-14 illustrate the design parameters selected for this loop based on equilibrating the heat delivered in a prior laser pulse within an assumed minimum 15 minutes between tests.

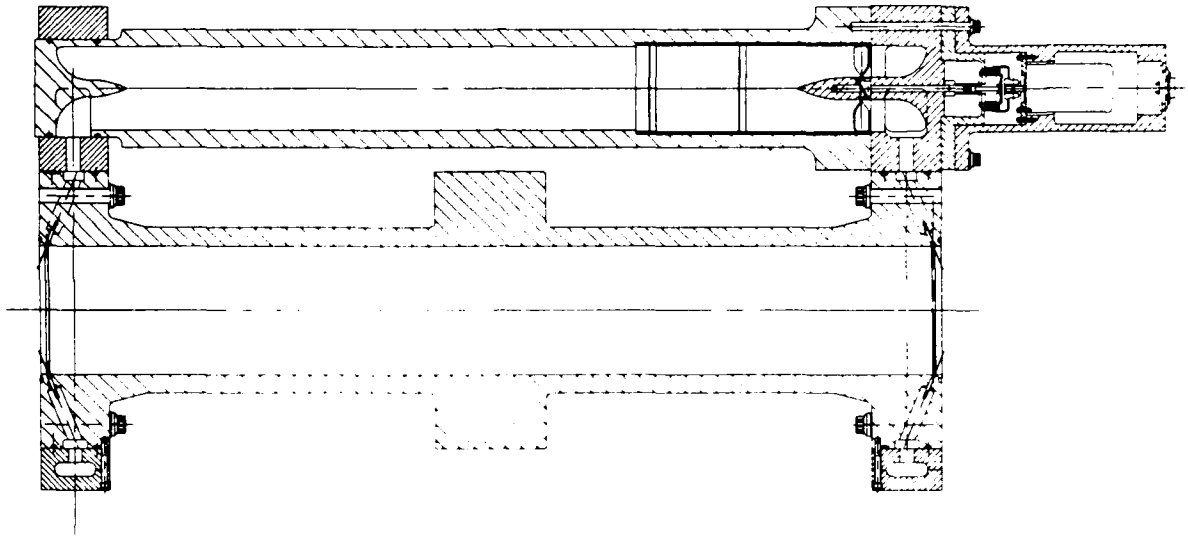

Figure 5-12. Recirculation assembly.

Impingement on window will be used to equalize temperature with the cell after each test

- **Cools to within 0.1 K in 15 min**
- **Assures uniform xenon temperature**
- **Complete equalization not necessary if flowing during test**

Turbulent flow assures complete mixing at any cross-section: Re = 200000

Velocity at edge of beam path is 0.94 x V_{max}

Friction heating is low: 1.36°F/hr

Pressure gradient low: $\Delta P = 0.32$ psi for entire loop

Power requirement for turbine/fan: 0.8 W

Velocity should not cause vibration: 7.2 ft/s in injector hole

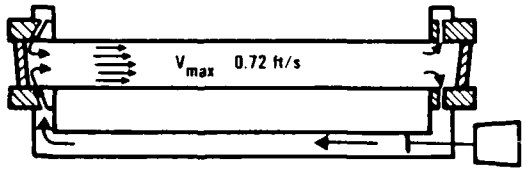

Figure 5-13. Static cell recirculation loop.

Criteria: media OPD along light path $\leq \lambda/10$ maximum

Turbulent flow OPD analysis indicates $\Delta T_{maximum} = 0.1\ K = 0.18F$ if over entire light path

Analysis at right applies 0.1 K criteria to pulse heated window and nearby media (conservative)

A recirculation Reynolds number of 200000 restores thermal uniformity in 15 minutes with above assumption

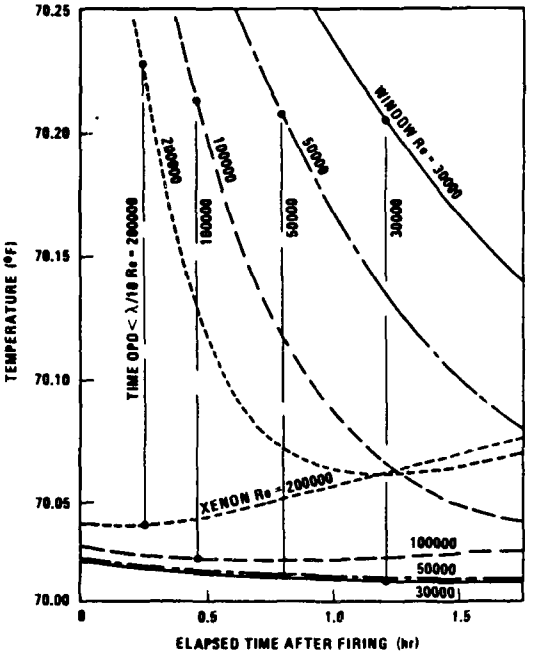

Figure 5-14. Static SBS cell media OPD from prior test.

A schematic of the support system required to leak test, evacuate, fill and recover xenon from the static cell is shown in Figure 5-15. Many of the components shown are usable later in the support system for the flowing gas cell designed for the COS experiment.

5.4 BEAM PATH CONDITIONING ASSEMBLY

Figure 5-16 depicts the major requirements and trades leading to the selected design for the beam path conditioning system (BPCS). Briefly, the major portion of the optic path outside the vacuum duct assembly must pass through a gas containing very low concentrations of trace gases that absorb at HF wavelength such as CO_2, H_2O vapor and N_2O. Additionally, any large-scale index of refraction gradients normal to the beam's propagation direction must be held to very low levels or the beam will be bent so as to miss the tight spatial filter apertures. Such gradients usually arise from temperature gradients.

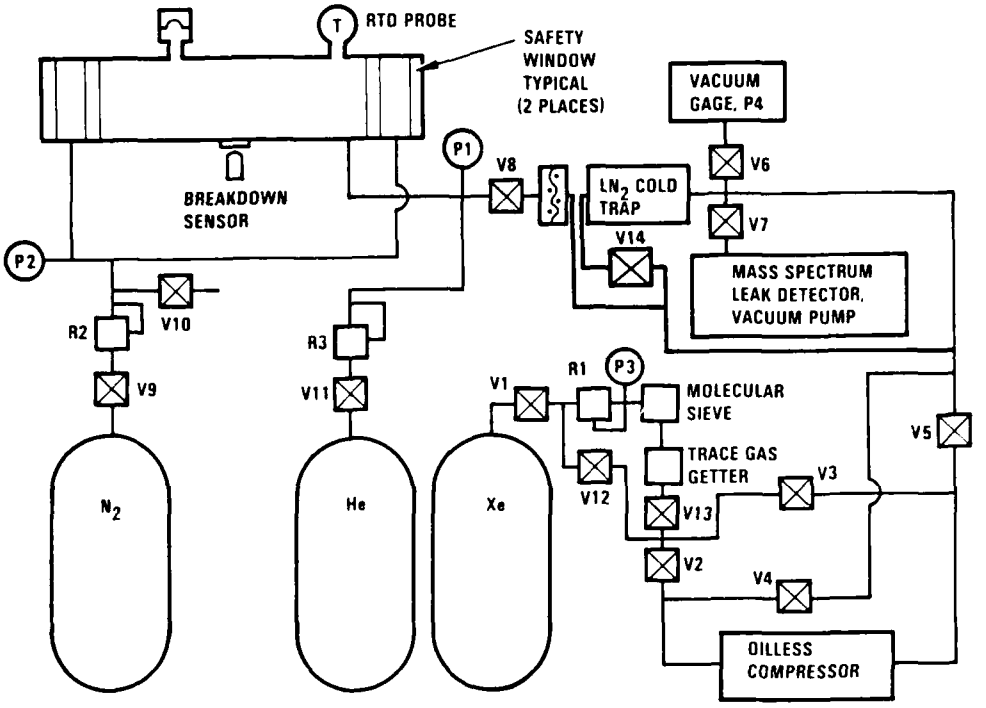

Figure 5-15. Static SBS cell support system.

Low absorption medium to limit power loss and thermal blooming

Filtration to class 10,000 clean room level to prevent contamination of optic components

Access and viewing of all experiment apparatus. Ability to change setup for later experiments without major redesign

Limit index of refraction gradients over beam path to satisfy tight beam steering and beam quality constraints

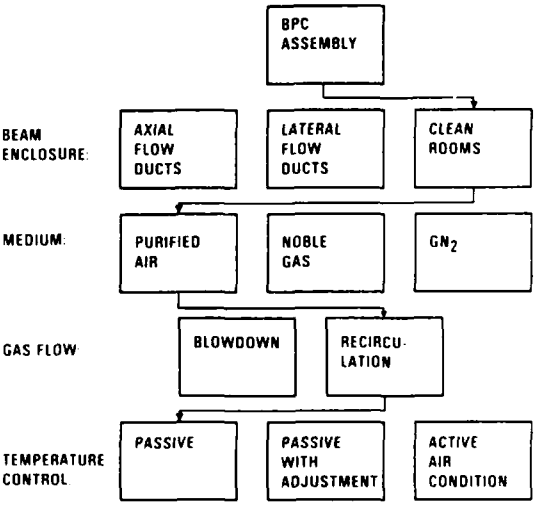

Figure 5-16. Beam path conditioning assembly (major requirements and trades).

The CLPCT BPCS requirements differ from several earlier programs in that a very large number of optical legs between approximately 50 mirrors must be conditioned and a sizable number of presently undesigned modifications to the optical train will be made as the experiments proceed. Providing individual ducts around each leg (as has been done on some programs) and modifying them throughout the program was visualized as extemely expensive. Instead the entire optic train will be enclosed in modular, commercial clean room enclosures that recirculate and filter the same BPC gas for contamination and equilibration control. Purified, manufactured air has been selected as the gas media in these enclosures to eliminate asphyxiation hazards to personnel. The air is mixed from cryogenic oxygen and nitrogen boiloff and contains a few parts per million CO_2 and H_2O. Table 5-2 outlines the plan.

The thermal requirements on various portions of this system are summarized in Table 5-3. The system depends largely on passive control, utilizing the building air conditioning as a small, nearly constant temperature sink, then attenuating the temperature swings of the recirculated air by equilibration with the large thermal masses of the delay line and concrete optical benches as shown in Figure 5-17.

Figure 5-18 shows the beam path conditioning enclosures installed in the APACHE building. Several zones are provided as opposed to one huge enclosure to maintain as much of the purified air charge as possible free from contamination when technicians must enter the enclosures to adjust or changeout optical components. The significance of this contamination by perspiration, respiration, and metabolic body heat is shown in Figure 5-19.

5.5 VACUUM DUCT ASSEMBLY

The essential requirements and trade issues involved in the design of the vacuum duct assembly are shown in Figure 5-20. A more complete listing of requirements versus capabilities is shown in Table 5-4. The resulting vacuum duct design is hown in Figures 5-21 and 5-22. The major portion of the 34-meter duct length is formed from flanged pipe sections. Both the oscillator and amplifier beams are introduced through separate windows in one end of the line and passed along the chamber length repeatedly for time delay and spatial filtering. The oscillator beam makes two passes along

TABLE 5-2. Beam Path Conditioning Assembly (Summary of Design).

Enclose entire beam train in zoned clean-room enclosures to avoid complexity of individual ducts. Use ducts in RPCL building where overhead is obstructed

Fill enclosures with CO_2, H_2O free purified air mixed on site to prevent beam absorption without safety hazard. Recirculate purified air to reduce supply costs and to equilibrate air with optic components

Provide adjustable thermal conductance between recirculating purified air and facility air conditioning outside enclosures

In local problem areas (e.g., mirrors with planes perpendicular to enclosure velocity) provide local fans and/or mixing screens

Temperature condition, new purified air to match enclosed components

Tune facility heat pump to reduce temperature variation outside insulated enclosures

TABLE 5-3. Beam Path Conditioning Assembly (HFC Beam Path OPD Distortions.

Beam Path Segment	Criteria	Path Length in BPCS (M)	Beam Width (Averaged) (cm)	Allowable (ΔT) Within Beam (K)	Allowable ΔT Air to Mirror (K)
Oscillator to oscillator Spatial filter	2 μrad Tilt	10.8	5.0	0.17	1.29
Oscillator spatial filter to amplifier spatial filter	2 μrad Tilt	32.6 to RPCL 21.7 post RPCL/	7.7 to RPCL input/12.0 Post RPCL	0.12	1.48
Amplifier spatial filter to SBS cell	BQ 1.020 (0.32 rms waves)	40.5	6.2	0.71	2.30
Diagnostic beamsplitter to diagnostic bench	BQ 1.020 (0.32 rms wave)	52.4	7.5	0.56	2.15

AD-A175 205 CHEMICAL LASER PHASE CONJUGATION TECHNOLOGY (CLPCT)(U) 2/2
TRW DEFENSE AND SPACE SYSTEMS GROUP REDONDO BEACH CA
APPLIED TECHNOLOGY DIV A D SCHNURR ET AL. 30 NOV 86
UNCLASSIFIED TRW-AP-0923 F/G 20/5 NL

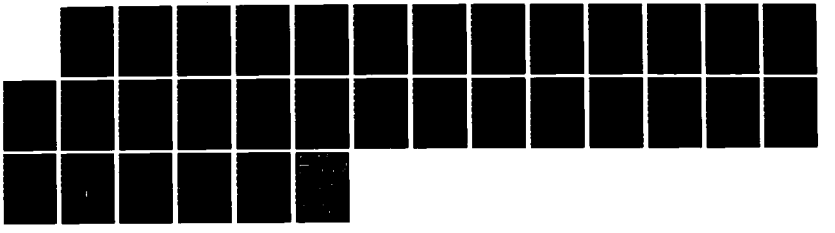

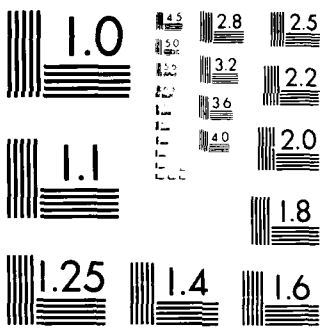

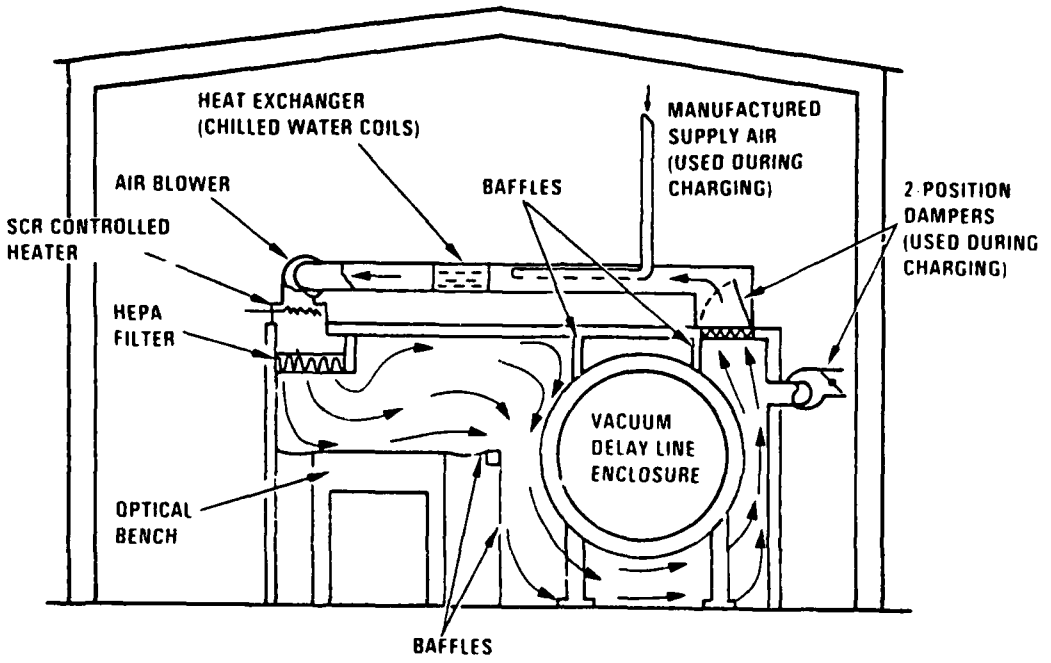

Figure 5-17. Beam path conditioning assembly design concept (clean enclosure subassembly CES).

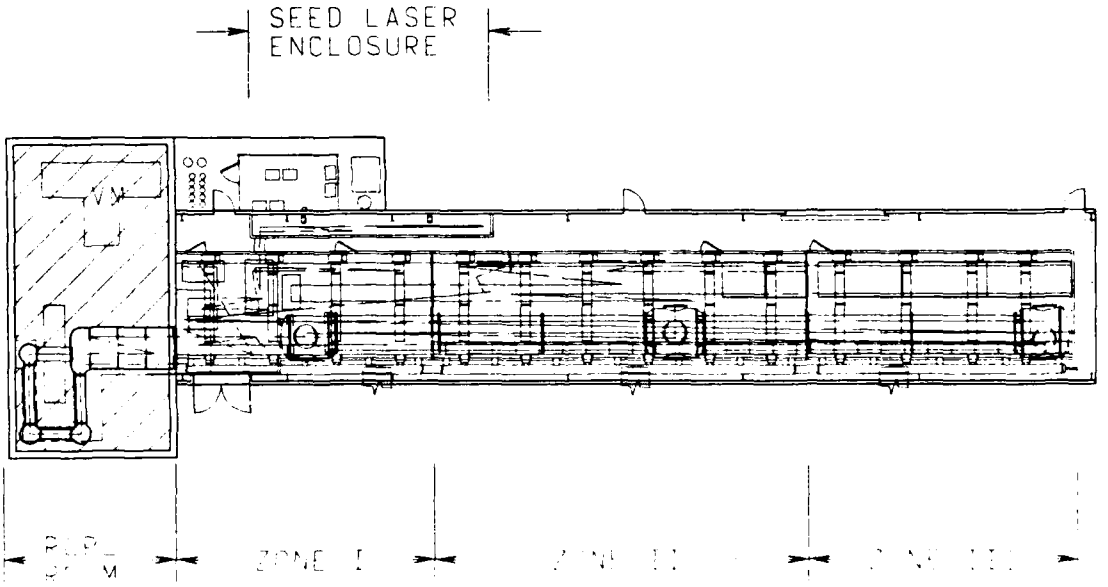

Figure 5-18. Plan of beam conditioning assembly.

Assume single worker, in diagnostics enclosure (126 m^3 volume, ≅ 50 m path)

25°C equilibration temperature

Conclude limited access to diagnostics may be made as long as $P_2(8)$ line is only concern (HFC)

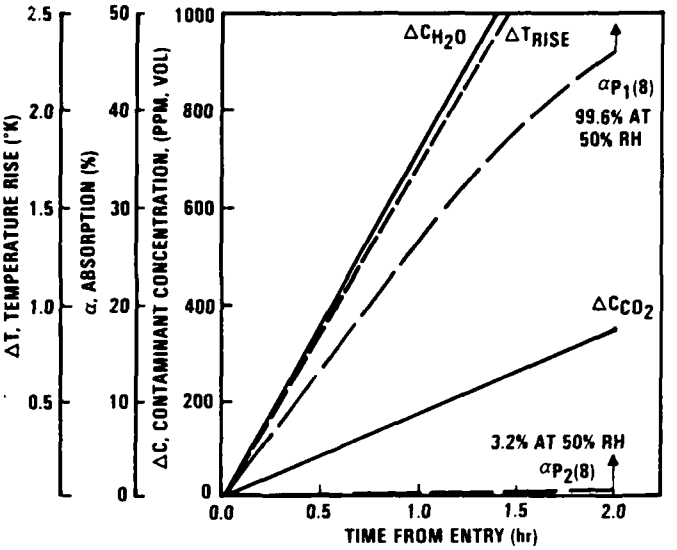

Figure 5-19. Personnel contamination of BPCS media.

Path length to isolate oscillator from return phase pulse, 320 m from SBS cell to oscillator

Pressure low enough to limit absorption, breakdown, and thermal blooming

Pumpdown in <30 min

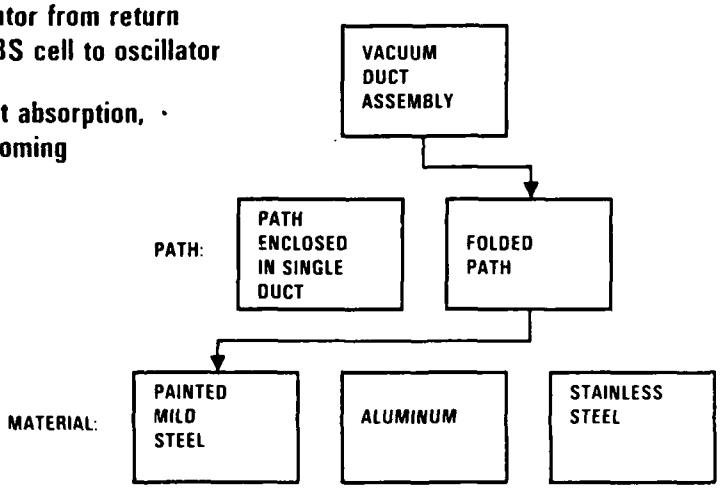

Figure 5-20. Vacuum duct assembly (major requirements and trades).

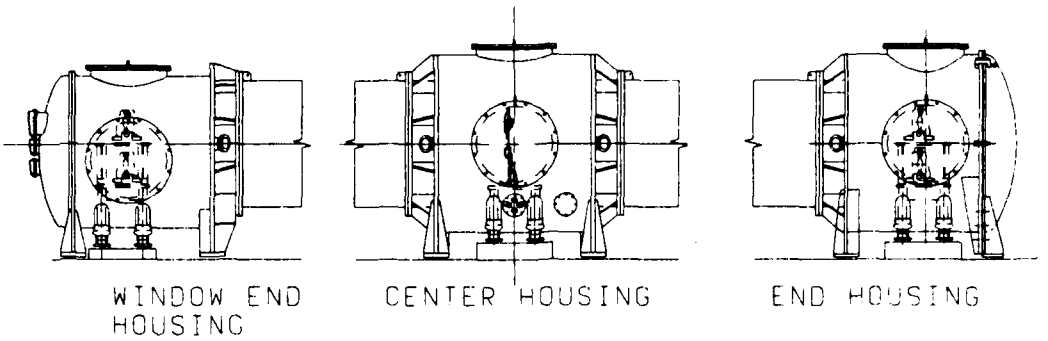

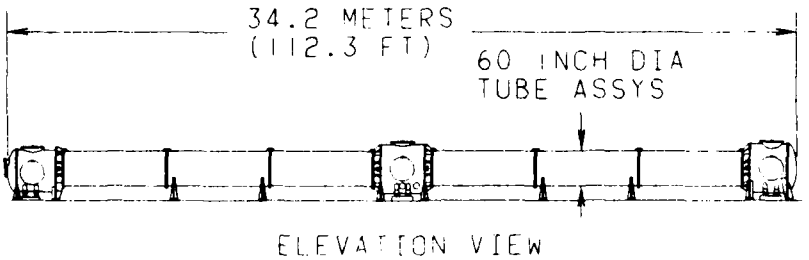

Figure 5-21. Vacuum duct enclosure.

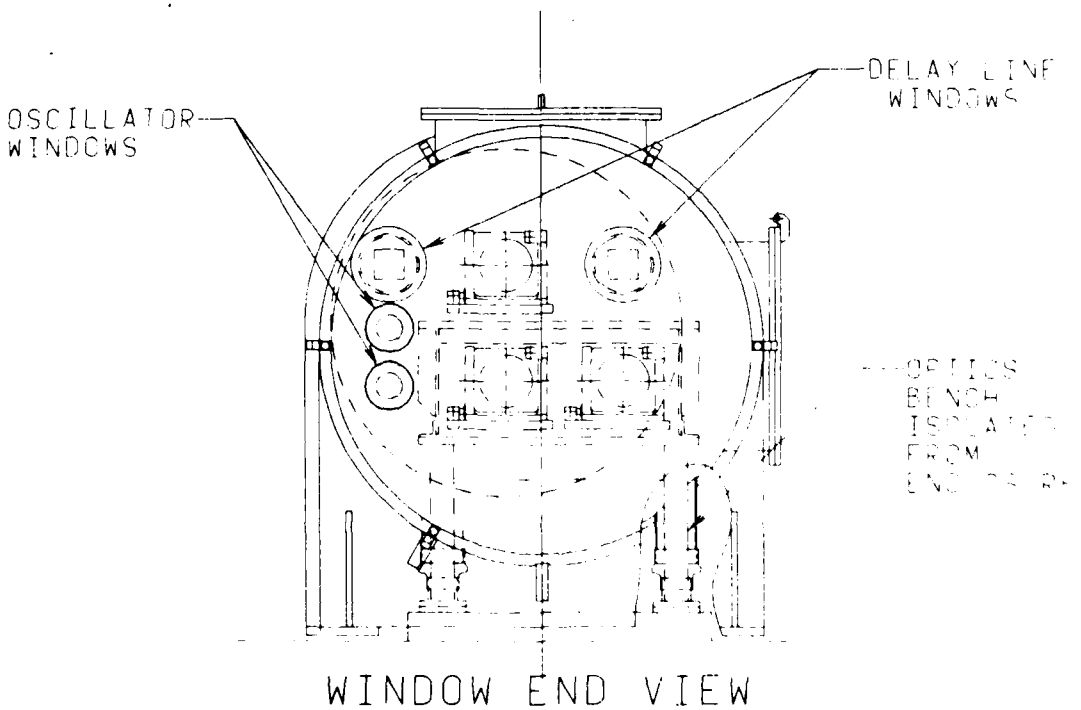

Figure 5-22. Vacuum duct enclosure.

TABLE 5-4. Vacuum Duct Assembly (Requirements Versus Capabilities).

Requirement	Relevant Features	Capability
Length • Sufficient to isolate a 1 μs FWHM pulse	Two passes of oscillator beam between optics 32 m apart plus eight similar passes of amplifier beam Total = 320 m	Total delay = 3.1 μs
Pressure • Low enough to prevent breakdown and single pulse thermal blooming	Hermetic welds Low-leakage seals	$<$ 5 torr
Medium • Absorptivity, particulates and trace gases low enough to prevent breakdown and thermal blooming	Mild steel vessel epoxy painted Clean before and after installation Gas vent valve connected to BPC assembly gas supply through particulate filters	Absorption = 6.1E-4% $P_2(7)$ (Grade B GN_2) Filtration: 0.3 μm
Windows: Satisfy • Fluence • Pressure • Beam quality • Power • Polarization • Alignment	CaF_2 material, Ar coated Mount design similar to RPCL Tilted to direct reflections out of train	See long-lead CDR
Accessibility • Access to optic components and diagnostics between tests • View ports • Feed throughs	Access ports top and both sides of three optical enclosures to reach two mounting levels Plexiglas viewports as required Electrical feed throughs for remotes	Complies
Pumpdown time • To operating pressure in $<$ 30 minutes	$>$ 500 ft^3/min pumping capacity Large diameter evacuation line LN_2 cold trap	760 to 5 torr in less than 30 min 1200 ft^3/min pump available surplus

the chamber while the amplifier beam is relayed through eight passes. Optical components requiring access for alignment or viewing are placed in three enclosures at the center and both ends of the duct. The end enclosures contain the relay mirrors on two level optical benches while spatial filtering is performed in the center enclosure.

6. HARDWARE ACQUISITION PLAN

Figure 6-1 shows the schedule for procurement of the various hardware and components required for the HFC experiment. Long-lead hardware was purchased under the CLPCT and NLOT programs whereas non-long-lead hardware was acquired under the APACHE program. Table 6-1 lists the long-lead hardware. Procurement of the long-lead transmissive CaF_2 optics was initiated in February 1986 with source selection being completed in March. It was expected that the long-lead schedule shown can be met, but only by employing extensive workarounds and deferring backup items beyond July 1.

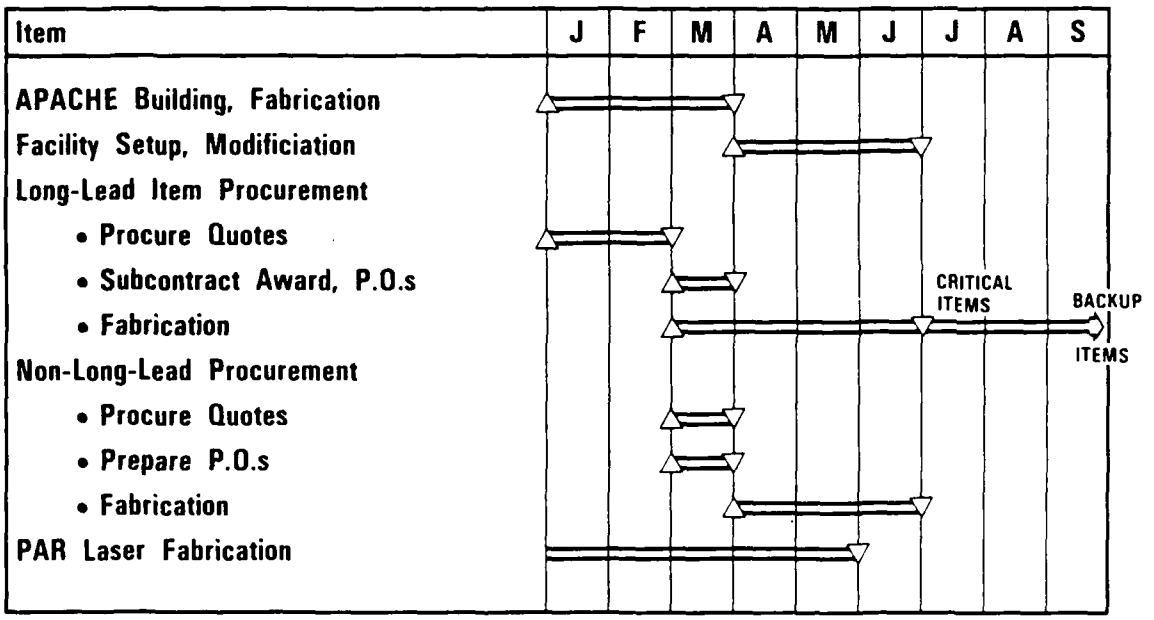

Figure 6-1. HFC hardware acquisition plan.

TABLE 6-1. Long-Lead Hardware.

Pockels cell

- Lithium-niobate crystal
- 20 mm x 20 mm clear aperture
- Damage threshold sample to preceed delivery
- Q-switch driver provides 10-ns switch time, ± 0.11 μs accuracy

Babinet compensator

- Magnesium-fluoride wedges
- 35 mm x 35 mm clear aperture
- Damage data from P. Nickles (classified)
- Micrometer provides wavelength adjustment

SBS cell windows, spatial filter alignment beamsplitters, back up spatial filter elements

- Calcium fluoride, uncoated
- Damage threshold of 700 J/cm^2
- SBS window 1,1,1 orientation provides additional damage resistance

Diagnostic beamsplitters

- Calcium-fluoride, AR coated one side only
- Coating damage threshold data form NWC (classified samples to preceed part)
- Uncoated surface provides 3% reflection

Delay line windows

- Calcium fluoride or alternative material to meet schedule needs
- AR coated both sides

RPCL amplifier windows, Brewster windows

- Calcium fluoride AR coated both sides

Polarizers

- Calcium fluoride
- Polarizing coated on front surface
- 100:1 extinction ratio
- Pair provides power throttling capability
- Damage threshold samples to preceed part

7. CONJUGATION SUBSYSTEM (COS) EXPERIMENT DESIGN TASKS

7.1 OVERVIEW OF COS EXPERIMENT DESIGN TASKS

7.1.1 Objectives of the COS Experiment

The Conjugation Subsystem (COS) Experiment consists of three separate subexperiments or test series, namely, COS 1, COS 2, and COS 3. The objectives of these experiments are defined in the following paragraphs:

COS 1. This is an SBS parameterization experiment that utilizes a static SBS cell to examine phase conjugation effects important to the design of an SBL system. The experiment will use the HFC experiment hardware (i.e., single line pulsed HF laser, optical delay line, spatial filter, static xenon SBS cell, etc.) to vary the following effects:

1) Incident energy

2) Cell pressure

3) Focusing telescope f/number

4) Beam quality aberrations (magnitude and spatial frequency)

5) Beam shape

6) Medium purity/absorption coefficient.

Effect Number 4 will be modeled by placing various aberrator plates in the beam and measuring power and beam quality, which allows calculation of conjugation reflectivity and fidelity. The lasers to be used are the RPCL and PAR devices.

COS 2. This is an experiment to examine the effects of focusing multiple lines in a single SBS cell, either in the same volume or angularly separated. The important issue is the effect of frequency and spatial separation of multiple lines within the SBS interaction volume. It will be designed to be a simple extension of the COS 1 test matrix, with a minor optical configuration change. The preferred laser device is the PAR PCL device since the RPCL power is not required and the PAR operating expense is less.

COS 3. This experiment examines the effects of a flowing SBS cell medium on SBS reflectivity and conjugation fidelity. The important parameters are those which affect thermal blooming and/or smearing of the phonon grating such as input energy power absorption coefficient, f/number, SBS medium purity, input beam quality and flow velocity or relative velocity due to a scanning

mirror. The COS 3 experiment will use a scanning mirror to simulate the effects of a flowing gas SBS cell; however, the design of the subscale flowing gas SBS cell will be taken to PDR level. The COS 3 apparatus will allow the beam to be slewed across the SBS medium at constant velocity. A goal is to use the same scanning mirror design as used for the CWCS experiment. The RPCL and PAR devices will be used for the experiments at CTS.

In summary, the COS 1 subexperiment will use the HFC experiment hardware to extend the parameter space. The COS 2 and COS 3 experiments will address the issues of multiline effects and moving SBS medium effects, respectively.

7.1.2 COS Design Tasks

The following hardware was designed for the COS experiment to a conceptual design review (CoDR) level:

1) COS 1 Hardware. The baseline COS 1 experiment will use precisely the same hardware as the HFC experiment. However, at the start of the CLPCT program it was desirable to consider a redesigned initiation assembly for the RPCL subsystem which would extend its available output energy and peak power. This design was not pursued past the conceptual design stage when it was discovered that (a) the baseline would yield sufficient power margin and (b) a higher energy RPCL would have the undesirable effect of shortening the pulse length.

2) COS 2 Hardware. The COS 2 experiment will use essentially the same hardware as the HFC and COS 1 experiments which were designed for single line SBS measurements. For the COS 2 (i.e., multiline) experiment, the grating will be moved from its original position (upbeam of the delay line) to a new position in the near field of the input beam just upbeam of the SBS cell.

3) COS 3 Hardware. The COS 3 experiment will use a modification of the HFC experiment hardware for the purpose of validating that a flowing gas SBS cell can be used to prevent thermal blooming. Initially the use of an actual flowing SBS cell was considered. However, the preferred approach is to use the HFC/COS 1 static gas SBS cell and to simulate the effects of a flowing gas SBS cell by the use of a beam scanning mirror. The concept is to scan the far-field focal spot within the static SBS cell with a velocity relative to the gas that would match the design flow velocity of the transversely flowing SBS cell. The scanning mirror or "beam scanner" is simply a rotating mirror which is synchronized so that the position of the focal spot will be centered within the SBS cell when the PCL fires.

In summary, the COS experiment design tasks led to the development of design concepts for the RPCL initiation system which was considered for the COS 1 experiment and a flowing gas SBS cell which was considered for the COS 3 experiment. Both design concepts, discussed in considerable detail in this report, were developed to a CoDR level during the CLPCT program. The RPCL initiation system upgrade is not required for the COS experiment so will not be further pursued. The flowing SBS cell is not required for the COS 3 experiment since the relative motion effects can be more easily studied with a beam scanning mirror. However, the design concept for a flowing gas cell will be further studied under the APACHE project.

7.2 COS REQUIREMENTS

Overall requirements on the COS experiment are given in Table 7-1. Many of these data, particularly those requiring wide SBS cell apertures, will be collected on the static SBS cell assembly designed for the HFC experiment. A flowing cell concept was developed to allow better definition of design that would be required to mock-up key aerodynamic

TABLE 7-1. COS System Level Requirements.

Requirement
Accommodate pulse lengths between 1–10 μs
Isolate oscillator
Find effects of flowing media/provide experiment flexibility
Static cell with material window
Flowing cell with aerowindow
Flowing cell with material window
Back-Injection Experiment
Path matching
Overlap of seed and pump beams
Seed beam power control
Seed beam frequency shift
Match seed polarization to Stokes
Two-Line Experiment
Far-field separation by 50 spot radii
Spatial filtering of separate lines

features. In the interest of utilizing the most realistic design approach, a concept design for a complete, fully assembled cell was developed.

Specific requirements on the transverse flowing SBS cell are given in Table 7-2. Perhaps the most important requirement is that the cell design be scalable to CW SBL conditions as there is neither interest nor need for a high-speed flowing cell applicable only to single-pulse testing. The goal of single-pulse testing with a flowing cell is to reach a combination of pulse duration and media velocity that simulates steady-state operation in the focal interaction volume. Since the dimensions of the interaction volume do not increase in scaling to a high-power SBL device, we are already testing an essentially full-scale flowing cell.

The design flow velocity range of 20 to 80 m/sec has been set based on hand calculations of the velocity necessary to hold thermal blooming distortion of the beam to a beam quality of 2.0. This requirement will be refined as thermal blooming, self-focusing, and phonon shifting effects are added to the BOUNCE and BRIWON SBS analysis codes.

7.3 RPCL INITIATION ASSEMBLY

7.3.1 Description of the Existing RPCL Initiation Assembly

The 50-liter cavity Repetitively Pulsed Chemical Laser (RPCL-50) is a photolytically initiated pulsed chemical laser which is capable of producing either an HF or DF pulsed beam which is repetitively pulsed (with a classified pulse repetition frequency). The flash photolysis initiation uses xenon flashlamps to produce ultraviolet phonons, which dissociate fluorine molecules, thus initiating the HF/DF chemical chain reaction. Figure 7-1 illustrates the 50-liter RPCL cavity with 40 ILC flashlamps on each side. The primary characteristics of the initiation system are as follows:

1) 80 ILC xenon flashlamps (arranged in 40 lamp-pair series circuits)
   - 4-mm ID
   - 30-cm length
   - UV efficiency, $\eta_{UV} \simeq 0.16$

TABLE 7-2. COS Flowing Cell Requirements Versus Capabilities.

Requirement	Capability
Scalability: concept shall permit operation under CW conditions and simulate SBL application to the greatest extent practical	Complies, consistent with funding limits
Media: xenon and consider other gases	Xenon at 40 atm examined
Cell pressure: 10 to 40 atm	Comply
Medium purity: as necessary to limit far-field spot size	$<$0.1 PPM of H_2O, CO_2, N_2O
Flow velocity: 20–80 m/s	20 m/s baseline 80 m/s can be reached for 1/4 test duration
Transverse velocity vector: adjustable with respect to beam centerline	Adjustment will be made in external train
Temperature uniformity, wall to medium	Several media aberrations require additional study
Aperture size: sufficient for single f/15 beam	Beam combination to be conducted in static cell
Media length: sufficient for 10 DOF of f/30 beam	f/10, f/40, and f/50 tests to be conducted in static cell
Entrance aperture OPD in accord with BQ budget	TBD
Media recycling in $\leq$45 min	Comply
Prevent liquid condensation in beam	Comply
Accommodate focus position tolerance of 0.5 cm axial and transverse	Comply
Limit Xe capacity to $50,000 per charge	Comply
Limit He flow requirements to that obtainable from existing facility ($\sim$3 lbm/s)	Comply

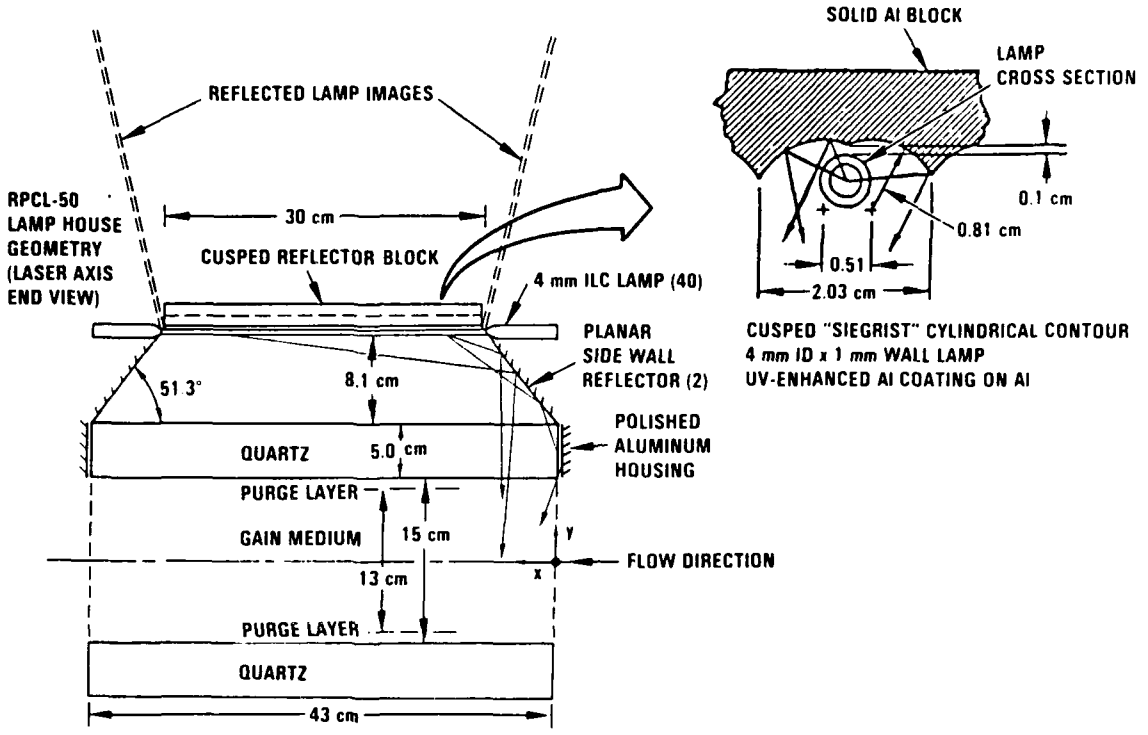

Figure 7-1. Existing RPCL-50.

2) Efficient lamphouse design

- Dual cylinder aluminum "Siegrist" reflector behind each lamp
- Sidewall reflectors (with UV enhanced reflective coatings)

3) 2.1 μs FWHM (full width half maximum) pulse duration

4) Electrical input energy, $E_E = \frac{N}{2} CV^2 = 11$ kJ (at 50 kV)

- 50 kV charging voltage
- 0.22 μF capacitor per circuit.

Figure 7-1 shows that the lamphouse is designed with highly efficient first surface quartz sidewall reflectors in order to couple the UV energy into the cavity. The following sections describe the pertinent performance parameters and scaling laws.

7.3.2 Performance Scaling Law

Section 3.2.2 contains a description of the scaling laws that apply to the prediction of laser pulse energy and pulse duration. The specific outcoupled laser energy, in Joules per liter-atmosphere of cavity size, scales according to the relationship,

$$\epsilon_L = K_\epsilon \, P_{F_2} \, \delta_{F_2}^{1/2} \, \alpha_{th}^{-1/6}$$

where

K_e = empirical energy constant ($J\ell^{-1}torr^{-1}$)

P_{F_2} = initial pressure of F_2 (torr)

α_{th} = rigrod parameter

Reference 15 gives the following equation for the fluorine degree of dissociation, F/F_2:

$$\delta_{F_2} = 0.090 \, \epsilon_E \eta_{UV} \eta_C \, P_{F_2}^{-1}$$

where

ϵ_E = electrical input energy per unit cavity volume ($J\ell^{-1}$)

$\eta_{UV} = \frac{\text{UV energy from flashlamps}}{\text{electrical energy to flashlamps}}$ = UV efficiency (-)

$\eta_C = \frac{\text{UV energy absorbed in cavity}}{\text{UV energy from flashlamps}}$ = coupling efficiency (-)

P_{F_2} = flourine partial pressure (torr)

It is seen that the degree of fluorine dissociation is directly proportional to the term, $\epsilon_E \eta_{UV} \eta_C$ (which is the UV energy deposited in the cavity) and inversely proportional to P_{F_2}.

Evaluating the fluorine dissociation for the baseline RPCL initiation system design with $\eta_{UF} = 0.16$, $\eta_C = 0.30$, $\epsilon_E = 11{,}000/50 = 220\ J\ell^{-1}$ and $P_{F_2} = 152$ torr:

$$\delta_{F_2} = \frac{0.090(220)(0.16)(0.30)}{152} = 0.00625$$

Note that the fluorine dissociation is proportional to the UV fluence at the lamp plane which can be evaluated:

$$e_{lamp} = \frac{NE_E\eta_{UV}}{A_{lamp}} = \frac{(5500)(0.16)}{(30)(83.2)} = 0.352\ J\ cm^{-2}$$

The average UV fluence coupled into the cavity (for two sided pumping) is:

$$e_{UV} = \frac{2NE_E\eta_{UV}\eta_C}{A_{cav}} = \frac{(11000)(0.16)(0.30)}{(43)(89)} = 0.138\ J\ cm^{-2}$$

Therefore the RPCL performance scaling laws indicate that the laser energy could be doubled by quadrupling the UV fluence from the initiation assembly. However, the SOSHF code (see Section 3.2.2) indicates the pulse duration scales as ϵ_L^{-1} so that doubling the energy would result in one-half of the original lasing pulse duration.

7.3.3 Motivation for Redesign Effort

The rationale and motiviation for the initiation assembly redesign effort can be summarized as follows:

- Increased lasing energy/SBS design margin - Increasing the available lasing energy by a factor of 1.4 to 2.0 will increase the lasing pulse peak power thus increasing the design margin (i.e., amount over SBS threshold power). It is important for the system to have adequate margin for the nominal case of best beam quality and largest initiation strength. COS tests will explore the effect of poor beam quality and decreased SBS cell pressure with both factors drastically reducing the design margin.

- Decreased potential project interference - Use of a dedicated initiation assembly for single-pulse APACHE tests would mean that this test program would not be affected by possible performance degradation and/or schedule slips caused by excessive usage on other repetitive pulse RPCL test programs.

7.3.4 Design Requirements

The objective of this effort is to redesign the RPCL flashlamp initiation assembly in order to increase the UV energy that is deposited in the laser cavity, thus increasing the outcoupled single pulse HF lasing energy. The requirement is to double the UV energy while preserving the effective flashlamp pulse duration at approximately 2 μs, which would increase lasing energy by 40 percent. The goal is to increase the UV energy by a factor of 4, thus doubling the HF lasing energy. The detailed design requirements are as follows.

- Single Pulse Operation. The flashlamp initiation assembly shall produce a single pulse of ultraviolet energy which will initiate HF chain reaction lasing in the 50-liter RPCL cavity. The pulse shall be triggered by the same signal which triggers the present repetitively pulsed initiation assembly. The capacitor banks shall be recharged in ≤30 sec.

- Average UV Fluence. The UV fluence, measured within the RPCL cavity at the plane of the quartz initiation windows, shall be temporally averaged over the first 2 μs of the flashlamp pulse and spectrally averaged over the F_2 absorption band of $240 < \lambda < 360$ nm. When spatially averaged over the area of the initiation window (i.e., the xz plane), the average UV fluence shall be as follows:

  1) Requirement:

     $\langle e_{UV} \rangle \geq 0.138$ J cm^{-2} (factor of 2 greater than original design)

  2) Goal:

     $\langle e_{UV} \rangle \geq 0.276$ J cm^{-2} (factor of 4 greater than original design)

- Spatial Variation of UV Fluence. The spatial variation of the UV fluence in the plane of the initiation windows influences the initiation uniformity and, hence, the cavity medium homogeneity. For a media contribution to the beam quality of 1.4 and treating this OPD as a deterministic sine distribution in the x direction results in the following requirement for spatial variation of UV fluence with respect to the x (i.e., flow) direction:

$$\frac{\Delta_{uv}}{\langle e_{uv} \rangle} \leq 0.15$$

This requirement governs the design of the sidewall reflectors which are on the sides of the flashlamp plane.

- Ease of Access and Removability. The initiation assembly shall be designed for ease of access and maintenance. Modular subassemblies and components shall be considered in the design. Ease of replacement of flashlamps (or flashlamp modules) and spark gaps is particularly important. This assembly shall be easily installed and removed from RPCL with a change-over time (including checkout tests) of ≤2 days.

- Flashlamp Lifetime. The initiation assembly flashlamps shall be operated at pulse energies well below the explosion limit, such that the average lifetime before failure is ≥1000 shots.

- Reflector Degradation. Long term degradation of the UV reflectivity of the flashlamp reflectors shall be avoided by (a) careful design of the lamphouse to prevent F_2 and HF intrusion, (b) consideration of protective UV reflective coatings, and/or (c) reflectors (for preventative maintenance).

7.3.5 Candidate Design Concepts

The approach taken for the redesigned initiation assembly was to increase the flashlamp UV fluence by (1) increasing the capacitance for each flashlamp pair and (2) increasing the flashlamp density. Reference 16 presents data that indicates the flashlamp diameter must also be increased for the increased capacitance in order to preserve the desired short flashlamp pulse duration. This reference also indicates that the UV efficiency is also affected by the capacitance and lamp diameter. Table 7-3 indicates the effect of increasing the lamp diameter, capacitance (per circuit) and packing density (N') relative to the UV energy deposited in the cavity and resultant lasing energy.

TABLE 7-3. Comparison of Initiation Assembly Redesign Options Relative to Increased UV Fluence/Energy.

Configuration	Lamp Dia. D_j (mm)	$\frac{C}{C_{BL}}$ (-)	$\frac{N'}{N'_{BL}}$ (-)	$\frac{E_E}{E_{E,BL}}$ (-)	η^{UV} (-)	η^{C} (-)	$\frac{E_L}{E_{L,BL}}$ (-)
Baseline	4	1.00	1.00	1.00	0.170	0.30	1.00
Option A	5	2.00	1.23	2.46	0.118	0.30	1.31
Option B	5	2.00	1.40	2.80	0.118	0.30	1.39
Option C	5	2.00	1.60	3.20	0.118	0.30	1.49
Option D	7	2.00	1.23	2.46	0.101	0.30	1.21
Option E	7	3.23	1.23	3.97	0.079	0.30	1.35
Option F	7	3.23	1.40	4.52	0.079	0.30	1.45

It is seen that Option C, which uses the 5-mm lamp diameter with the highest packing density, results in the largest increase in lasing energy. This option would yield an energy increase of 49 percent which would satisfy the requirement of at least 41 percent. Therefore, it was decided that this option would be continued to a CoDR level.

7.3.6 Conceptual Design

The candidate design (i.e., Option C) was developed to a conceptual design and actually breadboard tested in the laboratory. The resultant design, shown in Figure 7-2, uses a module that is the same size as the existing module, but fitted with 16 5-mm diameter lamps rather than 10 4-mm diameter lamps. Figure 7-3 shows the pulse forming network for a typical circuit which drives a pair of lamps. Compared to the original design, the significant design features are as follows:

- Use of 2 ILC model L5827 xenon flash lamps coupled in series to a 0.50 μF capacitor.
- Use of higher lamp packing density made possible by potting the lamp electrode ends in silicone rubber rather than damping them with phenolic blocks.
- Use of an improved spark gap which features smaller volume and lower jitter.
- More efficient packaging of components with emphasis on minimum inductance and adequate dielectric insulation (for 50 kV).

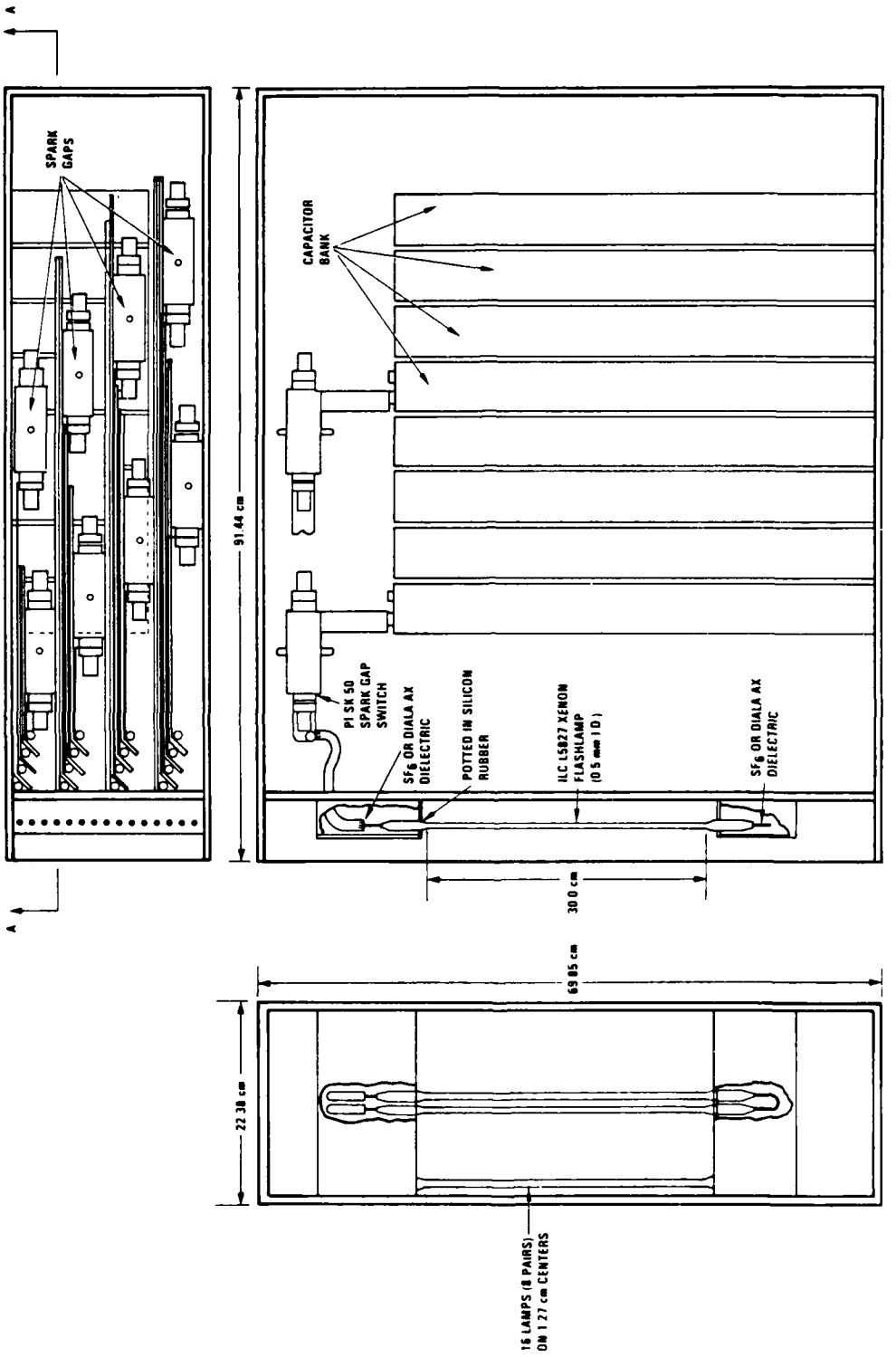

Figure 7-2. RPCL initiation assembly module design.

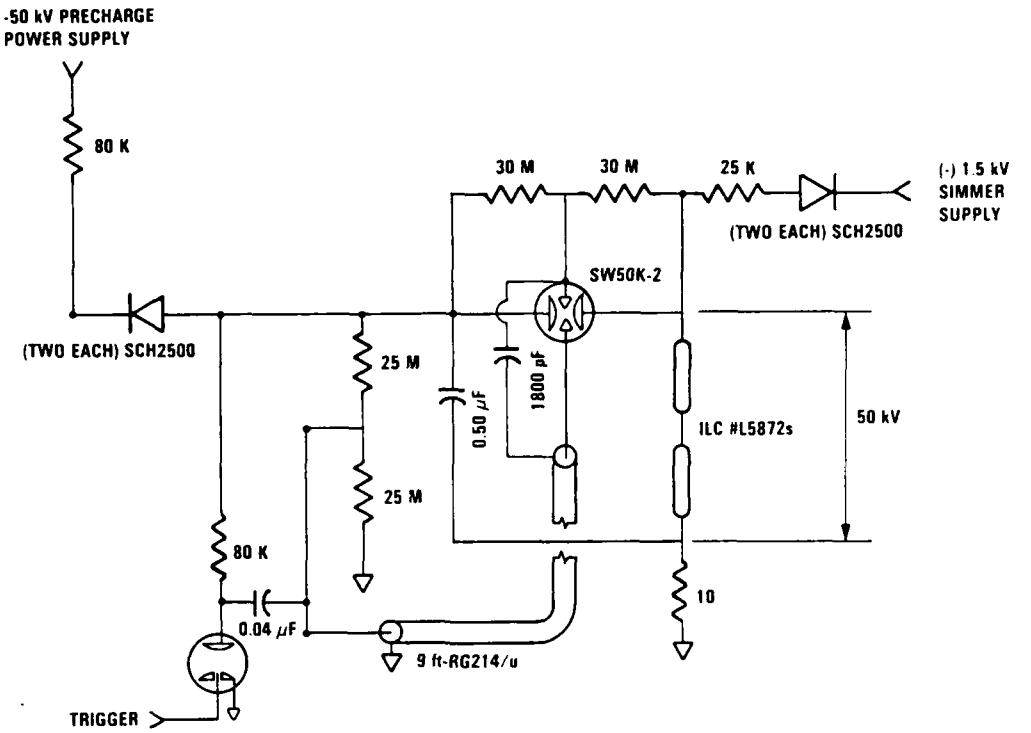

Figure 7-3. Pulse forming network design.

A breadboard test was conducted for a typical two-lamp, pulse-forming network which was packaged as it would be in the module. The results of the breadboard test proved that the design satisfies the design requirements listed in Section 7.3.4. The circuit successfully operated with a 50 kV charging voltage. Current waveforms and integrated, spectrally weighted UV fluence was measured.

7.4 FLOWING SBS CELL CONCEPTUAL DESIGN

7.4.1 Introduction

The objective of the flowing SBS design task on CLPCT was to define a conceptual design of a flowing gas SBS cell that could be used in ground-based aerodynamic and conjugation experiments and which is scalable to a system which could be used in the space-based APACHE device. As part of the work expected to follow this program, key elements of this conceptual design would be developed to a detail design and fabricated for experimental use.

7.4.2 Design Requirements

Table 7-4 summarizes the design requirements for an experiment-compatible flowing SBS cell. The SBS medium to be used is xenon at a pressure of 40 atmospheres and ambient temperature. The cell is to be designed to accommodate an f/number range of 15 - 30 with a cell length in excess of ten times the depth of field in order to allow adequate interaction length for the SBS process. It is also required that beam quality degradation within the SBS cell be less than 0.2 wavelength, and that no liquid condensation exists in the beam path. Flow rate requirements are that the cell has the capability of flowing the xenon between 20 and 80 m/sec. This requirement ensures adequate flexibility to operate at an optimum design point with regard to thermal blooming and forward SBS processes.

7.4.3 Trade Studies

As part of the concept design effort, several configurations were analyzed in a trade study to define the optimum concept. These design options are summarized in Table 7-5. The first configuration considered was that of a supersonic flow nozzle axially oriented with respect to the beam. Such a configuration acts to entirely eliminate the frequency shift of the SBS process by positioning the conjugation region at the sonic throat where the acoustic phonon field has zero propagation velocity. One very serious problem with this design is the condensation which occurs in the xenon shortly after the sonic nozzle in the supersonic portion of the flow field. Additionally, problems exist with regard to medium-induced defocusing of the beam due to transverse density gradients and with the excessively large amounts of xenon required to flow the gas at high pressures and sonic velocity. As a result of these design difficulties, a second design option was considered using a subsonic axial flow nozzle in order to reduce but not totally eliminate the SBS doppler shift. This design had the advantage of eliminating the condensation problem, because in this configuration the gas never flows supersonically. However, the problems of beam defocusing and large xenon quantities, although reduced in magnitude from the supersonic configuration, still raised major design issues.

TABLE 7-4. Design Requirements for the Flowing SBS Cell.

Optical requirements

- **SBS medium: xenon at 40 atm and 300 K**
- **f# range: 15-30 (based on the side of a square beam)**
- **Beam quality of 2.0 (OPD = 0.2 wavelengths)**
- **Beam defocusing less than double the spot diameter**
- **Length of cell: 10 x depth of field (11 cm at f#30)**
- **No liquid condensation within beam path**
- **Focus position uncertainty: ± 0.5 cm axial and transverse**

Flow requirements

- **Xenon flow at 20-80 m/s**
- **Xenon to be reused after each test (turnaround time under an hour)**
- **3 lbm/s helium flow, tentative maximum available at Capistrano Test Site**
- **40 kg supply of xenon in flow loop**

TABLE 7-5. Summary of Design Options Considered as Part of the Trade-Off Analysis of the Flowing SBS Cell Concept Design.

Flowing gas cell

- **Supersonic axial flow nozzle**

  Eliminate SBS frequency shift by conjugating in a long throat at Mach 1

  Technical issues: gas condensation, beam defocusing, very large requirement of gasses

- **Subsonic axial flow nozzle**

  Reduce SBS frequency shift by conjugating in a long throat at a Mach number between 0.75 and 0.99

  Technical issues: beam defocusing, large quantities of gas required

- **Modest subsonic transverse flow**

  Sweeps out the focal region on time scales much longer than the phonon rise time, but shorter than times for forward SBS and for significant temperature rise

  Technical issues: pressure matching the SBS cell to the aerowindow

Beam outcoupling

Axial flow aerowindow

While the axial flow configurations were being considered, a parallel study of the effects of SBS frequency shift on the amplifier extraction efficiency revealed that the shift had very minimal detrimental effect on the amplifier performance. As a result of this analysis and in recognition of the serious design problems associated with the axial flow design, a third option consisting of a low speed transverse flow design was considered. The motivation for this configuration is to provide continuous flow of gas within the conjugating region in order to eliminate thermal blooming and forward scattering processes from becoming important while accepting the SBS frequency shift without any attempt to reduce or eliminate it. This design significantly reduces the problems associated with beam defocusing and large xenon flow requirements.

In all of the configurations, it was recognized that a space-based system will have power levels far in excess of what could be tolerated by conventional transmissive optics, unless the cell was made excessively long in order to move the beam outcoupling port from the conjugation region near the beam focus. The concept adopted for beam outcoupling is an aerowindow which, owing to its low index of refraction, utilizes helium to accommodate the pressure matching between the high pressure xenon and the vacuum of space.

7.4.4 Description of Cell

Figure 7-4 shows a schematic layout of the flowing SBS cell conceptual design. The flowing cell system consists of five major elements:

- Flowing SBS cell
- Aerowindow
- Vacuum chamber
- Xenon cold trap
- Associated plumbing hardware.

Starting from the high pressure xenon storage supply tank, the gas is supplied to the SBS cell through a sonic orifice used to maintain constant flow rate. The gas enters the cell and passes through a high pressure drop screen bed used to uniformly distribute the flow downstream of the turn.

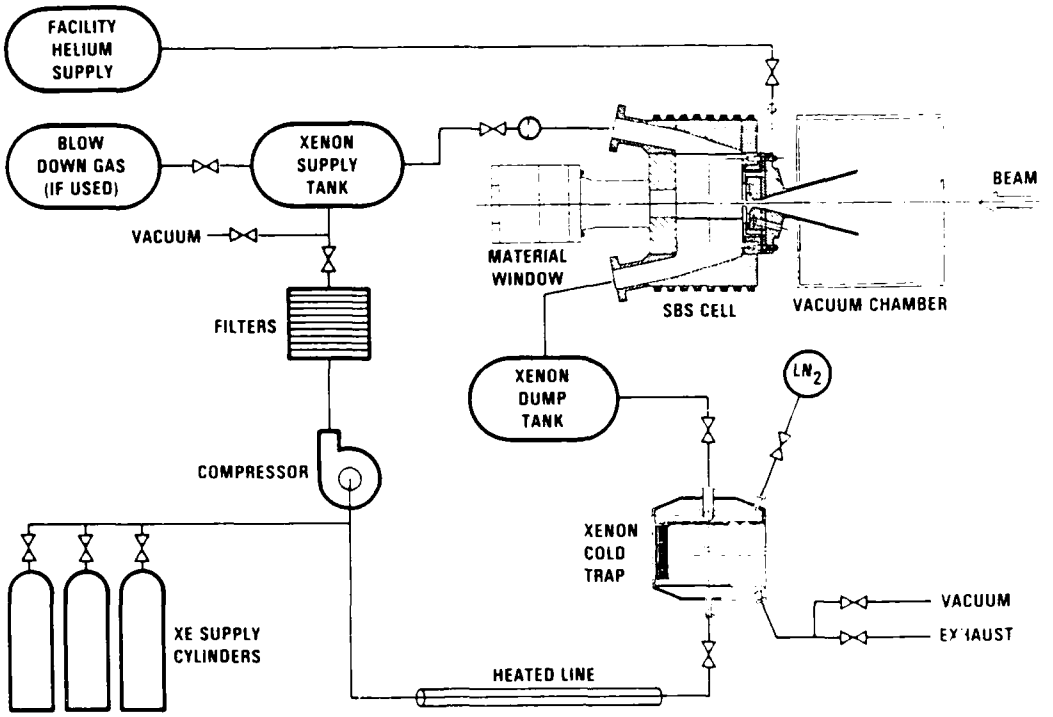

Figure 7-4. Block diagram layout of the flowing SBS cell conceptual design.

The gas flows downstream for a distance sufficient to attenuate turbulence from the flow distributor, after which it passes through the conjugating region. Once past the conjugating region, the gas leaves the cell and flows into a xenon dump tank which acts as a storage tank for the gas used during the run.

Following a run, the gas stored in the dump tank is slowly fed into a cold trap where the xenon is trapped out and any entrained helium from the aerowindow or other contaminants are removed; the gas is then repressurized for use on subsequent tests. Beam incoupling and outcoupling of the pump and Stokes beams are accomplished using a helium aerowindow. In the present design, helium is fed radially into a sonic orifice and expands in a conically shaped diffuser. In order to simulate a space-based environment, a vacuum chamber is placed downstream of the aerowindow.

Figure 7-5 presents dimensional information for the SBS cell conceptual design. The cell dimension in the direction of the beam axis is required to be larger than ten times the depth of field of the beam. For the f-number = 30 beam, with 0.5 cm margin on each side, this dimension is approximately 11 cm. A 2-cm aperture is required on the cell exit window to prevent the beam from striking the walls of the cell for the f-number = 15 beam. The 20-cm length of the cell in the flow direction is chosen to ensure adequate dissipation of the turbulence downstream of the flow distributor at the upstream entrance of the cell.

Figure 7-6 shows the conceptual design of the flowing SBS cell aerowindow. The throat diameter of 2.1 cm is chosen to accommodate the f-number = 15 beam without striking the walls of the device. A 15-degree conical nozzle is used to expand the gas to the low pressure conditions maintained in the vacuum chamber. The aerowindow design was sized to be compatible with existing helium supply facilities at the TRW Capistrano Test Site, which can provide helium mass flow rates of 3 lbm/sec.

Separating the high pressure xenon flow from the high velocity helium flow is a xenon-helium separation chamber which is depicted in Figure 7-7. Within this chamber, two low-speed streams of helium and xenon flow collinearly and provide a laminar interface between the large refractive index change from helium to xenon. With this design, this large index change occurs across a boundary which is nearly planar, thus minimizing the effects on optical phase distortion.

Figure 7-8 shows schematically the vacuum chamber layout. The low pressure conditions in the vacuum chamber are controlled using the existing 27,000 gallon vacuum vessel located near the COS experiment test stand.

The pumping capacity of the steam ejector is 0.6 lbm/sec of helium which is less than the maximum 3 lbm/sec mass flow rate of the helium aerowindow. Consequently, the vacuum conditions within the chamber cannot be maintained during the course of a run. However, the gas feed system design calls for the use of fast-acting solenoid valves and flow rates controlled with sonic orifices (as opposed to regulators) such that the establishment time for steady-state conditions is approximately 50 msec. During this time, under maximum helium flow rates the pressure within the combined

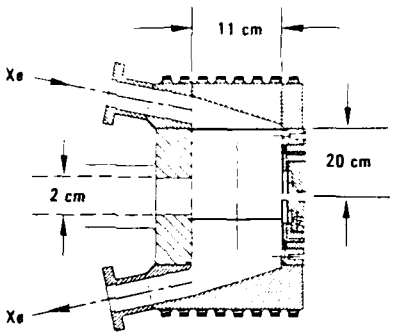

Length equals 10 times depth of field (ΔL) for an $f_s^\# = 30$ beam, plus focus uncertainty of 0.5 cm

$$L = 10 \cdot \Delta L + 0.5 = (10) \cdot 4\lambda \, (f_s^\#)^2 + 0.5 \cong 10.6 \text{ cm}$$

Width chosen to allow an $f_s^\# = 10$ beam to exit cell without striking walls

$$W = 2 \cdot \left[\frac{(5.5 + 0.5)}{2 \cdot f^\#} + 0.5 \right] \cong 2 \text{ cm}; \; f^\# = \frac{f_s^\#}{\sqrt{2}}$$

Height chosen to be sufficiently large to allow turbulence within the entering gas to decay

Figure 7-5. Conceptual design information for the flowing SBS cell.

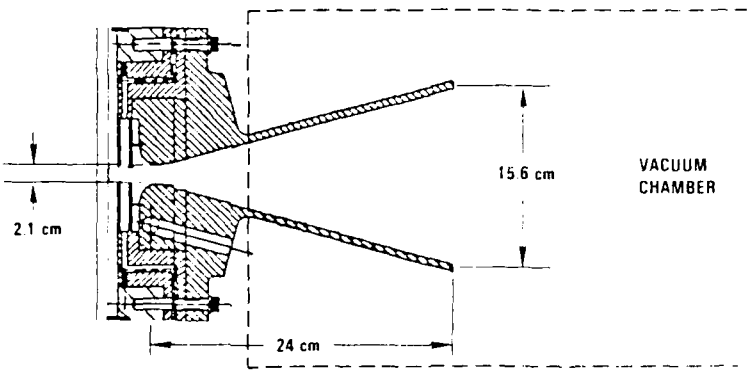

Helium supplied aerodynamic window to interface SBS cell to outside environment to prevent xenon condensation

Low index of refraction helium provides a smooth transition to a vacuum environment to reduce optical distortion

Helium exhausted by nozzle into a vacuum chamber

Helium flow rate 3 lbm/s

Figure 7-6 Aerowindow conceptual design for the flowing SBS cell.

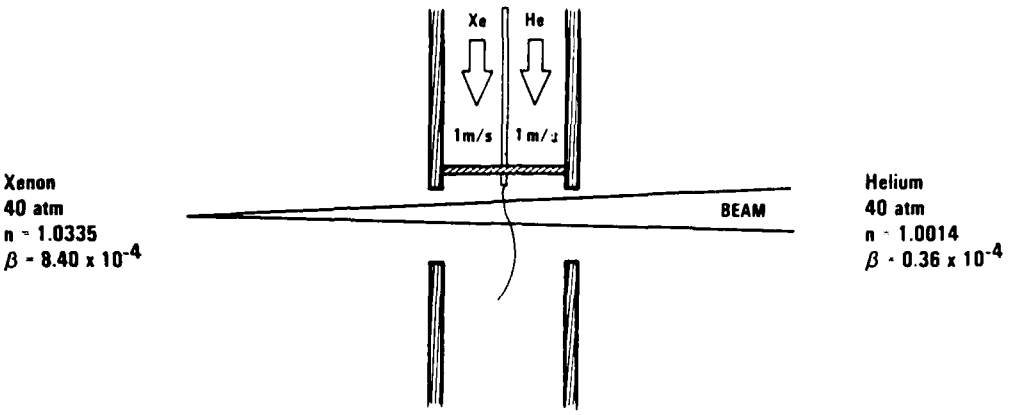

Match helium and xenon flow velocities at the interface to prevent turbulent shear layer, form a laminar wake to smoothly combine the two gases at the interface

Stable laminar interface minimizes optical distortion (i.e., perfect interface)

Flow velocity approximately 1 m/s

Flow rate approximately $\dot{m}_{xe} \sim 0.02$ kg/s / $\dot{m}_{he} \frac{4}{131} \dot{m}_{xe}$

Figure 7-7. Xenon-helium separation chamber.

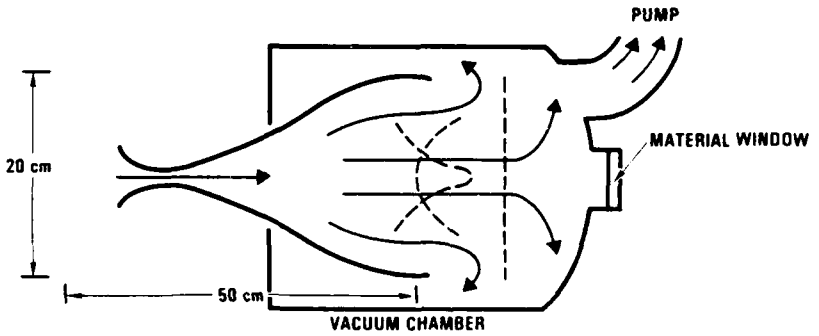

Vacuum chamber and steam ejector

- **Exhaust helium into a vacuum tank: flow rate 3 lbm/s**
- **Vacuum chamber volume: 10 m^3**
- **Ejector line volume: 40 m^3**
- **Ejector pumping capacity: 0.6 lbm/s**

OPD distortion

- **Pressure rise ~ 0.1 atm/s**
- **Flow establishment time: 50 ms**
- **Maximum pressure during flow establishment time: < 10 torr**

Figure 7-8. Vacuum chamber concept design.

volume of the vacuum chamber and the ejector line rises to less than 10 torr. Preliminary estimates of the effects of such pressure rise within the vacuum chamber on optical phase distortion indicate that the requirements on beam quality degradation (BQ <2) in the SBS cell will easily be satisfied using this configuration.

The conceptual design of the xenon cold trap used to separate the xenon spent during a run from entrained helium and other possible contaminants is shown in Figure 7-9. In this configuration, the gas collected in the xenon dump tank (Figure 7-4) is slowly passed through the trap where the xenon is frozen on a series of parallel plates. The residual gases and contaminants are pumped out using a vacuum pump. The cold trap is cryogenically cooled simply by filling the device with liquid nitrogen prior to a run and removing the nitrogen with a vacuum pump. The actual cryotrapping of the xenon during a run is accomplished with the thermal mass of the cold trap, as opposed to a more complex active cryogenic cooling system.

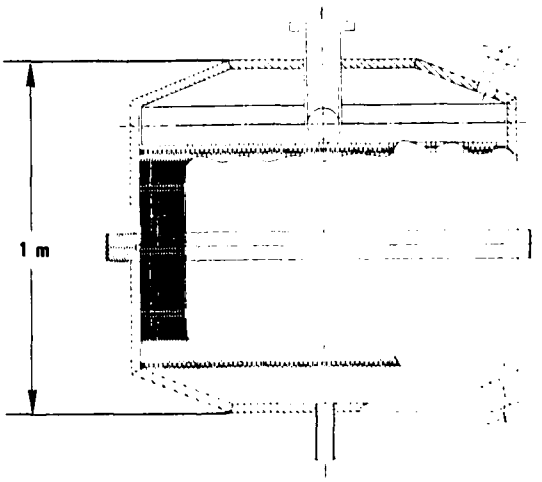

Design

- **99% efficiency in removing xenon from flow**
- **Remove 10 kg xenon per cycle maximum**
- **The order of a 30-minute cycle time**

Figure 7-9. Conceptual design of xenon cold trap.

7.4.5 Concluding Remarks

It is anticipated that, in programs following CLPCT, key features of the flowing cell conceptual design will be developed to a detailed design and fabricated for experimental investigation. During this detail design phase, additional analyses would be performed on computing the helium and xenon flow fields in the various sections of the cell and assessing the effects of medium-induced aberrations on optical phase distortion.

8. GLOSSARY

A/D	Analog-to-digital
BQ	Beam quality
CDR	Critical design review
CLPCT	Chemical laser phase-conjugation technology
CoDR	Conceptual design review
COS	Conjugation subsystem (experiment)
CTS	Capistrano Test Site (TRW)
FWHM	Full-width at half-maximum
GFE	Government furnished equipment
HEL	High energy laser
HF	Hydrogen fluoride
HFC	HF conjugation (experiment)
MO	Master oscillator
MOPA	Master oscillator, power amplifier
NRL	Naval Research Laboratory
PAR	Pacific Applied Research
PCL	Pulsed chemical laser
PDR	Preliminary design review
RPCL	Repetitively pulsed chemical laser
RPCL-50	50-liter RPCL
SBL	Space based laser
SBS	Stimulated Brillouin scattering
SDI	Strategic Defense Initiative
SDIO	Strategic Defense Initiative Operation

REFERENCES

1. Mangano, J.A., Limpaecher, R.L., Daugherty, J.D., and Russell, F., Appl. Phys. Lett., Vol. 27, pp. 293, 1975.

2. Chen, H.L., Taylor, R.L., Wilson, J., Lewis, P. and Fyfe, W., J. Chem. Phys., Vol. 61, p. 306, 1974.

3. Pulsed Chemical Laser Science and Technology, AFWL-TR-73-40, Air Force Weapons Laboratory, Kirtland Air Force Base, NM 87117, October 1973.

4. Hofland, R., Ching, A., Lundquist, M.L., and Whittier, J.S., J Appl. Phys., Vol. 47, p. 4543, 1976.

5. Design of a Pulsed DF Flowing Gas Laser, Boeing Report No. D180-25569-1, October 1979.

6. Weisbach, M.F., Buonsdonna, V.R., Artura, C.J., Shephers, W.B., Shrader, J.E., and McClure, J.D., PHOCL-50: A 50-Liter Photoinitiated Chemcial Laser, Boeing Final Technical Report D180-24898-1, November 1978

7. Kerber, R.L., and Hough, J.J.T., Applied Optics, Vol. 17, p. 23377, 1978.

8. TRW, Memorandum by J. Doyle on oscillator design, AP-0304, Redondo Beach, CA, 12 February 1986.

9. TRW, Memorandum by J. Doyle on performance budgets update, AP-0324, Redondo Beach, CA, 18 February 1986.

10. TRW, Memorandum by J. Lockwood on NLOT/CLPCT telescope design, revision A, AP-0201A, Redondo Beach, CA, 27 February 1986.

11. TRW, Memorandum by S. Quon on intensity profiles of the horizontal oscillator spatial filter, AP-0292, Redondo Beach, CA, 6 February 1986.

12. TRW, Memorandum by R.J. Wagner on spatial filter, AP-0263, Redondo Beach, CA, 8 January 1986.

13. Betts, J., SUB-PIRCL Contractor Selection Review, p. 151, 6 December 1978.

14. TRW Memorandum by D.C. Heiner on damage threshold of copper mirrors, AP-0216, Redondo Beach, CA, 12 December 1985.

15. J.A. Betts, et al., Repetitively Pulsed Chemical Laser Technology Assessment, prepared for US Army/MICOM, Confidential TRW Report S/N 37505, 29 August 1980.

END

2-81

DTIC